

University of Windsor

Scholarship at UWindor

Electronic Theses and Dissertations

Theses, Dissertations, and Major Papers

3-28-2023

Framework for the Design of Seismically Isolated Part 9 Structures

Nolan M. Stratton
University of Windsor

Follow this and additional works at: <https://scholar.uwindsor.ca/etd>



Part of the [Civil and Environmental Engineering Commons](#)

Recommended Citation

Stratton, Nolan M., "Framework for the Design of Seismically Isolated Part 9 Structures" (2023). *Electronic Theses and Dissertations*. 9050.

<https://scholar.uwindsor.ca/etd/9050>

This online database contains the full-text of PhD dissertations and Masters' theses of University of Windsor students from 1954 forward. These documents are made available for personal study and research purposes only, in accordance with the Canadian Copyright Act and the Creative Commons license—CC BY-NC-ND (Attribution, Non-Commercial, No Derivative Works). Under this license, works must always be attributed to the copyright holder (original author), cannot be used for any commercial purposes, and may not be altered. Any other use would require the permission of the copyright holder. Students may inquire about withdrawing their dissertation and/or thesis from this database. For additional inquiries, please contact the repository administrator via email (scholarship@uwindsor.ca) or by telephone at 519-253-3000ext. 3208.

Framework for the Design of Seismically Isolated Part 9 Structures

By

Nolan M. Stratton

A Thesis

Submitted to the Faculty of Graduate Studies
through the Department of Civil and Environmental Engineering
in Partial Fulfillment of the Requirements for
the Degree of Master of Applied Science
at the University of Windsor

Windsor, Ontario, Canada

2022

© 2022 Nolan M. Stratton

Framework for the Design of Seismically Isolated Part 9 Structures

by

Nolan M. Stratton

APPROVED BY:

O. Jianu

Department of Mechanical, Automotive & Materials Engineering

S. Das

Department of Civil and Environmental Engineering

N. Van Engelen, Co-Advisor

Department of Civil and Environmental Engineering

R. Ruparathna, Co-Advisor

Department of Civil and Environmental Engineering

September 9, 2022

DECLARATION OF ORIGINALITY

I hereby certify that I am the sole author of this thesis and that no part of this thesis has been published or submitted for publication.

I certify that, to the best of my knowledge, my thesis does not infringe upon anyone's copyright nor violate any proprietary rights and that any ideas, techniques, quotations, or any other material from the work of other people included in my thesis, published or otherwise, are fully acknowledged in accordance with the standard referencing practices. Furthermore, to the extent that I have included copyrighted material that surpasses the bounds of fair dealing within the meaning of the Canada Copyright Act, I certify that I have obtained a written permission from the copyright owner(s) to include such material(s) in my thesis and have included copies of such copyright clearances to my appendix.

I declare that this is a true copy of my thesis, including any final revisions, as approved by my thesis committee and the Graduate Studies office, and that this thesis has not been submitted for a higher degree to any other University or Institution.

ABSTRACT

Despite the recent advances in structural engineering made over the last century, earthquakes continue to pose a major risk to the lives and livelihoods of many communities. British Columbia is well known as a region at risk from seismic hazards, however, significant seismic risk extends to Canadians across the country as 70% of Quebec's population lives in active seismic regions. Most single-family residential structures in Canada are built using Part 9, Housing and Small Buildings, of the National Building Code of Canada (NBCC). Part 9 provides conservative simplified design and analysis methods that facilitate design without engineering involvement. It is generally believed that Part 9 single family wood frame residential structures are resistant to seismic effects, however, the aftermath of several earthquakes have demonstrated that, while life safety resilience is fairly good, the economic losses are unacceptably high. To protect against this danger to life and livelihood the NBCC provides several ways to design structures for seismic events. One of the most promising of these is an emerging technology known as base isolation.

Base isolators are specially designed structural components that effectively act as a suspension system, isolating the structure from the ground motion effects. While this technology has proven effective at protecting structures and their occupants, the current design methodology often requires custom base isolator designs and comprehensive engineering. This creates a significant cost barrier that disincentivizes application of base isolation to common Part 9 designed single family residential structures that normally avoid engineering involvement.

To eliminate this cost barrier to widespread adoption of base isolation, a program was developed to perform the engineering seismic design for a base isolated single family residential structure. Currently the NBCC does not provide a design methodology for base isolated structures, and so the program utilizes the ASCE design method adapted for NBCC requirements. The program performs the design of the base isolated structure using a catalogue of pre-certified isolators, and structural characteristics and seismic data available to non-engineer Part 9 designers. This makes the program usable by non-technical experts who will be aided through a series of recommendations and provisions. The program produces key design data and performance metrics such as base shear, maximum deflection, distribution of loads, and the number of isolators required and their placement.

The program was validated by time history analysis of common single family residential structure designs. Elastomeric isolators were proposed for the case study structures, and discussions and recommendations for the design of elastomeric bearings for Part 9 structures are proposed. It was determined that the developed program provides a suitable representation of the design characteristics and seismic response of single-family residential structures.

This research serves to address and remove many of the barriers which have prevented widespread adoption of base isolation in residential structures. Through the development of this design methodology base isolation will move towards becoming available for widespread use in Part 9 single family residential structures in vulnerable regions.

ACKNOWLEDGEMENTS

I would like to thank my advisor, Dr. Niel Van Engelen, for his continuous support and guidance over the last two years. Without whose patience and technical wisdom this research would not have been possible. I would also like to thank Dr. Rajeev Ruparathna for his support and my committee members, Dr. Sreeketa Das and Dr. Ofelia Jianu.

I wish to thank my family for the unconditional support and love they have given me. And a special thanks to Joanna for always sticking by my side and encouraging me throughout.

TABLE OF CONTENTS

Declaration of Originality	iii
Abstract	iv
Acknowledgements	v
List of Tables	ix
List of Figures	x
List of Appendices	xii
Chapter 1 Introduction	1
1.1 Earthquake Risk in Canada	1
1.1.1 Earthquake Risk in Canada	1
1.1.2 West Coast	2
1.1.3 Eastern Canada	3
1.1.4 The Risk to Single Family Residential Structures	4
1.2 Seismic Isolation in Canada	5
1.3 Objectives	6
Chapter 2 Literature Review	8
2.1 Base Isolation Theory	8
2.1.1 Characteristics of a Base Isolation System	9
2.1.2 Transmissibility	9
2.1.3 Dynamic Response	11
2.2 Isolator Systems	12
2.2.1 Sliding Isolators	12
2.2.2 Elastomeric Isolators	15
2.3 Base Isolated Structures	17
2.3.1 Examples of Isolated Structure Performance	17
2.3.2 Economics of Base Isolation	18
2.3.3 Isolation of Single-Family Residential Structures	19
Chapter 3 Review of Existing Base Isolation Standards	20
3.1 NBCC	20
3.1.1 Fixed Base Structures	20
3.1.2 Seismic Force Resisting Systems and Capacity Based Design	21
3.1.3 NBCC Base Isolation Provisions	22
3.2 ASCE Base Isolation Provisions	23
3.2.1 Response Spectrum	23
3.2.2 Analysis Methods	24
3.3 Base Isolation Standards Overview	25
Chapter 4 Adaption of ASCE ELF Procedure to NBCC Part 9	27
4.1 Method of Analysis	27

4.1.1	Key Parameters	27
4.1.2	Inputs.....	27
4.2	Equivalent Lateral Force Procedure Equations and Adaption	28
4.2.1	Maximum Displacement.....	28
4.2.2	Effective Isolated Period.....	28
4.2.3	Total Maximum Displacement of Isolator Units	29
4.2.4	Vertical Distribution of Forces	30
Chapter 5 Online Resource Methodology.....		32
5.1	The Online Resource.....	32
5.1.1	Existing Capabilities	32
5.2	Deficiencies Requiring Further Development	33
5.2.1	Structural Geometry.....	33
5.2.2	Structural Properties.....	33
5.2.3	Torsional Effects.....	33
5.2.4	Isolation System Layout.....	33
5.2.5	Site Specific Conditions.....	33
5.3	Improvements to the Baseline Program	34
5.3.1	Geometry Inputs and Analysis.....	36
5.3.2	Isolation Layout	37
5.3.3	Determine Tributary Areas	38
5.3.4	Distribute Loads.....	40
5.3.5	Calculate Axial Loads.....	41
5.3.6	Torsional Amplification Evaluation.....	42
5.3.7	Calculation of Floor Stiffness	43
5.3.8	Placement Results and Plot Results	44
5.3.9	Move Existing Add New Isolators.....	45
5.3.10	Determine Period and Design Displacement	46
5.3.11	Determine Forces and Response	49
5.3.12	Analysis Results.....	51
Chapter 6 Isolator Design		52
6.1	Introduction.....	52
6.2	Isolator Stability.....	52
6.2.1	Buckling Stability	52
6.2.2	Rollout Stability	53
6.2.3	Rupture Stability Check.....	54
6.3	Testing Requirements	56
6.3.1	Compressive Properties.....	56
6.3.2	Compressive Property Dependence	57
6.3.3	Shear Properties	57
6.3.4	Shear Displacement Capacity	58
6.3.5	Shear Property Dependence	58
6.4	Design Considerations for Part 9 Structures	59
6.4.1	Isolator Shape.....	59

6.4.2	Superstructure Performance and Shear Displacement	60
6.4.3	Applicability of Designs	60
Chapter 7 Case Studies		62
7.1	Program Methodology Validation	62
7.2	Model Structures	62
7.3	Isolator Properties	66
7.4	Time History Analysis	69
7.5	Results.....	71
7.5.1	Fixed Base Responses.....	72
7.5.2	Base Isolated Responses	73
7.5.3	Evaluation of Isolated Performance	75
Chapter 8 Conclusions and Recommendations.....		77
8.1	Introduction.....	77
8.2	Conclusions.....	77
8.3	Recommendations for Future Research	78
8.3.1	Rigid Floor Diaphragm	78
8.3.2	Isolation Layer Design and Axial Loading	79
8.3.3	Structural Geometry Considerations	79
8.3.4	Storey Stiffnesses.....	79
8.3.5	Superstructure Performance	79
References.....		81
Appendix A Baseline Program Process		88
Appendix B Beam Layout		92
Vita Auctoris.....		96

LIST OF TABLES

Table 5.1: CWC Normal and Heavy weight classification	42
Table 5.2 Damping Factor [42].....	48
Table 6.1: Compressive strain dependance test strains	57
Table 6.2: Compressive stress dependance test stresses	57
Table 6.3: UPD compressive stress loads	58
Table 7.1: Geometric data.....	63
Table 7.2: CWC weight class distributed dead loads.....	63
Table 7.3: Snow load values Vancouver.....	64
Table 7.4: Distributed live loads	64
Table 7.5: Mass and weight distribution	64
Table 7.6: Program stiffness distribution	64
Table 7.7: Model stiffness distribution	64
Table 7.8: Isolator axial loading of design 1 structure (kN)	66
Table 7.9: Isolator axial loading of design 2 structure (kN)	66
Table 7.10: Design axial loads for bearings (kN)	66
Table 7.11: Isolator characteristics	67
Table 7.12: Isolator properties	67
Table 7.13: Model Bouc-Wen Variables	69
Table 7.14: Ground motion records	70
Table 7.15: Fixed base structure base shear.....	72
Table 7.16: Fixed base lateral storey displacement and floor accelerations	73
Table 7.17: Fixed base interstorey drifts.....	73
Table 7.18: Difference factor between the program and THA (THA/program).....	73
Table 7.19: Base isolated displacement and base shear.....	74
Table 7.20: Base isolated lateral storey displacement and floor accelerations	74
Table 7.21: Base isolated interstorey drifts.....	75
Table 7.22: Difference factor between program and THA (THA/program).....	75
Table 7.23: Program responses	76
Table 7.24: THA responses.....	76

LIST OF FIGURES

Figure 1.1: Seismic hazard map of Canada [7].....	1
Figure 1.2: Lateral compressive stress orientation [8].....	2
Figure 1.3: Base isolation	6
Figure 2.1: Effects of period elongation on a) spectral acceleration b) displacement	8
Figure 2.2: Base acceleration of a) perfectly fixed b) perfectly detached and c) base isolated structures	9
Figure 2.3: Comparison of TR and frequency ratio	10
Figure 2.4: Mode shapes of a) fixed base and b) isolated 4-storey structures [38].....	11
Figure 2.5: Flat sliding isolator and FP sliding isolator	13
Figure 2.6: Hysteresis of flat and friction pendulum sliding isolators [46]	13
Figure 2.7: Triple friction pendulum isolator cross section [48]	14
Figure 2.8: Stiffness displacement profile of TFP	15
Figure 2.9: Lateral bulging: a) unreinforced b) with reinforcement	15
Figure 2.10: Rollover deformation: a) linear displacement b) partial rollover c) full rollover	17
Figure 3.1: Acceleration response spectrum	21
Figure 3.2: ASCE 7-16 design response spectrum [42].....	24
Figure 5.1: Program flow chart.....	35
Figure 5.2: Dimensions of floor plan a) with no offset and b) with upper storey offset.....	36
Figure 5.3: Variable floor plan types with a) a rectangular base and b) a L-shaped base ..	36
Figure 5.4: Division of structural plan in elements.....	38
Figure 5.5: L-shaped structure rounded elements for areas A, B and C	39
Figure 5.6: Element array generation of floors $k+1:1$ for $k = 3$	40
Figure 5.7: Structure load paths	40
Figure 5.8: Isolator placement for a) a rectangular and b) a L-shaped structures.....	44
Figure 5.9: Floor beams with offsets	45
Figure 5.10: Custom placement of isolators	46
Figure 5.11: Response spectrum interpolation.....	47
Figure 5.12: Comparison of fixed base and isolated spectral accelerations	48
Figure 5.13: Example of a vertical force distribution comparison.....	50
Figure 5.14: Displacement comparison	50
Figure 6.1: Rollout instability	54
Figure 7.1: Design 1 Ground floor plan and 2 nd storey plan.....	62
Figure 7.2 Design 2 ground floor plan.....	63
Figure 7.3: a) Design 1 floor beam layout and b) design 2 floor beam layout	65
Figure 7.4: a) Design 1 isolator layout and b) design 2 isolator layout	65
Figure 7.5: a) Force displacement hysteresis of design 1 and b) design 2.....	69
Figure 7.6: a) Design 1 response spectrum comparison and b) design 2 response spectrum comparison.....	76
Figure B.1 Floor beams for a) Rectangular and b) L-shaped structures	92
Figure B.2 Floor beams and isolator layout of example structure	93
Figure B.3 Division of a L-shaped structure.....	93
Figure B.4 L-shaped structure floor beam layout	94

Figure B.5 L-shaped structure floor beam layout with AB and AC borders	94
Figure B.6 L-shaped structure with AB and AC borders connected.....	95

LIST OF APPENDICES

Appendix A Baseline Program Process	88
Appendix B Beam Layout	92

CHAPTER 1

INTRODUCTION

1.1 Earthquake Risk in Canada

1.1.1 Earthquake Risk in Canada

Despite the engineering achievements of the last century earthquakes continue to be a serious threat to the lives and livelihoods of many communities. Since 1970, approximately 360 damaging earthquakes have claimed over 1 million lives worldwide [1]. In Canada there are approximately 4000 earthquakes annually, mainly concentrated in regions of high seismicity. British Columbia is well known as a region at risk from seismic hazards, however, significant seismic risk extends to Canadians across the country as on June 23, 2010, a 5.2 magnitude earthquake rocked a small Quebec town 60 km north of Ottawa [2]. The full extent of the hazard is illustrated in Figure 1.1. The threat posed to Canadians is further magnified due to the concentration of roughly 40% of the national population within areas of high seismicity [3]. In Quebec, 70% of the population lives in active seismic regions and three of the largest cities in eastern Canada – Montreal, Ottawa and Quebec City – are all located in earthquake-prone regions [4]. In British Columbia the hazard is even greater where over 80% of the population lives in active seismic regions [5]. Earthquakes tend to occur in specific geographical regions, but this in no way makes them predictable. For example, on August 16, 2019, there was a magnitude 4.1 earthquake 25 km east of Esterhazy, Saskatchewan, a low-risk area according to the Government of Canada [6].

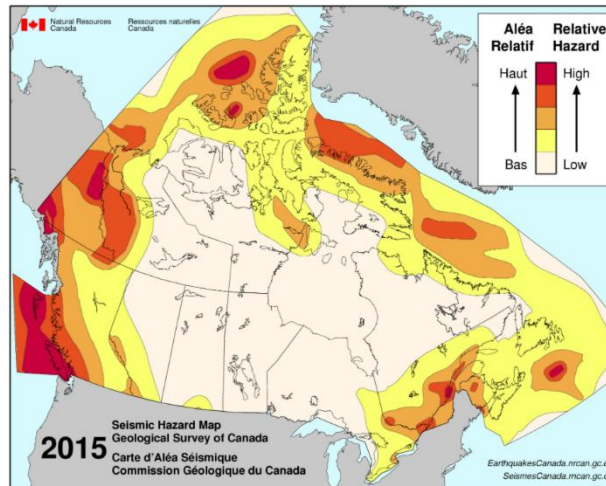


Figure 1.1: Seismic hazard map of Canada [7]

Studies have been performed to evaluate the potential risk posed by earthquakes to the West and East coasts, with the finding suggesting that a significant seismic event near a sizable urban center on either coast could result in tens of billions of dollars of damages [3]. This would make either of these potential events the costliest natural disaster in Canadian history. More importantly earthquakes of similar magnitude and proximity have resulted in deaths tolls ranging from hundreds to thousands, and the displacement of tens of thousands from their homes. To protect against this threat to the lives and livelihoods of local communities the National Building Code of Canada

(NBCC) has specified that structures be designed for a 2475 year return period rather than the typical 50 year return period prescribed for other load types [6]. This is partially due to the danger posed by seismic events and the difficulty in which they can be predicted.

1.1.2 West Coast

The West coast is commonly held as the region of Canada most prone to earthquakes and with good reason. The largest and most frequent of Canada's earthquakes occur along the west coast and originate from a variety of sources. The sources of earthquakes along the coastal regions of British Columbia (BC) are dominated by (NW-SE) strain built up due to the presence of the subduction zone known as the Queen Charlotte fault off the coast of BC, while approximately 150km inland the strain build up responsible for many inland earthquakes is heavily influenced by the northern drift of Oregon Block plate causing significant N-S compressive stresses within the plate to form as shown in Figure 1.2 [8].

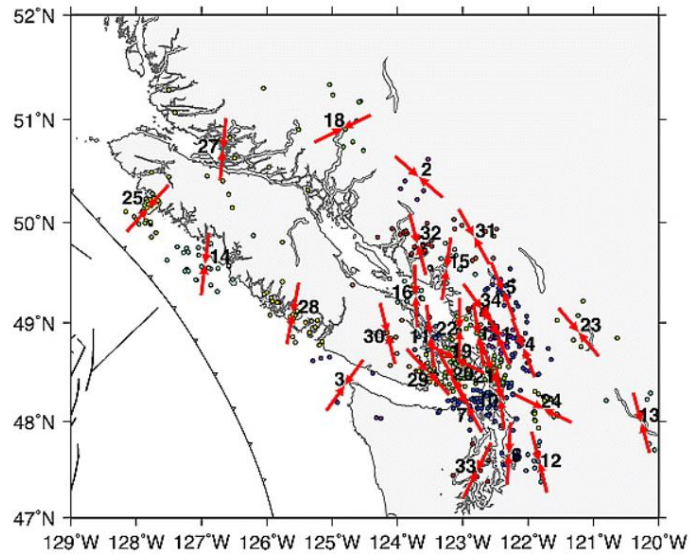


Figure 1.2: Lateral compressive stress orientation [8]

A subduction zone is the interface between two tectonic plates where the denser plate is forced under the less dense plate [9]. The plates may lock resulting in a buildup of stress until a slip occurs which results in a rapid realignment of the plates causing an earthquake. The Queen Charlotte fault is a result of the Pacific plate being forced beneath the North American plate which generates significant friction as the plates move past one another. This region makes up a small portion of the greater Pacific Ring of Fire; a term used for the areas in and around the Pacific Ocean where similar subduction induced earthquakes are frequent. The largest Canadian earthquake of the last century was the M8.1 (1949) Queen Charlotte earthquake which occurred just off the coast of the Queen Charlotte Islands [10]. Due to the sparse population of the island the quantity of damage was low, however, reports of collapsed chimneys and ground motions strong enough to throw people off their feet were reported. The largest known earthquake in Canada was the 1700 M9.0 megathrust earthquake which occurred off the southern coast of Victoria Island near Victoria, BC [11]. Oral traditions of the native communities of Vancouver Island give descriptions of the

devastation and long duration shaking that occurred, while over 7000 km away Japanese sources document the tsunami that hit the east coast of Japan as a result of the event [10]. Geological evidence indicates that 13 of these large events have occurred over the last 6000 years with another similar event expected in the future. An analysis of the potential destruction a repeat of the M9.0 1700 earthquake could result in an estimated \$74.7 billion CAD in damages, with \$58.6 billion originating directly from ground shaking [10]. To further compound the issue, less than a third of the loss would be insured meaning losses would be directly inflicted onto the property owners resulting in widespread destruction of people's livelihoods and savings. A bigger risk to the west coast might come from a smaller event located closer to a large urban center. In the last 130 years, four M7.0+ events have occurred inland in BC and northern Washington state [12]. In 1995 an inland M6.9 earthquake 20km from Kobe Japan, which has a similar population to the Vancouver Metro, resulted in over 6000 deaths, left over 300,000 people homeless, and caused 200 billion CAD in damages due to initial and long term losses [13]. An event of similar magnitude and proximity could result in a proportionally equivalent loss of life, and the destruction of tens of thousands of people's homes and livelihoods.

1.1.3 Eastern Canada

The east coast is another area within Canada where significant seismic risk exists. Three main areas of seismicity exist within eastern Canada: Western Quebec along and North of the Ottawa river; the lower St Lawrence River Valley; North of the St Lawrence River in Charlevoix Quebec. Charlevoix, Quebec, has been a continuous source of many small earthquakes but is also responsible for some of the largest earthquakes in eastern Canada [14]. Most of the earthquakes in Eastern Canada are upper to mid crustal earthquakes resulting from thrust (reverse) faulting mechanisms from compressive stresses within the rock [15]. These types of earthquakes occur mostly around areas of crustal weakness which may be correlated with the St Lawrence River system and the Charlevoix impact crater. This potential impact zone of these events are amplified as the effects of seismic events are transmitted further through the Canadian shield such that an M6.0 earthquake could be felt up to 1000 km away [15]. This provides for a potential scenario where communities could be affected by events that occur sizable distances away. The risk in Eastern Canada is made more significant by the concentration of its population and large urban centers around areas of known seismicity, such as Montreal, Ottawa and Quebec City [16]. In 1663 an M7.0 earthquake occurred in Charlevoix, Quebec, the effects of which were felt over the entirety of eastern North America. At the time most settlements were a significant distance from the estimated epicenter, as such most of the reported damage was fairly limited [17]. An analysis of the potential destruction caused by an M7.1 earthquake, similar to the 1663 earthquake, resulted in \$60.6 billion CAD in damages of which 45.9 billion would be due to direct property damage, almost all directly from the ground shaking [10]. As earthquakes are typically not perceived as high risk in much of Eastern Canada, only about one sixth of the damage inflicted would be insured. Due to this gap in insurance coverage the total uninsured damage due to this event would be comparable to the uninsured damage due to the discussed M9.0 west coast scenario. In Quebec as of 2017 only about 3.4% of homeowners had earthquake insurance compared with 64% in Victoria and

Vancouver, BC, meaning that most uninsured losses would be directly inflicted on the average citizen leading to the destruction of potentially hundreds of thousands of livelihoods [16].

1.1.4 The Risk to Single Family Residential Structures

The National Building Code of Canada Part 9, Housing and Small Buildings, applies to structures with total areas of 600m² or less and 3 storeys or less in height [6]. If a structure exceeds these parameters Part 4, Structural Design, of the NBCC must be followed and the approval of the design by a qualified professional engineer is required. Part 9 allows relatively small and simple structures to be designed without engineering involvement by providing simplified methods of design and analysis where acceptability of the design is evaluated based on the designer's selections.

For most common single-family dwellings typically referred to as a house, Part 9 prescriptive design methodologies are employed to ensure the structure will be resilient enough to withstand the applied load conditions, including seismic loads. For structures vulnerable to dynamic excitations, or with complex or irregular designs, a dynamic analysis utilizing time histories developed based on historical earthquake data must be conducted. Simpler structures can be evaluated using the equivalent static force procedure given in Part 4 of the NBCC utilizing regional seismic data. In Canada, and especially in eastern Canada, many residential structures were built prior to the current building code standards and are significantly more vulnerable to seismic hazards. Many modern single-family residential structures are composed primarily of wood members due to their relatively high strength to weight ratio. When subjected to seismic loads these structures typically perform well relative to masonry due to their low weight to high stiffness ratio; the flexibility of these structures; and the system redundancy of the members [18].

In recent years the performance of single family wood frame residential structures has come under scrutiny due to the aftermath of several seismic events near urban centers. The traditional measure of disaster intensity is generally the casualty figures, which for many events in North America in recent years have been low compared to other events around the world, especially in developing countries. However, the economic losses and people left homeless remain shockingly high for moderate and strong events such as the 1994 Northridge earthquake [19]. The Northridge earthquake was a M6.7 event that occurred in the Los Angeles area of California. This event is notable due to the magnitude of the event as well as its proximity to an urban center which resulted in 57 fatalities and between \$25 - 40 billion USD in losses [20, 21]. Of the 57 fatalities, 25 were a result of building damage and 24 of those occurred in wood frame residential structures, with half or more of the \$40 billion in property damages being from wood frame structures [20]. Of the 64,000 damaged homes inspected after the disaster over 10% were deemed unsafe for habitation, leaving many homeless. The portion of damaged homes in this case represents 25% of the total number of homes within a 20 km radius of the fault rupture plane. Over the following years \$20.9 billion USD (adjusted for inflation) would be provided to over 500,000 homeowners for mainly minor structural and nonstructural damages. 265,000 homeowners would receive an average of \$50,000 USD in insurance payments; 74,000 homeowners would obtain low interest loans from the Small Business Administration, averaging \$51,500 USD; and 288,000 homeowners received an average of \$5,000 USD from other federal programs [19]. The inflicted losses, even for

superficial damage are quite high, usually averaging \$50,000 USD or \$64,500 CAD which is greater than the yearly median provincial household income of Canadians across all provinces [22]. The potential loss of over a year's worth of income, or the potential loss of their home, which is the largest single asset of many Canadians, would be a catastrophic loss for the affected individuals.

The damage suffered by a structure does not need to be structurally debilitating to be economically significant as many structures can be structurally sound but suffer significant damage to nonstructural components. Damage to structures from an economic perspective can be categorized as either damage due to excessive interstorey drift, or damage due to excessive floor accelerations. Interstorey drift is the relative lateral displacement between floors due to the ground motion effects. Drift sensitive components such as drywall and wall studs can be compromised if the interstorey drift becomes too significant leading to cracking. Acceleration sensitive components are possessions that are not fixed to the structure such as ceiling tiles, small appliances or other furnishings, which may become damaged when exposed to strong accelerations. Superficial damage to drywall can occur at interstorey drifts as low as 0.1%-0.5%, with significant cracking and crushing occurring between 2%-5% drift. More concerning permanent damage to the wall frame has been observed to occur for an interstorey drift of 1-2% which may result in a loss of structural integrity and leave the structure more vulnerable to additional seismic events [23]. Loss of structural integrity due to a previous event was a significant issue in the 2011 Christchurch earthquake when the CTV building that had been previously damaged during an earlier earthquake in 2010 collapsed resulting in the deaths of 119 people [24]. Drifts of around 2% damage to the wall may be extensive enough as to be a complete economic loss and necessitate the complete repair or reconstruction of the wall [25]. While structural collapse may be avoided due to the flexibility of wood frame structures, significant economic losses may be incurred as a result of that increased flexibility and deformation of the structure. Slight damage to acceleration sensitive objects begins to manifest when objects are subjected to around 0.25g - 0.50g, while complete damage often occurs around 2.00g [26]. Roughly 60-80% of a building's value is its non-structural components and contents [27]. During seismic events low-rise wood frame structures, typically for common Canadian homes, are usually structurally resilient. However, they may suffer significant damage to its contents and its nonstructural components resulting in significant economic losses. In addition to the direct economic losses the loss of property and the potential need to seek temporary accommodations while repairs are underway may result in a substantial disruption to affected people's lives.

1.2 Seismic Isolation in Canada

The potential for losses and disruptions to the livelihoods of owners of Part 9 designed low-rise single-family residences are both serious and unacceptable. While fairly resilient from a life safety standpoint, the structures are often unable to prevent the contents and interior of the structure from experiencing significant damage during moderate to strong earthquakes, which can induce significant and potentially devastating losses to people's livelihoods. There have been many methods employed to increase the seismic resilience of structures collectively known as anti-seismic techniques. Currently over 20,000 structures across 30 countries utilize such techniques [28]. One of the most popular modern techniques is known as base isolation, which has shown great success in preventing damage to structures during a variety of earthquakes. Base isolation prevents

the structure from experiencing the effects of the strong ground motions by decoupling the structure from strong ground motions as illustrated in Figure 1.3 [29].

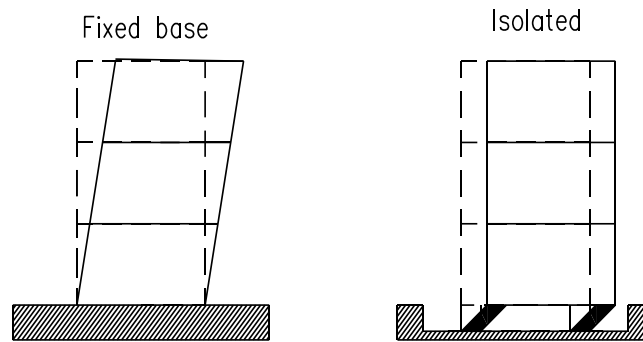


Figure 1.3: Base isolation

The decoupling significantly reduces the transfer of forces from the ground motion to the overlying structure, protecting the structure and its occupants from harm even during large earthquakes [30, 31]. The properties of base isolation make it a suitable candidate for single family residential structures as it has shown its ability to protect against structural damage as well as economic losses, a characteristic many residential structures have, as previously discussed, been shown to lack [32, 33].

While this technology has proven effective at protecting structures, its use has been mainly limited to large high importance structures. Currently no simplified method for the design of base isolated structures exists in the NBCC in Part 4 or Part 9 [7]. Low-rise residential structures are usually designed based on the prescriptive requirements outlined in Part 9 of the NBCC. A lack of prescriptive standards for the design of a base isolated residential structure means that inclusion of a base isolation system would require the involvement of an engineer familiar with base isolation. This verification is to ensure the system would operate as intended, and the requirements outlined in Part 4 and Part 9 of the NBCC have been met. The current requirements outlined in the NBCC require a rigorous series of tests to verify the properties of base isolators before they can be certified for use in a structure. The custom base isolator design process and comprehensive engineering requires a significant capital expenditure making the application of this technology cost prohibitive for Part 9 single family residential structures. While significant research has been done to improve the economics of base isolation, namely via the development of low-cost bearings, little research has been conducted to address the cost barriers created by testing, design, and analysis costs.

1.3 Objectives

The objectives of this research are to:

- reduce or eliminate the cost barriers related to seismic isolation by developing a prescriptive Part 9 compatible design and analysis methodology, and,
- facilitate the application of seismic isolation to Part 9 structures.

To achieve the objective, research is conducted to develop a program capable of performing the design of the base isolated structure using only the inputs that would be available to a Part 9 designer and a catalogue of pre-certified isolators tailored for use in residential structures. This will remove the need to conduct a comprehensive engineering design of the structure, and eliminate the costly custom testing and design of the base isolators by designing based on existing and well understood isolators. The development of this approach will enable the widespread application of seismic isolation by significantly reducing the required capital investment.

CHAPTER 2

LITERATURE REVIEW

2.1 Base Isolation Theory

Base isolation is a method of seismic protection which has proven effective at protecting structures and their contents from the damage caused by the strong ground motion generated by earthquakes. A base isolated structure is augmented by a flexible isolation layer usually located between the foundation and the ground floor. This layer decouples the structure from the strong ground motions experienced by the foundation, significantly reducing the transmission of ground accelerations to the structure. This is achieved by elongating the fundamental period of the structure. The advantage to elongating the structure's fundamental period is that the spectral acceleration experienced by the structure will decrease. A typical low-rise wood frame structure has a fundamental period of 0.2s [34], extending that period from 0.2s to 2.0s, which is very achievable for base isolated structures which often have much longer periods [35], would substantially reduce the forces the structure must endure to remain linear elastic and avoid damage. The decoupling of the structure from the ground motions causes large relative displacements between the structure and its foundation. The relation between structural displacement, D , period, T , and spectral acceleration, S_a , is given by:

$$D = \frac{S_a g T^2}{4\pi^2} \quad (2.1)$$

The relation between period, spectral acceleration and displacement, and the effect of base isolation upon them are illustrated in Figure 2.1 a) and b).

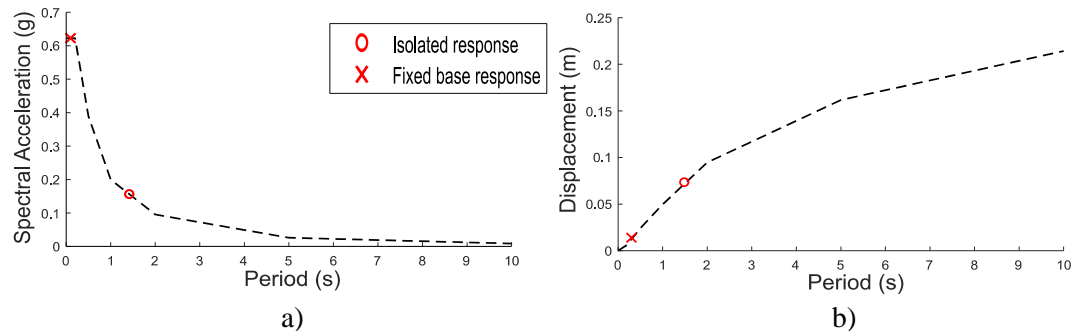


Figure 2.1: Effects of period elongation on a) spectral acceleration b) displacement

The design methodology inherent to base isolation is the reduction of loads experienced by a structure, rather than reinforcing the structure to overcome them. The addition of a base isolation system to a traditionally designed single family residential structure would significantly reduce the lateral forces experienced by the structure and allow for better performance and reduction or elimination of the economic losses caused by ground shaking [35].

2.1.1 Characteristics of a Base Isolation System

The three main characteristics of a base isolation system that determine its performance, are its lateral stiffness, vertical stiffness and damping characteristics [36]. The characteristic most relevant to the fundamental principles of base isolation is the lateral stiffness of the isolators. The lateral stiffness of the base isolators influences the fundamental period of the structure, and also indirectly influences other important dynamic characteristics such as transmissibility and the modal influences. A fixed base rigid structure would move rigidly with the ground motion and would in turn experience base total accelerations, \ddot{U} , equivalent to the ground acceleration, \ddot{U}_g , as shown in Figure 2.2 a). If the reduction of stiffness between a structures foundation and the ground is significant enough, theoretically the base of the structure would be isolated from the ground accelerations and would experience total accelerations near 0 g as shown in Figure 2.2 b). It is possible to create a region of low lateral stiffness between the foundation and superstructure using an isolation layer, substantially reducing the base accelerations as illustrated in Figure 2.2 c). Assuming vertical stability is maintained the superstructure would remain rigidly elastic and would experience relative displacements equivalent to the ground displacement.

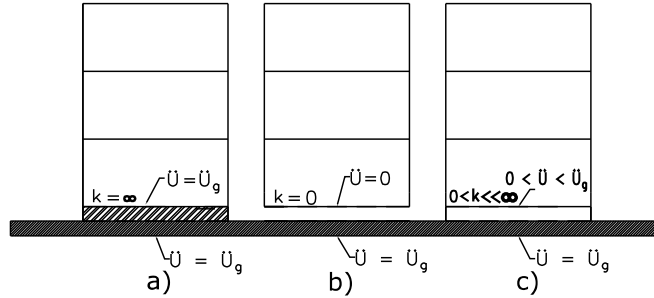


Figure 2.2: Base acceleration of a) perfectly fixed b) perfectly detached and c) base isolated structures

2.1.2 Transmissibility

The relation between reduced stiffness of the isolation layer and the forces experienced by the structure is due to the relation between the dynamic transmissibility of the fundamental mode and the stiffness and damping of the isolation layer. Transmissibility, TR , is the ability of a response characteristic to be transferred from a source of excitation to a structure and is defined as:

$$TR = \left\{ \frac{1 + [2\zeta(\omega/\omega_n)]^2}{[1 - (\omega/\omega_n)^2]^2 + [2\zeta((\omega/\omega_n))]^2} \right\}^{\frac{1}{2}} \quad (2.2)$$

where ω is the angular frequency of excitation, ω_n is the natural frequency of the structure and ζ is the damping ratio.

Plotting the relation between TR and ω/ω_n as shown in Figure 2.3 reveals that for a structure with a very high ω_n relative to ω would yield a TR of 1 for that mode. However, when ω_n is low

relative to ω the value of TR is substantially reduced. The region of concern is when ω_n and ω match closely as TR will be very large and can substantially amplify the loads.

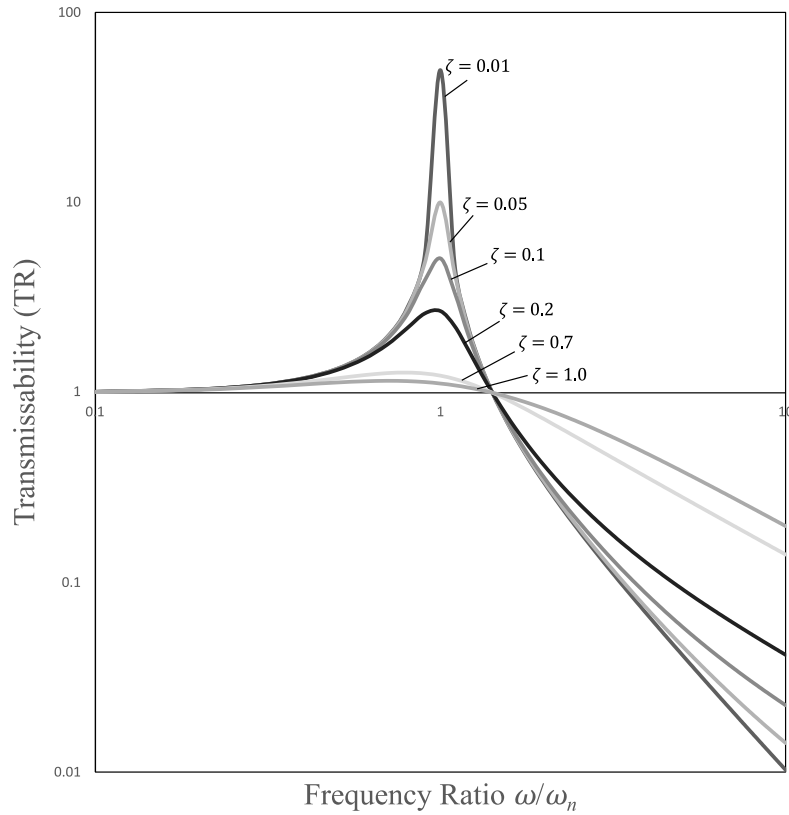


Figure 2.3: Comparison of TR and frequency ratio

One of the main objectives of reducing the lateral stiffness is to reduce the fundamental natural frequency of the structure to a region well below the frequencies of greatest earthquake energy, with the goal of achieving a TR value substantially less than unity [36]. Each earthquake ground motion record can be expressed as the sum of an infinite number of sinusoidal functions in the form:

$$\ddot{u}_g(t) = \sum_{i=1}^{\infty} A_i \sin(\omega_i t) \quad (2.3)$$

Each of these functions will have a different frequency of oscillation as well as a different amplitude. Certain functions will be more dominant than others in the overall seismic response, and in general the frequencies of highest energy content will be within the range of 0.2 – 0.3 s, which also tends to align with the fundamental frequency of many low-rise structures [37].

2.1.3 Dynamic Response

The total response of a structure can be described by the summation of the response of individual modes of vibration. The modes of a structure are a product of the structure's mass and stiffness and correspond to a specific frequency of vibration. Depending on the dynamic characteristics of a structure some modes can dominate the overall response by contributing proportionally more than other modes. Each mode will have an independent transmissibility amplification factor, whose magnitude will be based on how closely the frequency profile of the exciting forces matches the modal frequency, as seen in Figure 2.3 when ω/ω_n approaches unity. Since the frequency excitation profile of an earthquake is composed of many frequencies, with the most significant being concentrated at the lower periods, an increase of the structures period results in the most influential modes having very high ω/ω_n ratios which result in very low modal transmissibility factors.

Each mode excites a structure to vibrate in a specific manner. The relative motion of a structures degree of freedom can be described by a mode shape which describes the motion of a structure when excited at the modal frequency, as shown for a 5-storey structure in Figure 2.4 a). Typically for a fixed base structure, the first/fundamental mode will be dominant, however, the higher modes will have a significant influence on the response of the structure. The addition of an isolation layer causes the mode shapes of the structure to be altered such that the fundamental mode generates a substantial response at the isolation layer while the overlying structure behaves near-rigidly. Significant interstorey drifts are present in the higher modes of the isolated structure, with the higher modes often referred to as its structural modes. The difference in mode shape between a fixed base and isolated structure are illustrated in Figure 2.4 a) and b) for a 5-storey building respectively.

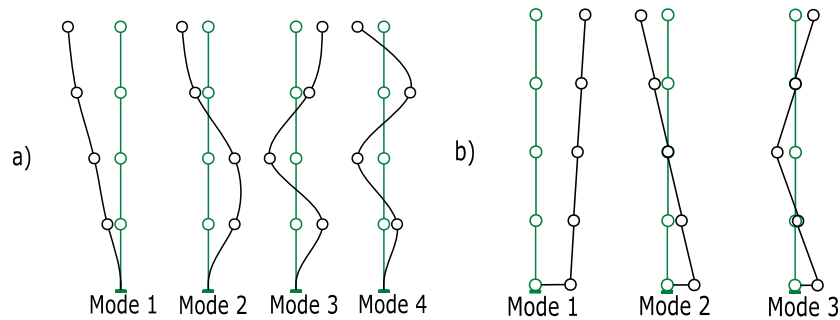


Figure 2.4: Mode shapes of a) fixed base and b) isolated 4-storey structures [38]

One of the key concepts of seismic isolation is that if the fundamental period of the fixed-based structure is much shorter than the fundamental period of the isolated structure, the higher modes will have small participation factors [38, 39]. This characteristic of a base isolated structure means that if the transmissibility of the fundamental mode is low then the overall response of the overlying structure will also be reduced. This is especially beneficial when considering that the main source of interstorey drift and floor accelerations of a base isolated structure originate from the response generated by the higher modes. This allows interstorey drifts and floor accelerations of base isolated structures to be substantially reduced, as the isolation mode will dominate the response. This is also the reason why base isolation is rarely used in structures with a fixed base

period similar to that of the desired isolation period, as isolation will have a reduced beneficial effect on the structure's overall response [40].

The vertical stiffness and damping of an isolation system are parameters that are instrumental to the performance of the complete system. During an earthquake the vertical component of ground motions is often disregarded [6]. This is due to the assumption that the vertical strength offered by the gravity resisting system of a structure provides sufficient stiffness and strength to resist serious damage. To avoid invalidating this assumption the vertical stiffness of the isolation system should be sufficiently high to allow the isolation layer to behave equivalently to that of a traditional fixed based structure. The damping of the isolator system is also crucial to ensuring the isolation system can dissipate sufficient energy to reduce displacements [39].

2.2 Isolator Systems

Base isolators are devices that are generally installed between the foundation and superstructure, with the goal of achieving the isolating effect as described in section 2.1. These devices are required to exhibit the desirable properties of low lateral stiffness, high damping, and high vertical stiffness to perform adequately. The two main types of isolators can broadly be classified as either sliding or elastomeric, although there are many other unique proprietary devices available. These two isolator types achieve desirable structural performance during seismic events but do so by differing means.

2.2.1 Sliding Isolators

Sliding isolators achieve the decoupling of a structure from strong ground motions by utilizing a low friction interface between the upper and lower faces of the sliding interface. A theoretical system with a coefficient of friction of zero at the interface would remain in its original position while the ground displaced laterally beneath it. This would theoretically eliminate the lateral forces experienced by a structure during seismic events [41]. However, such a system would require additional mechanisms to restrain the structure when subjected to wind loads and would have no means of rectifying relative displacements between the structure and its foundation after the seismic event. The issues of relative displacement between a structure and its foundation have led to code requirements such as in ASCE 7-16 [42], for isolator systems to generate a minimum restoring force to return a structure to its original position with respect to the foundation. Friction systems which utilizing a flat surface and Coulomb friction are known as pure friction systems and must be augmented with additional mechanisms to provide this restoring force, as the isolator alone has no means to restore the structure to its initial position [43]. Other systems such as friction pendulum (FP) systems, incorporate the restoring force into their design and rely on gravity to return the isolator to the initial position [44]. This is achieved by the sliding bearing resting inside a concave housing which allows the bearing to return to its initial position. A comparison between the design of a flat isolator and a friction pendulum isolator can be seen in Figure 2.5. In all cases the damping properties of sliding isolators is dependent on the energy dissipated by the sliding friction and is equivalent to the area enclosed by the hysteresis curves of the displacement force relationship.

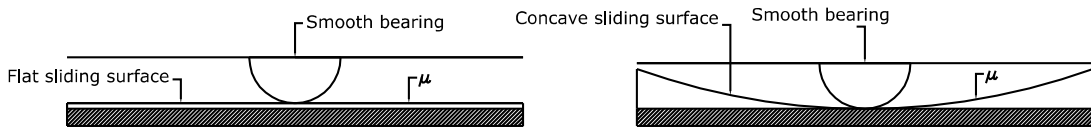


Figure 2.5: Flat sliding isolator and FP sliding isolator

The design of friction pendulum isolators produces a fixed period of oscillation, which pure friction systems lack [45]. To avoid resonance with an earthquake's dominant excitation frequencies, a long period is desirable. This is achieved by increasing the housings radius of curvature which effectively reduces its lateral stiffness, altering the period of oscillation in the same manner as discussed in section 2.1.1. The stiffness of the system is constant and is dependent on the weight of the overlaying structure, W , and the FP's radius of curvature, R :

$$K_{restore} = \frac{W}{R} \quad (2.4)$$

The directional lateral strength of a FP is variable and increases as the structure is displaced in the relevant direction. This is not true for flat systems which provide lateral resistance equivalent to the friction force. A comparison of the lateral strength profiles of a flat and sliding isolator can be seen in Figure 2.6.

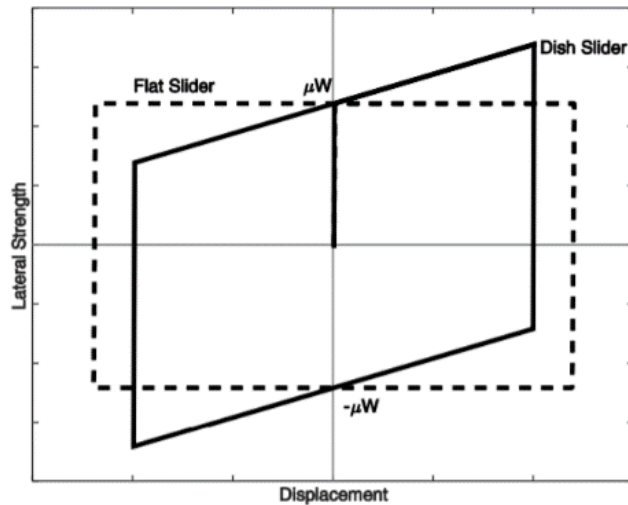


Figure 2.6: Hysteresis of flat and friction pendulum sliding isolators [46]

Another type of sliding isolators that further alter the stiffness properties are known as sliding multi-friction pendulum systems, with the triple friction pendulum isolator (TFP) being one of the most popular variants. These devices consist of multiple concave sliding interfaces and an articulating slider, as shown in Figure 2.7 which allow for larger structural displacements relative to the diameter of the bearing. In addition, the stiffness and displacement properties of these

bearings evolve nonlinearly over the course of the seismic event allowing the structure to avoid resonance and further improve its performance [47].

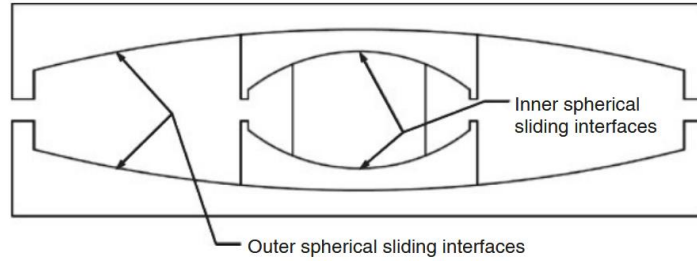


Figure 2.7: Triple friction pendulum isolator cross section [48]

A TFP utilizes three pendulum mechanisms consisting of four sliding interfaces. To achieve advantageous adaptive characteristics each mechanism is designed with a progressively higher coefficient of friction, μ_i , such that it only activates at a specific force threshold, and a specially detailed pendulum length, L_i , which alters its sliding stiffness. The effective pendulum length given by:

$$L_i = R_i - h_i \quad (2.5)$$

where R_i is the radius of curvature of the dish, and h_i is the slider height [48].

The properties of each pendulum mechanism are selected to target isolation system hysteretic properties that depend on the level of displacement response, and the corresponding level of seismic hazard. Isolation systems must have a sufficiently high initial stiffness to avoid undesirable motion due to wind excitation or small seismic events, the first layer of the sliding system is thus designed such that only sufficiently large seismic events will trigger the sliding mechanism. The first layer is designed with the shortest pendulum length as high initial stiffness to control motion during small and medium seismic events is desirable. For large events, a stiff isolation layer is not desirable as higher stiffness will increase the transmission of loads from the ground to the superstructure. At larger forces the second sliding interface will trigger as μ_2 is overcome. This layer is designed with the largest pendulum length to provide the system with a softening effect. At even larger forces the 3rd mechanism will be activated as μ_3 is overcome. This regime's pendulum length is designed with a moderate length such that $L_1 < L_3 < L_2$. This regime continues to soften the overall stiffness of the system until the 2nd mechanism reaches its displacement limit. When the 2nd mechanism reaches its displacement limit the stiffness of the system will sharply increase to constrain displacement. If even larger forces occur the 3rd mechanism will also reach its displacement limit and only mechanism 1 will remain causing stiffness to increase further. The total forces and displacements at which each of these transitions occur is a function of the dish diameter, and produces a stiffness displacement profile equivalent to that shown in Figure 2.8.

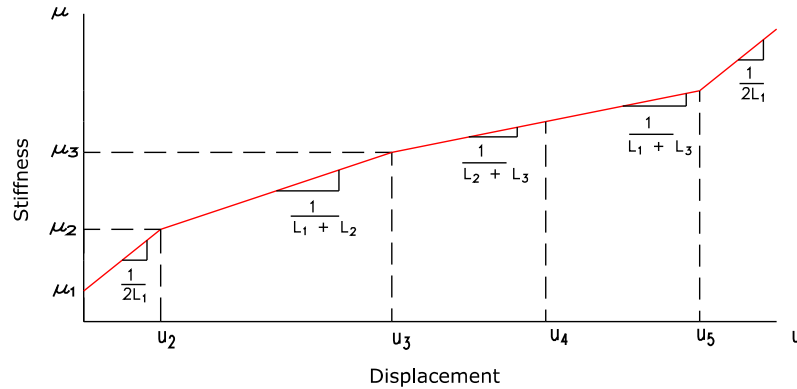


Figure 2.8: Stiffness displacement profile of TFP

2.2.2 Elastomeric Isolators

Elastomeric isolators are primarily large rubber bearings. The rubber has a relatively low lateral stiffness which elongates the fundamental period of the structure. The properties of the rubber allow it to experience large recoverable strains which allow it to withstand cyclical loading and deformation without lasting damage or residual displacement. However, unconstrained rubber bearings have a vertical stiffness similar to its lateral stiffness and will undergo large vertical deformations during seismic events due to the vertical component of the ground motion. This was a significant issue for the first building designed with such bearings, an elementary school in Skopje Macedonia, as during an earthquake the structure experienced significant rocking and bouncing which mitigated the usefulness of base isolation [29]. To mitigate this deficiency, reinforcement was added to the isolator to improve the vertical stiffness preventing large vertical displacements and rocking. The elastomer employed in the bearings is effectively incompressible, as such any vertical deformations result in lateral bulging of the bearing as shown in Figure 2.9 a).

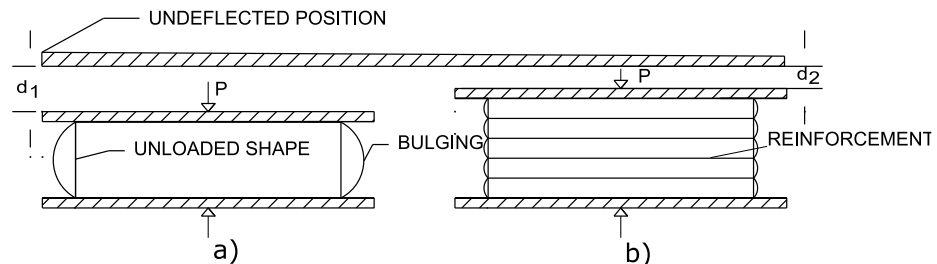


Figure 2.9: Lateral bulging: a) unreinforced b) with reinforcement

Adding horizontal layers of reinforcement in the form of steel plates or fiber layers distributed through the bearing allows for layers of the elastomer to be bonded to the reinforcement which restricts the ability of the bearings to laterally bulge when a vertical load is applied, as shown in Figure 2.9 b). Steel is the most common reinforcement used and this type of elastomeric isolator is known as a steel-reinforced elastomeric isolator (SREI). Due to the incompressible nature of the elastomer the lateral bulging restraint provided by the reinforcement results in a vertical stiffness several orders of magnitude greater than the lateral stiffness [49]. The addition of reinforcement does not result in substantial increases in the lateral stiffness of the isolators. It was demonstrated

that the ratio of the plan area to the perimeter area of an elastomeric layer does not substantially influence the lateral stiffness of the bearing, while the ratio of the bearing width to the total thickness of elastomer layers proved much more influential [50]. In the simplest case, the lateral stiffness of elastomeric isolators, k_H , is given by:

$$k_H = \frac{GA}{T_r} \tag{2.6}$$

where G is the shear modulus, A is the contact area and T_r is the total thickness of the elastomer layers. From equation (2.6), the lateral stiffness of an elastomeric bearing is directly proportional to its contact area and inversely proportional to the total thickness of the elastomeric layers. Additionally, the lateral stiffness is inversely influenced by the applied axial compressive load, where increases in the compressive load leads to reductions in lateral stiffness and in extreme cases may cause buckling to manifest [51].

Another type of elastomeric isolator is the fiber-reinforced elastomeric isolator (FREI). This isolator was conceived as a method to reduce the weight of individual isolator units by replacing heavy steel reinforcement plates with much lighter fiber meshes capable of restraining lateral bulging to a similar degree. In addition, it was theorized the cost could also be substantially reduced by cutting large pads into smaller isolator units during fabrication [52]. A notable difference between SREIs and FREIs is the lack of flexural rigidity provided by the fiber reinforcement [53]. A variant of the FREI is known as the unbonded fiber-reinforced elastomeric isolator (UFREI) which is not fixed to the foundation or overlying superstructure. The friction between the bearing and its supports is generally sufficient to prevent slip, however, if the vertical compressive stress is low and lateral loads are sufficiently high slip may still occur under these conditions [54]. This particular design further improves the economic feasibility by eliminating the requirement for custom mechanically fastened connections between the bearing and its supports used in bonded elastomeric bearings.

Due to the lack of fastened connections and flexibility of the fiber reinforcement, UFREIs develop adaptive stiffness characteristics. This means that depending on the intensity of shaking the lateral stiffness of the bearing will vary to achieve better structural performance. The initial stiffness of the bearing is sufficient to prevent unwanted motion due to wind loads and smaller seismic events. During a large seismic event the bearing will begin to displace following a linear stiffness profile as shown in Figure 2.10 a). If displacement continues a softening regime begins, which allows the structure to undergo large displacements while transmitting relatively low forces to the overlying structure during moderate to severe seismic events. The change in stiffness is caused by the bearing reducing its effective plan area as the initial contact surfaces lose contact with the supports as shown in Figure 2.10 b). This loss of contact area is a phenomenon known as rollover, which is a desirable characteristic of FREIs.

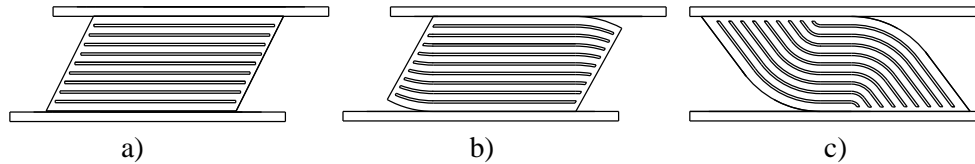


Figure 2.10: Rollover deformation: a) linear displacement b) partial rollover c) full rollover

At higher displacements the stiffness of the bearing increases as the bearing completes its roll-over action and the initially vertical faces of the bearing contact the supports as shown in Figure 2.10 c). This sharply increases the shear resistance of the isolator which constrains the maximum displacement of the structure and prevents dangerously large displacements from occurring during exceptionally large seismic events.

The properties of elastomeric isolators will vary over time due to aging and exposure. Aging has a variety of sources such as light, temperature, ozone and other environmental effects [55]. Tests on the properties of aged elastomeric bearings indicate that the stiffness and damping properties of the bearing had increased while the vertical stiffness had decreased. As a result, the design of structures utilizing elastomeric bearings should consider the aged and unaged conditions of the bearings.

2.3 Base Isolated Structures

While the vast majority of structures in regions of high seismicity are constructed using traditional fixed foundations base isolation is gaining notoriety due to its demonstrated efficacy at preventing damage [28]. Several isolated structures have been subjected to earthquakes in the past decades and in each case if the system was properly detailed the structure performed very well. This however, was not the case for several nearby traditionally designed structures that were significantly damaged. While any sort of damage is unfortunate the contrast between the performance of isolated and fixed base structures provides engineers and designers with a proof of concept that may in the future result in isolation becoming a prominent or even dominant method of design in regions of high seismicity.

2.3.1 Examples of Isolated Structure Performance

In 1990 there were between 102-125 structures designed with a base isolation system [56]. 20 years later it was estimated that the number of base isolated structures exceeded 10,000 with the vast majority being within Japan and China [28]. A sharp rise in the construction of isolated structures has occurred over the last decades as the response of real isolated structures has served to validate the theoretical benefits of isolation. The performance of isolated structures also extends to preventing nonstructural damage by substantially reducing interstorey drifts and floor accelerations [57]. The relative performance gap between isolated and fixed base structures was more significant for shorter than taller structures, which is in agreement with the theory presented in section 2.1.3. Examples of isolated structures performing well during seismic events include the 1988 East Tokyo Earthquake [56], the 1994 Northridge earthquake [58, 59], the 1995 Kobe Earthquake [60] and the 2011 Christchurch earthquake [61]. The East Tokyo earthquake provides a case study of the performance of isolated structures during real seismic events. The isolated

structure experienced about 50% lower accelerations, and much lower interstorey drifts compared to fixed base models and nearby structures. Northridge, Kobe and Christchurch provided further examples where in each case significant damage causing billions in damage in each was inflicted upon the local area, however, in each case the isolated structures escaped without damage and were ready for operation immediately afterwards.

2.3.2 Economics of Base Isolation

Due to economic constraints base isolation is more readily used on larger structures than smaller residencies due to the lower proportional cost of the isolation system. Due to the superior performance of isolation of large structures research has been conducted to evaluate and increase the economic viability of isolating small and moderately sized structures. When the same level of seismic performance of a structure is required from a fixed base and an isolated structure, isolation generally offers a more economically design option in all cases [51]. This observation is due to the reality that the level of performance and damage prevention provided by base isolation is extremely costly to achieve through traditional fixed base design methods, as the reinforcement required to ensure an elastic structural response would be prohibitively costly [62]. Armenia, despite being a developing country, has been one of the most enthusiastic adopters of base isolation with the 2nd highest number of isolated structures per capita, only surpassed by Japan [28]. One of the explanations of this supposed anomaly is due to the cost savings that have been seen for structures adopting base isolation. Isolation allows the superstructure to remain elastic and thus the substantial material reinforcement and seismic detail typically required for fixed base structures is substantially reduced, resulting in cost savings estimated between 30 - 40%, relative to conventional fixed base structures, without loss of performance [63].

Due to the gap in performance between isolated and fixed base structures, it is often the case that traditionally designed structures, and their contents, can be severely damaged during seismic events as discussed in section 1.1.4. In the case of a strong seismic event the economic loss difference between an isolated and non-isolated structure described in section 1.1.4, would be enough to justify the initial cost of including an isolation system. Methods to reduce the cost of isolation systems have also been investigated to decrease the initial cost and promote adoption. Traditional SREIs can be substituted by elastomeric bearings which can achieve the same level of seismic performance but at a fraction of the cost due to the reduced bearing weight and less expensive manufacturing requirements (e.g., FREIs) [53, 64]. This type of bearing is used in housing in seismically at-risk developing countries to provide structures with a proportionally less expensive system [65]. It is possible to apply the same design methodology to housing elsewhere to achieve cost effective isolation. Additionally, due to the performance of isolated structures, it has been suggested that earthquake insurance may become redundant as the cost of damages is unlikely to exceed the deductible for a base isolated structure [61]. If earthquake insurance were forgone than the initial cost of the isolation system would be recovered within a decade. However, as insurance companies become more aware of base isolation it is likely more favourable premiums will be offered to acknowledge the effectiveness of seismic isolation.

2.3.3 Isolation of Single-Family Residential Structures

The idea of seismically isolating low rise residential structures is not novel, as several single-family homes were constructed using base isolation as far back as 1977 in France [56]. While general advances have been made to improve the viability of base isolation, special attention has also been given to smaller residential structures within the last decades. Shake table testing of a model 1-storey base isolated wood frame, and a 2-storey base isolated masonry building were conducted to evaluate the efficacy of isolation of single-family residential structures. The performance was compared to the linear response of fixed base models, and it was concluded that the isolated wood frame and masonry structures experienced a 66% and 74% reduction of peak acceleration, respectively [34]. These results are notable as the reduction of forces is generally larger than the reduction experienced by other larger structures due to the generally lower fixed base period, demonstrating that isolation is not only feasible for smaller structures but is particularly effective.

The development of cost-effective systems has also been of primary interest. A cost-effective design methodology for isolated light frame structures was proposed in [46]. The proposed method involved tailoring the isolation systems to the unique structural characteristics of light frame structures mainly their high stiffness to weight ratio. It was proposed that isolators could be designed to transfer larger forces to the structure to reduce the design displacements of the isolators and thus their size and cost. This method however, also required changes to the design of the superstructures framing to keep interstorey drifts within the damage threshold. The structures were isolated using high friction low-cost bearings and the performance was evaluated for various ground motions. The isolated structures achieved base acceleration reductions as high as 2.7 times for the larger events and around 50% reductions for weaker events which is in alignment with performance of other systems discussed in section 2.3.1.

Investigations were conducted in California to produce a cost effective base isolated single family residential structure. The cost of the structure was estimated at 400,000 USD while the isolation system would cost only 15,000 USD, less than 4% of the total construction cost [66, 67]. This figure is in agreement with the cost estimates made for cost effective isolators, that were estimated as costing hundreds of dollars per unit [64, 46], and the number of isolators utilized in the designs of the isolated single family residential structures tested in other studies [34, 46]. The cost of isolation systems will vary depending on the design and local seismic hazard, but the cost of the isolation system relative to the structural value is of key interest. Insurance deductibles in British Columbia typically range between 5 – 20% of the value of the structure [68], meaning that only damage exceeding that proportional cost will be covered by earthquake insurance. It may be the case that the cost of the isolation system is lower than the deductible of earthquake insurance. Since it is well established that isolated structures will experience minimal, if any damage during seismic events, earthquake insurance could feasibly be abandoned in favour of more cost-effective isolation systems. This would protect the structure and save the owner the cost of the deductible payment, as well as annual premium costs. Base isolation also has the advantage of insulating owners from more moderate damages caused by smaller but more common events that could cause damage below the deductible threshold. Designing structures with isolation systems could thus be a more economically sound option than traditional earthquake insurance, especially in areas with high deductibles and premium rates.

CHAPTER 3

REVIEW OF EXISTING BASE ISOLATION STANDARDS

3.1 NBCC

The National Building Code of Canada provides a general standard regarding the requirements for seismic design in Canada [6]. The NBCC contains two sections of interest when investigating the stability of structures under seismic loads: Part 9 Housing and Small Buildings, and Part 4 Structural Design. Part 9 applies exclusively to buildings with total areas of 600m² or less and 3 storeys or less in height, while Part 4 requires engineering analysis but can be used for all buildings. Part 9 relies on a prescriptive design methodology to ensure sufficient structural resistance is provided to maintain stability. While this is sufficient for the design of the superstructure it fails to provide any clear instruction regarding the use of base isolation systems for structures that Part 9 applies to. It is thus necessary to utilize the requirements presented in Part 4 when designing low rise residential structures with base isolation systems.

3.1.1 Fixed Base Structures

Fixed base structures constitute the overwhelming majority of the structures detailed for seismic resistance, thus many of the standards regarding base isolation are either adapted from, or used to augment, existing fixed base standards. Part 4 offers two main methods of analysis, the dynamic analysis procedure (DAP) and the equivalent static force (ESF) procedure. The DAP involves the use of modelling software to investigate the dynamic response of the structure by subjecting the structure to earthquake time history records. This method is complicated and time intensive, thus the 2015 NBCC also provides the simplified ESF procedure which can be used for certain types of structures in regions of low seismic hazard. Clause 4.1.8.7 describes the conditions that must be met for application of the ESF procedure. The conditions are as follows:

1. The design spectral acceleration, $S_a(T)$, at a period of 0.2s is constrained such that:
$$I_E F_a S_a(0.2) < 0.35$$

I_E : Importance factor
 F_a : Site coefficient
2. Or, the structure is classified as regular as per clause 4.1.8.6 and is less than 60 m in height with a fundamental lateral period, T_a , less than 2 s in each of two orthogonal directions as defined in clause 4.1.8.8
3. Or, the structure contains an irregularity of Type 1, 2, 3, 4, 5, 6 or 8 as defined in Table 4.1.8.6, and is less than 20 m in height with a fundamental lateral period, T_a , less than 0.5 s in each of two orthogonal directions as defined in clause 4.1.8.8

Requirement 1 is a restriction of the level of ground motion a structure may experience, as the approximations inherent in the ESFP are unlikely to have serious consequences for the relatively low ground motions. Requirements 2 and 3 ensure that the structure's response is dominated by the 1st mode and can thus be analyzed more easily by static methods. The shorter period required for structures with irregularities is to reflect that those irregularities have a minimal effect on the dynamic response of short-period structures. However, torsional irregularities are still restricted in all cases as large rotations can occur regardless of the fundamental period.

Both the dynamic and simplified analysis methods can be used to determine important design parameters such as the force and moment distributions, and the maximum displacements and interstorey drifts. The site-specific response spectrum required by the NBCC presents the ground motion accelerations that a structure will experience. The spectral response acceleration is based on the fundamental period of the structure, and the probable seismic hazard at the site.

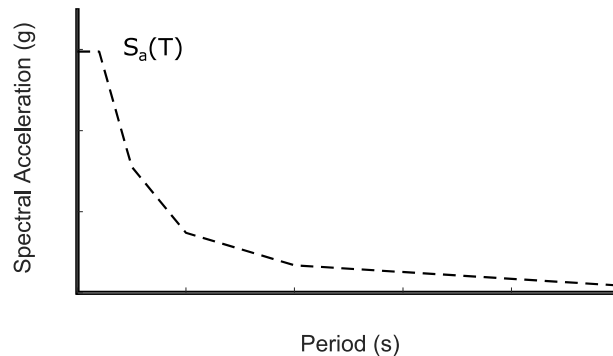


Figure 3.1: Acceleration response spectrum

The NBCC provides values of $S_a(T)$ at periods of 0.2 s, 0.5 s, 1.0 s, 2.0 s, 5.0 s and 10.0 s. For intermediate periods interpolation is employed to determine the design spectral acceleration. The ground motions are then scaled based on the local site soil conditions. The values of $S_a(T)$ provided by the NBCC are derived using seismic hazard analysis techniques which investigate the probability that a structure at a specific site will experience a specific level of ground shaking. The NBCC utilizes a uniform probability of exceedance for all regions across Canada, which allows for each location to be designed for the same level of hazard. The design probability of experiencing a certain level of ground motion is a 2% chance of exceedance in 50 years. The design response spectrum can be used to determine the design response acceleration in the ELF procedure to select earthquake time history records for use in a detailed dynamic analysis.

3.1.2 Seismic Force Resisting Systems and Capacity Based Design

Regardless of the method of analysis a structure must be designed with a dedicated seismic force resisting system (SFRS) specifically designed to resist and dissipate seismic forces while maintaining the overall structural stability. Generally, it is uneconomical to design fixed base structures to remain undamaged, as the cost of reinforcing a structure to resist seismic forces elastically would make most structures prohibitively expensive to construct. To control costs and ensure adequate seismic performance SFRSs are detailed to allow for a level of ductile action to occur within a structure. This ductile action is controlled by detailing certain sections of the

structure to remain undamaged while others deform and dissipate energy in a controlled manner such that overall stability is maintained. To account for the ductility the NBCC ascribes a ductility factor, R_d , and an overstrength factor, R_o , to a SFRS, such that the forces the system is designed to withstand are reduced by a factor of $R_d R_o$ [69]. This method of design is known as capacity-based design, and it allows structures to undergo substantial plastic deformation and dissipate much of the energy imparted to the structure during seismic excitation. This method, while able to control the response by ensuring plastic deformation occurs under control, leads to substantial plastic deformation within the structure requiring extensive repairs after experiencing large seismic forces.

3.1.3 NBCC Base Isolation Provisions

Part 4 of the NBCC, unlike for fixed base structures, does not present a simplified method of analysis for base isolated structures and instead requires that a detailed non-linear dynamic analysis be conducted to investigate the structural response. Clause 4.1.8.20 of the NBCC also provides several prescriptive requirements to ensure the base isolated structure performs as intended. The main requirements of note are [6]:

1. The period of the isolated structure shall be greater than three times the fixed base period.
2. The isolation system shall produce a restoring force to prevent residual displacements.
3. The stiffness and damping characteristics of the isolation system must be validated by testing at least two full-size specimens of each predominant type and size of isolator, and a representative sample of the isolator units to be installed shall be validated by tests prior to their installation.
4. A lateral load carrying diaphragm, or lateral structural elements located above the isolation interface shall transmit forces due to non-uniform ground motions from one part of the structure to another.
5. The isolation system shall limit lateral displacement due to wind loads across the isolation interface to a value equal to $1/500$ the least storey height.
6. All structural framing elements shall be designed for the forces where $R_d R_o = 1.0$, such that they will remain elastic, and the SFRSs shall be detailed to meet $R_d \geq 1.5$.

The requirement of an elongated isolated period is to promote a first mode dominant response of the seismically isolated structure. Unlike the items 1 - 5, item 6 applies specifically to the analysis and design of the superstructure. The superstructure of a base isolated structure is expected to remain undamaged during a seismic event, this is reflected by the requirement that the superstructure be designed without force reduction allowed through ductile action. While the frame is designed to resist elastic loads pertaining to $R_d R_o = 1.0$, the structure must still be detailed for a level of ductile behaviour to prevent collapse in the event of inelastic deformation.

The requirements the NBCC provides for base isolated structures require significant testing and validation of the finished isolator units, and the expertise of an engineer with knowledge of both dynamic modelling and base isolation design. The detailed testing and analysis requirements provided are reasonable for large dynamically complex structures, as the performance of such structures cannot be simplified adequately, however, they may prove unnecessary for structures whose behavior is more easily predicted.

3.2 ASCE Base Isolation Provisions

While the NBCC does not currently provide significant guidance on the design of base isolated structures, ASCE standards contain a suite of potential analysis and design methods for both fixed base and isolated structures. ASCE 7-16 Minimum Design Loads and Associated Criteria for Buildings and Other Structures [42] contains several chapters with similar provisions to those outlined in Part 4 of the NBCC. ASCE 7-16 provides both a detailed dynamic analysis method and a simplified method for both fixed-base, and base isolated structures. As the NBCC does not provide a simplified method of analysis, it is possible to adapt the simplified base isolation analysis methods provided in ASCE 7-16 Chapter 17 to be compliant with the requirements given in the NBCC. While the NBCC and ASCE standards use similar methods to calculate the seismic response of structures there are several notable key differences that must be considered to adapt ASCE methods for use in Canada.

3.2.1 Response Spectrum

To evaluate the loads experienced by a structure from a seismic event, ASCE 7-16 utilizes a response spectrum similar to that constructed in the NBCC. ASCE develops the response spectrum by employing a piecewise function to describe the spectral acceleration for different period ranges such that:

$$S_a = \begin{cases} S_{DS} \left(0.4 + 0.6 \frac{T}{T_0} \right) & 0 \leq T \leq T_0 \\ S_{DS} & T_0 \leq T \leq T_s \\ \frac{S_{D1}}{T} & T_s \leq T \leq T_L \\ \frac{S_{D1} T_L}{T^2} & T_L \leq T \end{cases} \quad (3.1)$$

S_{DS} : Design earthquake spectral response at short periods

S_{D1} : Design earthquake spectral response at 1s periods

T_0 : $0.2S_{D1}/S_{DS}$

T_s : S_{D1}/S_{DS}

T_L : Long period translation period

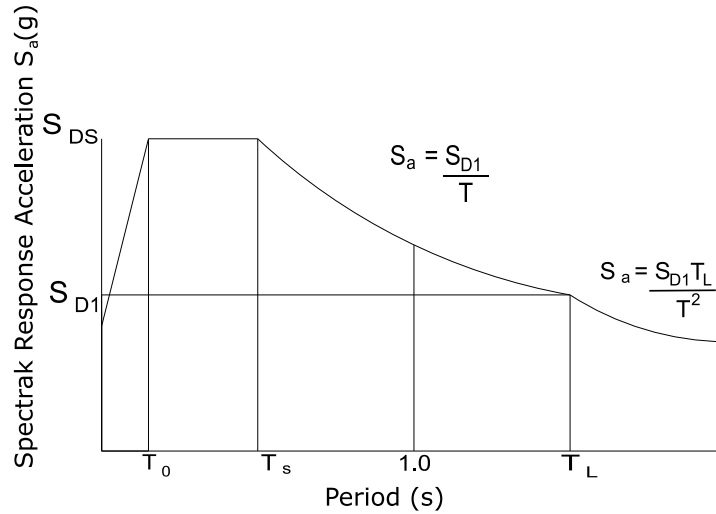


Figure 3.2: ASCE 7-16 design response spectrum [42]

While the ground motions for a specific site are obtained by similar hazard analysis techniques the construction of the response spectrum is significantly different than that presented in the NBCC. The period range between T_0 and T_s represents the constant acceleration range, while the range between T_s and T_L represents the constant velocity range. For periods longer than T_L , $S_a(T)$ is a function of assumed constant displacement.

3.2.2 Analysis Methods

The fixed base and base isolated methods presented in ASCE are designed to calculate the same key performance parameters (e.g., the distribution of forces and maximum displacements) as the methods presented in the NBCC. The equivalent lateral force procedure is the simplest method presented in Chapter 12 as it does not require detailed modelling. The Chapter 12 ELF procedure can be utilized for fixed base structures similar to the NBCCs ESF procedure. This method was further adapted in Chapter 17 to analyze base isolated structures as well. To ensure the results produced by this procedure will be representative of the real seismic base isolated response the following criteria are imposed:

1. The structure is located on a Site class A, B, C, or D
2. The effective period of the isolated structure at the maximum displacement is less than or equal to 5.0 s.
3. The structure above the isolator interface is less than or equal to 19.8 m in height
4. The effective damping of the isolation system at the maximum displacement is less than or equal to 30%

5. The effective period of the isolated structure is greater than three times the elastic fixed base structure above the isolation system
6. The structure above the isolation system does not have any structural irregularities as defined in section 17.2.2
7. The isolation system meets the following requirements:
 - a. The effective stiffness of the isolation system at the maximum displacement is greater than $\frac{1}{3}$ of the effective stiffness at 20% of the maximum displacement
 - b. The isolation system is capable of producing a restoring force
 - c. The isolation system does not limit the maximum displacement to less than the total maximum displacement D_{TM}

The ELF procedure is based on the assumption that the structure will be dominated by the isolation mode (i.e., displacements concentrated at the isolation layer). The conditions of applicability listed above are to ensure that the dynamic performance of the structure matches the assumptions of the ELF procedure, as the equations used in the ELF procedure determine the loadings independent of the dynamic influence of higher modes. The maximum period and damping restrictions not found in the NBCC ensure conservative estimates, as some formulas are unconservative at high levels of damping and long isolation periods [70].

3.3 Base Isolation Standards Overview

The NBCC contains two main areas of interest in regards to the seismic design of an isolated structure: Part 9, which details the prescriptive requirements used to ensure the strength of typical low rise residential structures, and Part 4 which contains provisions regarding more detailed seismic analysis. Part 9, while sufficient to ensure adequate life safety performance of low rise residential structures, does not provide direction regarding base isolation or more detailed seismic design. Part 4 provides several methods of analysis including the simplified equivalent static force procedure for fixed base structures. Part 4 provides design requirements for base isolated structures, but due to the lack of a simplified method of analysis and expense of the mandated dynamic analysis and testing, research is required to develop an economical base isolation design methodology for low rise residential structures. ASCE 7-16 contains several sections regarding seismic design of structures, with Chapter 17 being entirely dedicated to the analysis and design of base isolated structures. Chapter 17 includes the equivalent lateral force procedure which is a simplified method of analysis for base isolated structures.

Notable commonalities include the analysis of the structure based on a 1st mode dominated response, and the provisions included to ensure 1st mode dominance. While the theory behind the NBCC and ASCE methodologies and requirements are the same, some component of the analysis differ. Most of the differences between the NBCC and ASCE requirements are prescriptive,

however, the most prominent variation is the construction of the response spectrum. The NBCCs response spectrum is developed via uniform hazard points with linear interpolation, while ASCE constructs its response spectrum based on a piecewise equation with assumed trends. It is thus proposed that the simplified ASCE procedure be adapted to comply with the NBCCs standards for inclusion in Part 9.

CHAPTER 4

ADAPTION OF ASCE ELF PROCEDURE TO NBCC PART 9

4.1 Method of Analysis

The NBCC currently does not provide a simplified method of analyzing base isolated structures. Additionally, the design of isolated structures requires a costly and complex dynamic analysis to be employed to analyze the performance of the base isolated structure regardless of the dimensions and properties of the superstructure. The ASCE provides a simplified method of analyzing base isolated structures which recognizes that certain structures can be analyzed by simpler means. The ELF procedure provided in ASCE 7-16 is in agreement with current structural dynamics theory and can thus be adapted to comply with the NBCC and used to analyze certain types of base isolated low rise residential structures in Canada.

4.1.1 Key Parameters

The analysis of a structure requires several parameters to be extracted to ensure the performance of the structure is desirable. These parameters of interest are:

D_M : Maximum translational displacement of the center of rigidity of the isolator system

D_{TM} : Total maximum displacement of isolator units, including torsional amplification

T_M : The fundamental period of the isolated structure at D_M

V_b : Lateral forces below the isolation layer (foundation)

V_{si} : Total seismic shear within the elements above the isolator layer (ground level)

F_x : Vertical distribution of forces in the superstructure at the x^{th} level

n : Number of isolators used in the isolation layer design

$X_i Y_i$: Plan coordinates of the i^{th} isolator unit

Δ_k : Interstorey drift of storey k

a_x : Floor acceleration of the x^{th} floor

4.1.2 Inputs

The ELF procedure is a simplified analysis method, and thus the required inputs are also deliberately minimized to promote accessibility. The required parameters for analysis are:

1. The height distribution
2. The vertical mass distribution of the structure
3. The damping, $\zeta_M(D_M)$, and stiffness, $k_M(D_M)$, as a function of isolator displacement
4. The fundamental period of the fixed base structure, T_{fb}

4.2 Equivalent Lateral Force Procedure Equations and Adaption

The equations derived for the ELF procedure are generally based on the dynamic concepts of the performance of base isolated structures. While the requirements and code provisions for the ELF procedure have been discussed in sections 3.1.1 and 3.2.2 it is important to discuss additional concepts that are more appropriately discussed alongside the equations.

4.2.1 Maximum Displacement

To calculate D_M an expression is given in the ELF procedure such that:

$$D_M = \frac{S_{M1}gT_M}{4\pi^2B_M} \quad (4.1)$$

where:

g : The acceleration caused by gravity,

T_M : The effective period of the seismically isolated structure at the maximum displacement

S_{M1} : The 5% damping spectral acceleration parameter at a 1.0 s period

B_M : The numerical coefficient correcting for the effective damping of the isolation system

Equation (4.1) is developed for the ELF procedure by modifying the fundamental dynamic equation which relates the seismic displacement response of a structure to the pseudo acceleration. The factor B_M accounts for higher or lower levels of damping provided by the isolator system relative to the commonly assumed 5%. To adapt equation (4.1) to the requirements of the NBCC the input from ASCE's response spectrum must be replaced by the equivalent inputs of the NBCCs response spectrum. The variable S_M from the ASCE response spectrum will be replaced by $S_a(T_M)$ as determined by the NBCC response spectrum producing:

$$D_M = \frac{S_a(T_M)gT_M^2}{4\pi^2B_{Mj}} \quad (4.2)$$

4.2.2 Effective Isolated Period

The effective period of an isolated structure is a product of the instantaneous properties of the isolated structure. Since the stiffness of isolators varies nonlinearly with displacement the period at the maximum structural displacement, T_M is of particular interest. To determine T_M the ELF procedure uses:

$$T_M = 2\pi \sqrt{\frac{W}{k_M n g}} \quad (4.3)$$

where W is the effective seismic weight of the superstructure above the isolation layer, and k_M is the effective isolator stiffness at D_M . As previously mentioned, D_M must be determined by an

iterative process, and the same process is required to determine T_M . As shown in equation (4.2) D_M is dependent on T_M , and T_M is dependent on k_M which is a function of D_M .

4.2.3 Total Maximum Displacement of Isolator Units

D_{TM} is a combination of D_M and the amplifying effect of actual and accidental torsion. D_{TM} refers to the maximum displacement of an individual component of the isolator system and thus can be used to evaluate the most extreme displacement of any component of the system at the isolation layer. The equation to determine D_{TM} is given as:

$$D_{TM} = D_M \left[1 + \left(\frac{1}{P_T^2} \right) \frac{ye}{r^2} \right] > 1.15D_M \quad (4.4)$$

where:

- y: the distance between the centers of rigidity of the isolation system and the element of interest measured perpendicular to direction of loading;
- e: the structural eccentricity including accidental eccentricity

$$e = \left[(CR_x - CM_x)^2 + (CR_y - CM_y)^2 \right]^{\frac{1}{2}} + 0.1D_n \quad (4.5)$$

$CR_{x,y}$: the center of rigidity X and Y coordinates;

$CM_{x,y}$: the center of mass X and Y coordinates;

D_p : the longest plan dimension of the structure perpendicular to the direction of loading;

r: the radius of gyration;

P_T : the ratio of the effective translational period of the isolation system to the effective torsional period of the isolation system.

Accidental eccentricity accounts for the likelihood that CM and CR will deviate from the calculated values due to unintended irregularities in the mass or rigidity of the structure [71]. Equation (4.4) is the result of modifications to the approximation of D_{TM} which was derived from the modal analysis of a simplified base isolated structure with 3 degrees of freedom, 2 lateral and 1 rotational at the isolation layer [51]. For equation (4.4) to be conservative the rotational and translational modes must be well separated [51].

The P_T term in equation (4.4) accounts for torsional stiffness and torsional damping by applying a factor of $1/P_T^2$, where P_T is given as:

$$P_T = \frac{1}{r_1} \sqrt{\frac{\sum_{i=1}^n (x_i^2 + y_i^2)}{n}} \quad [72] \quad (4.6)$$

X_i, Y_i = lateral distance from the center of mass to the i^{th} isolator unit;

n = number of isolator units;

For $\omega_\theta > \omega_0$ P_T will be greater than 1 and the torsional component of displacement will be suppressed due to the relatively torsional higher stiffness and damping compared to the translational

stiffness and damping. Equation (4.6) is based on an approximation that has an error that approaches zero as the eccentricity between the center of mass and center of rigidity diminishes, thus it is required that the eccentricity of the isolation system be minimized [72]. The ASCE ELF procedure does not consider torsion caused by local stiffness variations as it is assumed that the lateral stiffness of bearings will be homogenous regardless of direction of loading.

4.2.4 Vertical Distribution of Forces

The maximum shear force within an isolated structure will occur at the foundation. The same is generally true for fixed base structures as the forces generated by inertia are transferred through the superstructure to the foundation. The ELF procedure provides the equation to determine the base shear, V_b as:

$$V_b = k_M D_M \quad (4.7)$$

The ELF procedure recognizes that the sum of the lateral forces within the superstructure will be transferred to the foundation through the isolation layer. The total lateral forces to be distributed over the height of the superstructure, V_s is given as:

$$V_s = \frac{V_{st}}{R_1} \quad (4.8)$$

$$V_{st} = V_b \left(\frac{W_s}{W} \right)^{(1-2.5\zeta_M)} \quad (4.9)$$

where:

R_1 : the numerical coefficient related to the type of SFRS

W : the effective seismic weight of the structure above the isolation interface

W_s : the effective seismic weight of the structure above the isolation interface excluding the base level

ζ_M : the effective damping of the isolation system at the displacement D_M .

The sum of lateral forces distributed over the superstructure above the isolation layer are not equivalent to V_b . The reduction of V_b to V_{st} presented in equation (4.9) is to account for the often-significant inertial forces caused by a concentration of mass at the base level. The base inertial forces significantly influence V_b but have a reduced effect on the overall force distribution. The factor R_1 presented in equation (4.8) fulfils a similar purpose to the $R_d R_o$ factor within the NBCC, however, the NBCC does not allow any reduction due to ductility to occur to ensure elastic behavior of the superstructure and thus equation (4.8) can be simplified to:

$$V_s = V_b \left(\frac{W_s}{W} \right)^{(1-2.5\zeta_M)} \quad (4.10)$$

The force distribution method proposed by the ELF procedure is referred to as a k distribution (not to be confused with the variable k used to represent the storey) such that:

$$F_x = C_{vx} V_s \quad (4.11)$$

$$C_{vx} = \frac{w_x h_x^k}{\sum_{i=2}^n w_i h_i^k} \quad (4.12)$$

$$k = 14 \zeta_M T_{fb} \quad (4.13)$$

where:

F_x : lateral seismic force at level x , $x > 1$;

C_{vx} : vertical distribution factor;

w_i w_x : portion of W_s located at level i or x ;

h_i h_x : height above the isolation interface of level i or x ;

T_{fb} : fundamental period of the structure above the isolation interface.

The lateral seismic force at the base level/ground floor, F_1 , is determined separately as:

$$F_1 = V_b - V_s \quad (4.14)$$

The k parameter represents the curvature of the force distribution with $k = 0$ representing a uniform distribution and $k = 1$ representing a linear distribution. For substantially long periods and high values of damping the k values will become large and will result in unconservative results [70]. As mentioned in section 3.2.2, the maximum values of T_{fb} and effective damping are restricted to prevent this. The linear distribution represented by $k = 1$ is in line with the response expected of a 1st mode dominated fixed base structure, while the uniform distribution represented by $k = 0$ conforms to the response expected of a 1st mode dominated isolated structure. The assumption of perfectly uniform behavior is only valid for structures when the isolation system responds linearly and the isolation period is well separated from the superstructure period [70, 51]. High damping systems tend to exhibit nonlinear behavior which has been shown to excite higher modes of response which can increase the forces in higher stories relative to the base shear [73]. To avoid conservatively applying a linear distribution to the structure above the isolation layer the k distribution applies a nonlinear force distribution to account for higher mode contributions that are expected for various levels of damping and the fundamental period length.

CHAPTER 5

ONLINE RESOURCE METHODOLOGY

5.1 The Online Resource

The ASCE equations presented and adapted for use with the NBCC require an iterative design process to determine several key structural characteristics such as T_M , D_M , k_M and ζ_M . To accommodate an iterative design process, it was proposed by [74] to develop a program to use the input parameters described in section 4.1.2, to produce the key outputs outlined in section 4.1.1. The Government of Canada provides an online tool to generate the design response spectrum for any given location in Canada [75], and it was proposed that the developed program could be made available in a similar method for ease of use.

The online resource methodology is similar to the prescriptive design methodology utilized in Part 9 of the NBCC, as both methods eliminate the need for in-depth engineering. It is desirable to align the online resource closely with Part 9 as base isolation is intended to augment the performance of structures already designed to achieve sufficient life safety performance. The combination of a superstructure designed according to Part 9 of the NBCC and an isolation system designed by the online program will remove the need for custom seismic engineering. To further reduce costs and improve ease of use, it was proposed that the properties of the isolator used in the design program be from pre-approved and tested isolators designed for Part 9 structures. The program method was developed using MATLAB [76]. The full program is available upon request to the author or primary supervisor

5.1.1 Existing Capabilities

The program described by [74] has seen development mainly around establishing a baseline program capable of analyzing rudimentary base isolated structures by adapting the ELF procedure to NBCC requirements. The baseline program was developed with only the simplest structures and responses in mind to validate the process. Substantial additions to the existing program were required to expand its capabilities and enable the analysis of more complex structures. Before discussing the expanded capabilities of the new program, the capabilities and limitations of the baseline program developed by [74] are discussed. The baseline program produces several of the parameters listed in section 4.1.1, such as:

1. The determination the number of isolators required to support the gravity loads
2. The ability to solve through iteration the design values of D_M , k_M , ζ_M and T_M
3. The design response spectrum acceleration $S_d(T_M)$
4. The vertical force distribution

In addition, the design is checked for compliance with the ASCE and NBCC requirements, and a comparison between the expected performance of the isolated structure and the fixed base structure is provided. The full details of the existing baseline program are discussed in more detail in Appendix A.

5.2 Deficiencies Requiring Further Development

5.2.1 Structural Geometry

The structural geometry currently considered by the existing program is limited to structures with rectangular plan areas for each storey, where storey heights and plan areas are uniform across the structure. Many Canadian structures have geometries that cannot be idealized as rectangular or uniform across their height. Work must therefore be done to expand the applicability of the program to a wider range of structures.

5.2.2 Structural Properties

The current program only considers structures where the mass and stiffness of each storey are equal. This assumption is somewhat acceptable for the idealized structures currently considered by the baseline program, but for structures that are asymmetric in plan area, and contain nonuniform floor plans the assumption is invalid. A more accurate estimation of storey mass and stiffness would allow the vertical force distribution and displacement response of each storey to be determined more accurately.

5.2.3 Torsional Effects

Torsional effects are not considered by the baseline program. Even for idealized structures where the center of mass and center of rigidity overlap, accidental torsion will still result in eccentricity within the structure and cause additional displacements to occur. The effects of torsion can substantially increase the displacement of components of the isolation system by as much as 30% depending on the relative difference in plan dimension lengths [42].

5.2.4 Isolation System Layout

A major output requirement is to provide the user with a design of the isolation system layout capable of both good seismic performance and capable of carrying the gravity loads of the system. The isolation layout must be placed to interface with the existing structural load path conventions, such that a continuous transfer of gravity loads is facilitated. The baseline program analyzes each isolator as supporting an equal axial load within the system, which will not be the case for most structures, and so a means of approximating the axial loads on individual bearings is required.

5.2.5 Site Specific Conditions

Site conditions such as soil and wind loading are currently not evaluated by the baseline program. The program currently assumes site class C soil conditions, however, the effect of soil

conditions on the magnitude of ground shaking can be quite substantial. Both ASCE and the NBCC specify that the isolation system should possess an initial stiffness sufficient to resist the design wind loads which also need to be incorporated.

5.3 Improvements to the Baseline Program

To remedy the deficiencies highlighted in section 5.2 several subprograms were created to improve the applicability of the program, reduce simplifying assumptions, and produce more complete designs. The subprograms are designed to balance accessibility and performance such that the user inputs are restricted to only information that would be readily available to a non-specialist designer. The required information is used to generate approximations of performance close to the structural reality, with minimal simplification or assumptions. The user enters the input variables via spreadsheet which highlights all required data in green. The sequence in which subprograms run is illustrated in Figure 5.1. The function of each subprogram, the required user inputs, and the design choices for each step are discussed.

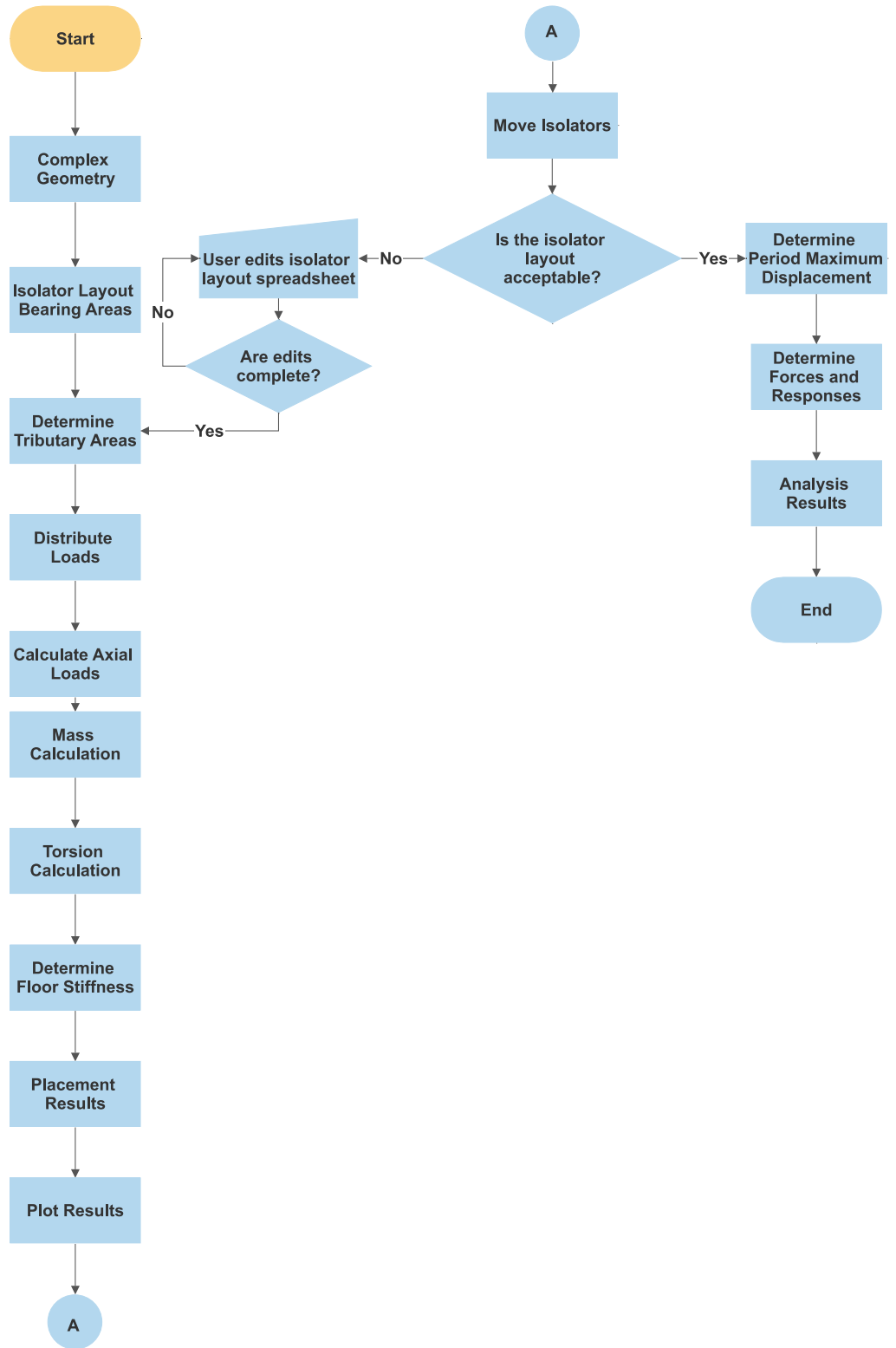


Figure 5.1: Program flow chart

5.3.1 Geometry Inputs and Analysis

The first input by the user is the number of floors of the structure, N . The user then inputs $X1$, $X2$ and $Y1$, $Y2$ which correspond to the dimensions as shown in Figure 5.2 a). For rectangular structures the user inputs $X2$ and $Y2$ as equal to zero. The L-shaped structure is analyzed as oriented in Figure 5.2 a). The user selects values of $X1$, $X2$ and $Y1$, $Y2$ for each storey of the structure. If the perimeter walls of a storey do not overlap fully the user can insert X_{ref} and Y_{ref} to define the geometry of the upper floor with respect to the bottom left corner of the ground floor as shown in Figure 5.2 b). The user is not constrained to one type of floor plan for each storey in the structure. While uncommon, the overlying storey of a rectangular floor plan may be L-shaped as shown in Figure 5.3 a). The reverse is also possible as shown in Figure 5.3 b). A check is performed to ensure the selected plan dimensions do not produce overhangs.

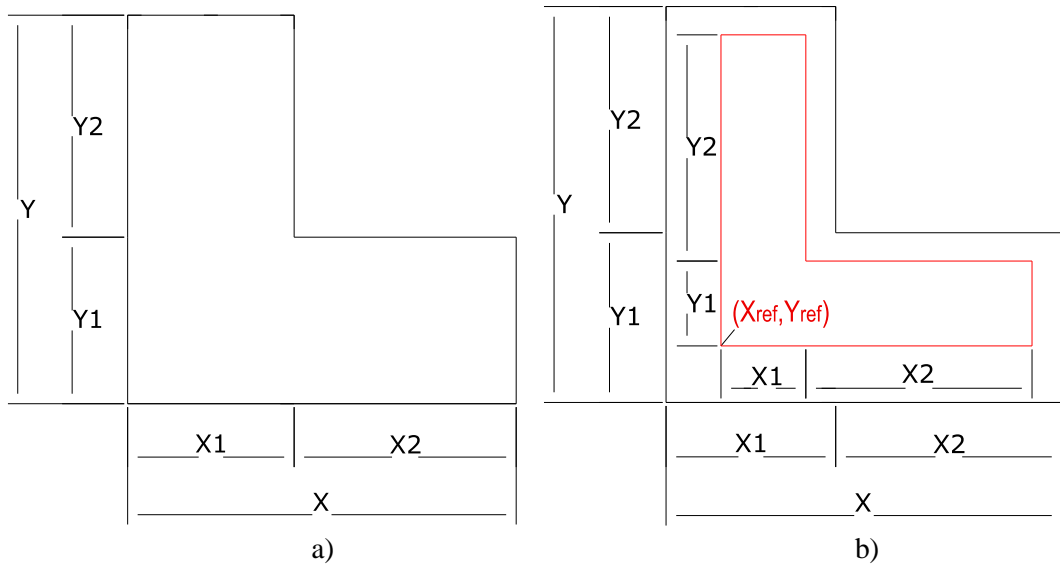


Figure 5.2: Dimensions of floor plan a) with no offset and b) with upper storey offset

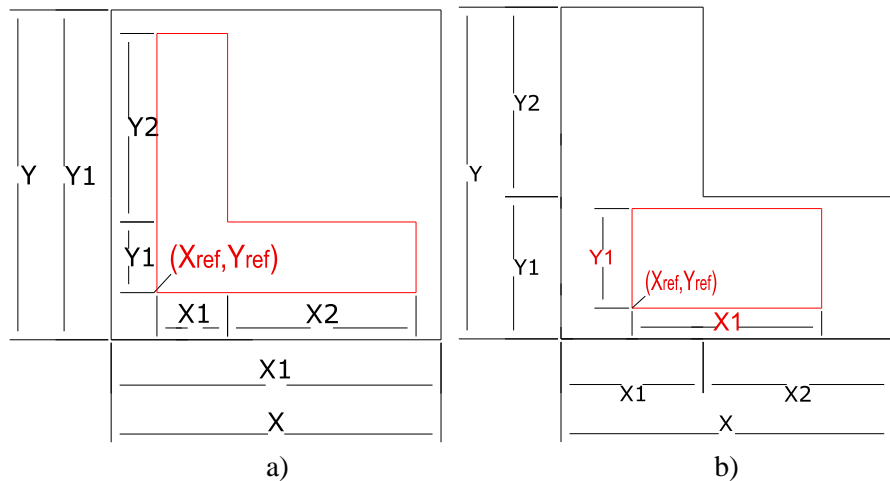


Figure 5.3: Variable floor plan types with a) a rectangular base and b) a L-shaped base

5.3.2 Isolation Layout

One of the challenges with developing a method of design and analysis for base isolated single-family residential structures, is ensuring that the isolator layout is detailed to carry the gravity loads of the structure. In addition, the design should not require substantial changes to the traditional design of the superstructure. Part 9 of the NBCC directs designers to design housing and small buildings in accordance with the practices outlined in the Canadian Wood Council Engineering Design Guide, henceforth referred to as the CWC guide [77]. It is therefore set as a requirement that the isolation system designed by the program should conform with the practices outlined in the CWC guide to ensure load paths are preserved [77].

Requiring the user to define the locations of all gravity walls was deemed too complicated and to require too much input from the user. A more efficient design method is proposed to design the isolator layer based on the design of the ground floor system. The CWC guide outlines that the floor system must be tailored to act as a load path to enable the transfer of gravity loads to the supports of the joist floor system, which must either be structural walls, lintels or beams. In the case of a ground floor system that does not rest directly upon the foundation, such as a structure with a crawl space, the floor system will rest upon floor beams which transfer the loads to piers or posts, typically located at the end nodes of the beams. In the case of an isolated structure a void will be present between the ground floor system and the foundation and the piers or posts that would support a fixed base structure will be replaced by the isolator bearings. The program designs the isolation system with this in mind, where the user highlights the location of the floor beams that support the floor joist spans and the program places bearings at the end nodes to ensure load paths are maintained.

The main concepts are summarized regarding the designation of beam locations for rectangular and L-shaped structures, for a more detailed description see Appendix B.

1. Isolators are placed at the corners of the exterior walls by default.
2. The user defines the location of longitudinal and lateral beams by selecting an X and Y coordinate respectively.
3. The number of beams is limited in either direction due to the realistic number of joist spans expected.
4. For L-shaped structures the user can further alter the beam layout to account for several relevant configurations that may be applicable.
5. The layout of isolators is then produced by assigning coordinates based on the intersection of floor beams.

5.3.3 Determine Tributary Areas

The previous subprograms estimate the placement of isolators such that they interface with the existing gravity loads carrying system of the superstructure. An array of elements for each floor of the structure is generated, such that each element will have a known centroid and a known tributary area assigned to it. The element arrays for each level are produced in descending order from the roof down. The number and size of elements for each level is dependent on the area of each floor plan, and the element size defined by the user. Element size is determined by U , a variable which represents the side length of the square elements the area will be divided into.

For rectangular structures the number of elements is determined by dividing the $X1$ and $Y1$ floor dimensions by U and rounding up to determine $nx1$ and $ny1$, the number of elements in the X and Y directions. Thus the total number of required elements is $nx1 \cdot ny1$. If rounding was required then special rounded elements will be generated at the extreme X and Y ends of the array as shown in Figure 5.4. These rounded elements will have reduced surface areas and side lengths compared to standard U by U elements. The purpose of these elements is to avoid potentially large approximations of the structure's total tributary surface area through excessive rounding.

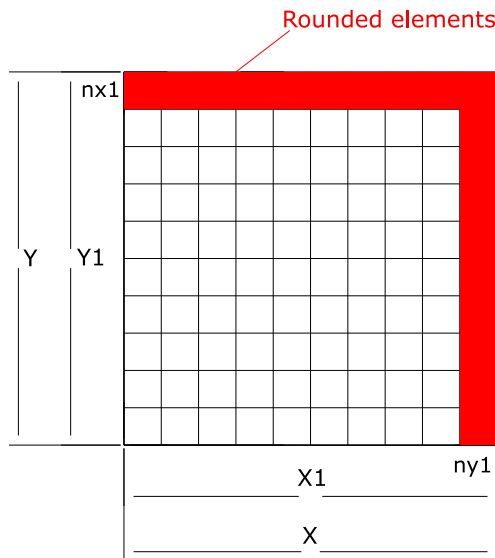


Figure 5.4: Division of structural plan in elements

L-shaped structures are more complicated to analyze as L-shaped structures effectively have 3 sub areas to analyze which correspond to areas A, B and C as defined in Appendix B. The total number of elements required to represent each of the 3 sub areas is determined, and if rounding occurred for the sub areas the rounded elements will be produced at the extreme extents of X and Y for that sub area as illustrated in Figure 5.5.

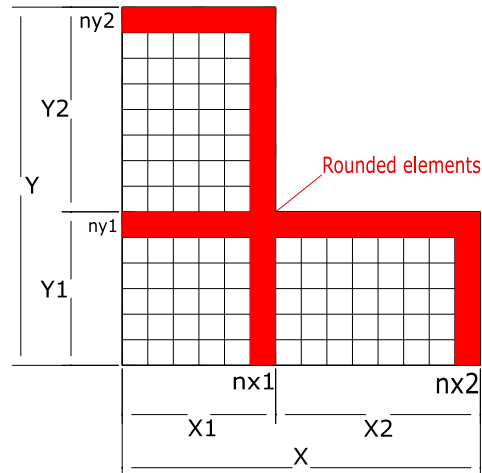


Figure 5.5: L-shaped structure rounded elements for areas A, B and C

The coordinates of the element's centroid and surface area of the generated element are determined. Based on the location of the centroid of each element tributary areas are assigned. There are 3 types of tributary area that can be assign: internal slab area, wall area, and roof area. The three area types exist to account for the different distributed load each area type will receive depending on the studied load case. Elements are assigned tributary areas based on the position of the centroid relative to the layout of the structure. The assignment of each element as internal or external is done by comparing the coordinates of its centroid to the perimeter bounds of the $k+1^{\text{th}}$ storey. If the centroid of an element is within the bounds of the overlying storey, then its surface area of the element will be designated as internal, otherwise it is defined as a roof element. This has the potential to cause minor errors as it is possible that an element is divided unevenly by the bounds of the upper storey, meaning that some of the element will be assigned to the incorrect area type. This however, does not produce significant errors as elements are small and the case loads between external and internal are often not vastly different. To improve accuracy the user may select a smaller U size which will reduce the approximation error by producing a finer mesh of elements.

All elements within the roof level analyzed are assigned as roof elements as none will be internal. Wall loads are assigned to the elements that form the perimeter of the level. This means that for the floor level analyzed, k , the perimeter elements of that floor will be assigned the surface area of the entire wall segment that spans between floors k and $k-1$. This division of tributary areas between floors is illustrated for an $N = 3$ structure in Figure 5.6. The wall area assignment convention of assigning the entire wall area to the upper storey does not affect the accuracy of the analysis. Normally the wall's mass would be divided between the two bounding storeys. However, since the following subprogram eventually transfers all tributary area values to the ground splitting the wall area between the two storeys would be redundant. Storey masses are calculated independently of the element assignment convention, and wall masses are distributed conventionally when determining the storey masses.

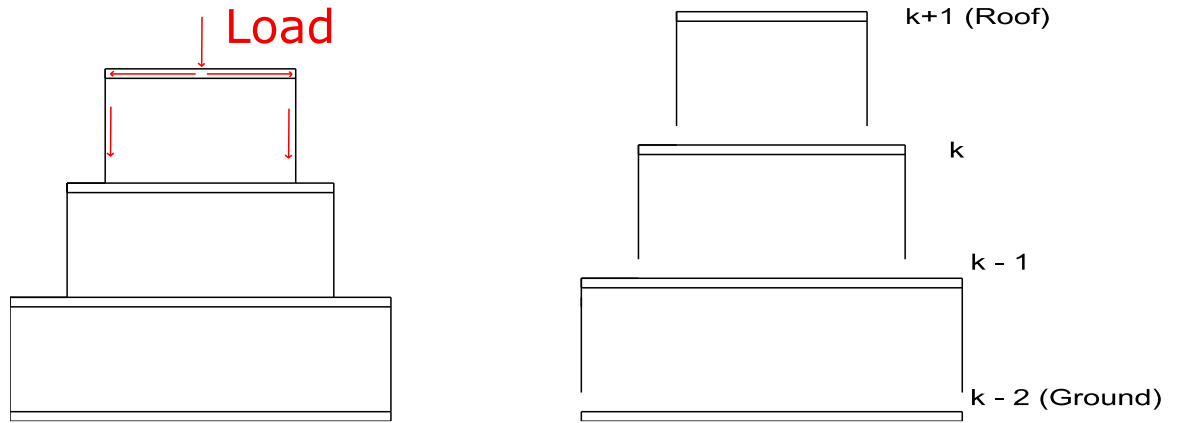


Figure 5.6: Element array generation of floors $k+1:1$ for $k = 3$

Once the element array generation of each floor is complete a record containing the sum of the internal, wall and roof tributary area of each floor is produced. The element arrays of each floor level are combined into a single array which defines the elements of all $k+1$ levels. After the total number of elements required to represent the floor is determined, the location, surface area, and tributary areas assigned to element i is determined independently before progressing to the generation of element $i+1$.

5.3.4 Distribute Loads

The load path distribution is intended to approximate the real structural load paths and allow the development of a more accurate estimate of the loads applied to each individual isolator unit. The tributary areas from each element within the structure are distributed along designated load transfer systems and onto the bearings composing the isolation system. This allows the tributary area carried by each isolator to be approximated and the axial load under each load case to be determined for each isolator unit. For light-frame wooden structures this would follow the load path as shown in Figure 5.7. Loads are transferred from the plan surface area, along the joists, to the beams and finally towards internal or external structural wall elements in the case of the upper storeys, or to the underlying isolator units in the case of the ground level.

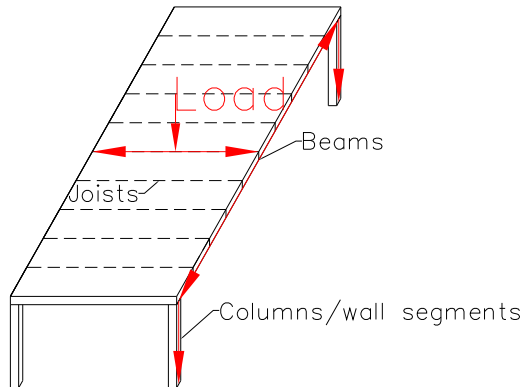


Figure 5.7: Structure load paths

The finite element approach distributes the tributary areas on floor k from individual elements to the elements whose coordinates match with the coordinates of known structural loadbearing elements. In practice this means distributing tributary areas to the elements that align with the coordinates of the perimeter walls. In this way the program allocates the distributed tributary areas along known load paths to approximate the real distribution of loads more accurately than by simply distributing tributary areas by proximity. To achieve this the tributary areas assigned to element i are added to the nearest loadbearing element before setting element i 's tributary loads to 0, thus transferring the tributary load along the approximated load path. This allows the finalized distributed array of elements of floor k to be added to the elements of floor $k-1$ by proximity, as the elements of floor k will have been distributed to the elements that would transfer load directly onto the underlying level.

However, a situation may arise where the distance from the i^{th} element to the closest known loadbearing/perimeter wall element is significant, and in such cases, it is unreasonable to approximate the load path by transferring tributary area from that element to the closest wall element. The limiting distance selected is half the maximum joist span on floor k . If an element is further than half the joist span to a wall element it will be distributed to the lower levels by an undefined structural element as the interior configuration is not a required input. To account for the internal distribution the tributary load from these elements will be added directly to the underlying elements of $k-1$ by proximity. This approximation is less accurate than transferring to a known structural element, but achieves the load distribution without requiring substantial and complex design inputs from the user.

This distribution and transfer process is continued for each floor until tributary loads are distributed to the ground floor. The tributary areas from ground floor elements will then be distributed to the isolators by proximity to determine the total internal, area and wall area supported by each isolator. A check is performed where the total internal, wall and roof areas supported by each isolator unit are calculated and the sums are compared to the total tributary areas for each category previously determined to ensure the totals are correct.

5.3.5 Calculate Axial Loads

Once the approximate tributary interior wall and roof areas are known for each isolator the axial load on each isolator can be determined. The gravity loads that the isolation layer must carry are found by analyzing the 4 relevant load cases from the NBCC [6]:

Case 1: 1.4Dead

Case 2: $1.25\text{Dead} + 1.5\text{Live} + 1.0\text{Snow}$

Case 3: $1.25\text{Dead} + 1.0\text{Live} + 1.5\text{Snow}$

Case 4: $1.0\text{Dead} + 0.25\text{Snow} + 0.6\text{Storage}$

Cases 1-3 are the static cases while case 4 is the dynamic case due to the inclusion of lateral seismic excitation. For the design to be acceptable the stability of the bearing must be assured under static and seismic axial load conditions. The dead loads for the 3 area types of the structure can be

determined based on the weight class selected by the designer. The CWC guide utilizes a metric known as weight class to provide the expected unfactored distributed loads for different structural areas. The distributed loads for various area types are shown for normal and heavy structures in Table 5.1. This metric is useful as it requires minimal input from the user and produces all the relevant dead load data for a single-family home.

Table 5.1: CWC Normal and Heavy weight classification

Structural Component	Normal Weight Construction	Heavy Weight Construction
Floor	0.5 kPa	0.5 – 1.5 kPa
Roof	0.5 kPa	0.5 – 1.0 kPa
Exterior Wall	0.32 kPa	0.32 – 1.2 kPa
Partition Wall	0.5 kPa	0.5 kPa

The live loads for the interior and roof areas are selected based on the NBCC prescribed residential loads; the unfactored live loading of the interior and roof areas is 1.9 kPa and 1.0 kPa, respectively. The snow loads are site specific and must be inputted by the user after being calculated using the methods within the CWC guide [77]. Storage loads are not considered as the low-rise residential structures the program is designed for do not typically contain substantial storage areas.

For each load case the three distributed loads are determined: *Load areas*, *Load roofs* and *Load walls*. These distributed loads represent the factored combination of loads for internal, wall and roof areas respectively. The distributed loads are determined for each load case by a subsidiary subprogram *Mass Calculation*. For the seismic case, case 4, the floor mass of each level, and the coordinates, CM_x and CM_y , of the structural center of mass are calculated. These variables are only determined for the seismic case as only the mass and center of mass for the seismic case will be used to determine the response of the structure during seismic excitation.

The loads carried by the individual isolators are determined by applying the distributed loads for each case. The maximum load on an isolator from the static cases is the critical static axial load and governs the acceptability of the static axial capacity of the bearing. The maximum and minimum dynamic axial loads determined from case 4 are used to verify the stability of the bearing under lateral seismic excitation. The subprogram checks these design axial loads against the bearings acceptable limits to ensure gravity load stability is obtained. If the capacity is insufficient the designer will be alerted and they can either make modification to the isolation layer layout, or restart the analysis using a different isolator. The axial loads calculated by the program will vary based on overturning moment leading to load concentrations on one side of the structure. These effects are not currently considered by the program.

5.3.6 Torsional Amplification Evaluation

After both the layout of the isolation system and the structural center of mass have been determined it is possible to determine the torsional amplification of displacement each isolator will experience. First the center of rigidity of the isolation layer is calculated. This calculation is simplified by assuming each isolator will have identical stiffness, and the properties are independent of the direction of loading. The assumption regarding uniform properties reflects that

most isolated structures use symmetric bearings which are either square or circular. It is also desirable to limit the type of allowable bearings to bearings of uniform lateral stiffness properties to both reduce the required design inputs and, as discussed in section 4.2.3, it allows the approximated response to ignore torsional effects caused by significant differences of lateral stiffness.

Once the coordinates of the center of rigidity, CR_x and CR_y , are known the eccentricity of the structure can be calculated using equation (4.5). The parameter P_T is also calculated and is used to account for the effects of torsional stiffness and damping as previously stated in section 4.2.3. The local eccentricity of each isolator, as described in section 4.2.3 is calculated. The torsional amplification of each isolator is calculated using equation (4.4) for both directions of loading, and the worst case is selected. If the amplification effect of an isolator is less than a 15% increase a minimum amplification factor of 1.15 is applied to ensure conservatism [42].

5.3.7 Calculation of Floor Stiffness

Interstorey drifts can be used to determine if significant non-structural or structural damage will occur to low rise residential structures as previously discussed in section 1.1.4. To determine the interstorey drifts the program must be capable of estimating both the vertical force distribution and the stiffness of each floor level. A modal analysis of the structure is used to determine the stiffness of each storey based on the following fundamental equation:

$$\det([K] - \omega_1[M]) = 0 \quad (5.1)$$

where ω_1 is the fundamental fixed base angular frequency, $[M]$ is the mass matrix and $[K]$ is the stiffness matrix of the structure. The mass and stiffness matrices of an $N = 3$ structure are given in (5.2) where m_k and k_k are the k^{th} storey mass and stiffness respectively.

$$[M] = \begin{bmatrix} m_1 & 0 & 0 \\ 0 & m_2 & 0 \\ 0 & 0 & m_3 \end{bmatrix} \quad [K] = \begin{bmatrix} k_1 + k_2 & -k_2 & 0 \\ -k_2 & k_2 + k_3 & -k_3 \\ 0 & -k_3 & k_3 \end{bmatrix} \quad (5.2)$$

For low rise residential structures, the values of fundamental period will typically be bounded by 0.1s and 0.3s [34]. The stiffness for each floor is determined for each assumed fundamental period, but an assumed value of 0.3s will result in a significantly softer structure producing larger interstorey drifts. For multistorey structures ($N > 1$) the solution to the equation is not unique as there will be three unknown variables in the in the characteristic polynomial. In the case of an $N = 3$ the characteristic equation is:

$$(k_1 + k_2 - \omega_1 m_1)(k_2 + k_3 - \omega_1 m_2)(k_3 - \omega_1 m_3) - (k_1 k_3^2 + k_2 k_3^2 - \omega_1 m_1 k_3^2) - (k_3 k_2^2 - \omega_1 m_3 k_2^2) = 0 \quad (5.3)$$

This situation necessitates that the storey stiffnesses must be related to one another to obtain a non-trivial solution by solving the roots of the N degree polynomial.

A relationship between storey stiffnesses was developed by relating the relative lateral load resisting capacity of each level to their relative stiffness. This relationship assumes that the stiffness of a storey scales linearly with its strength, and that the superstructure will be designed based on fixed base loads. The relative stiffness of the upper floor, x , to the ground floor stiffness, k_l , is determined by calculating the relative fixed base load distribution using the following formula:

$$k_{1:x} = \frac{\sum_{i=1}^N W_i h_i}{\sum_x^N W_x h_x} \quad (5.4)$$

The stiffness ratio can then be used to define the stiffness of the upper storeys in terms of k_l . The storey stiffnesses produced for $T_{fb} = 0.1s$ and $0.3s$ will be used in later subprograms to evaluate the interstorey drifts of the structure.

5.3.8 Placement Results and Plot Results

The reality of single-family homes is that they often do not conform perfectly to the generic layout generated by the previous subprograms. While most of the structure can be accurately modelled where the program generates similar recommendations for the placement of isolators to traditional footing layout of a single-family home, some nuance must be allowed to enable the user to make edits to the layout of isolators to better conform to the realities of a structure's layout not accounted for in the program.

To enable users to evaluate the placement of isolators and make the required adjustments to the existing layout, if any, the *Placement Results* subprogram generates a log of the existing isolator layout, their approximated tributary internal, wall and roof areas, as well as the total load. This log is then exported as a spreadsheet, *Isolator_data*, which can be reviewed by the user. This user review is supported by the layout figure produced by a separate but related subprogram *Plot Results*. The plot highlights the selected floor beam locations (red dashes), perimeter of the structure (solid black), and the placement of each individual isolator unit (red crosses) as shown in Figure 5.8 a) and b) for a rectangular and L-shaped structure. The results produced enable the user to make necessary changes to the isolation layer to provide a system better suited to facilitate the load paths of the structure.

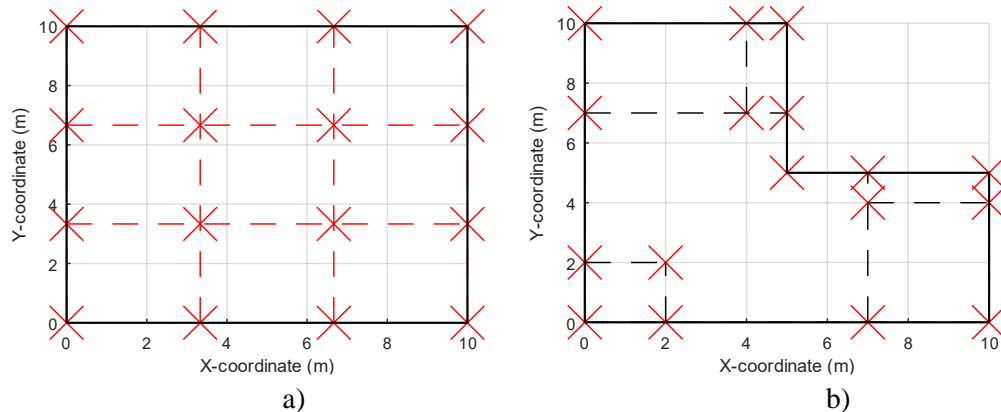


Figure 5.8: Isolator placement for a) a rectangular and b) a L-shaped structures

5.3.9 Move Existing Add New Isolators

As previously stated, it is not possible for the program to accurately estimate the optimal configuration of the isolated system for every structure. This is due primarily to the deliberate choice to minimize user input. This provides the user with an intuitive and relatively expedient means to generate a design, but at the cost of losing some the benefits or requirements that can be found when the entire structural layout is known. For instance, some structures will have discontinuities between the structural system and floor beam layouts of the foundation system such that an offset is required as shown in Figure 5.9. This creates a situation where it is not possible to select two parallel floor beams, while simultaneously it is not reasonable to select a single continuous floor beam to represent the foundation layout. This necessitates the ability for the user to manually alter the placement of bearings to apply an offset such that the isolators can more accurately be placed along the true floor beam layout of the structure.

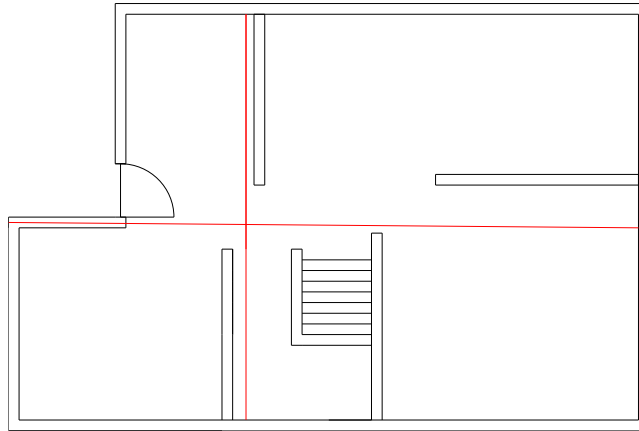


Figure 5.9: Floor beams with offsets

There may also be cases where it is necessary, or simply more expedient to manually place the isolators rather than trying to align the floor beam input selection to align with the structural plan. This may be the case where isolator units are placed to support load concentrations such as stairwells or other load concentrations are not accounted for by the program. Openings such as doors may also require custom placement.

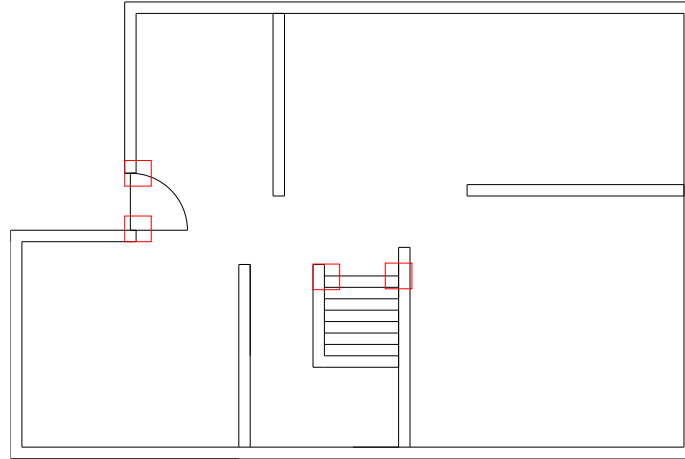


Figure 5.10: Custom placement of isolators

The interactive process between the user and the subprogram whereby edits to the placement may occur is illustrated in Figure 5.1. To make edits the user alters the previously produced *Isolator_data* spreadsheet. The user alters the coordinates of existing isolators by applying the desired ΔX and ΔY , or adds a new isolator by entering the X, Y coordinates of the new unit into the spreadsheet. All placement alterations made by the user must conform to CWC design requirements to ensure load paths and stability are maintained.

The changes made by the user are evaluated to ensure that the moved or added isolators are within the perimeter of the structure. If the changes in placement are acceptable a new list of isolators and their coordinates are produced. The loads and torsional amplifications are recalculated and a new placement graphic is produced. This is achieved by re-running several subprograms using the new isolator coordinates as illustrated by Figure 5.1. This process repeats until the layout and loading is acceptable. It is currently not possible to remove an isolator once added to the program, so the user must rerun the *Import Sheet* subprogram if they wish to remove an isolator or floor beam that was added erroneously.

5.3.10 Determine Period and Design Displacement

The purpose of the previous subprograms was to develop an isolation system that would be integrated into the load paths of the superstructure. In addition, several parameters of interest were also generated to determine the seismic response of the isolated and fixed base structures more accurately. These parameters are:

- The weight of each storey
- The maximum, minimum, and average loads on the isolators
- The number of isolators
- The torsional amplification to the displacement of each isolator
- The structural stiffness of each storey
- The isolator critical static axial load
- The isolator maximum and minimum dynamic axial loads

This program determines the dynamic properties of the isolated structure by iterative methods to determine the maximum lateral displacement, D_M , and the isolated period of the structure at the maximum displacement, T_M . As discussed in section 4.2.1, the maximum displacement of the structure is of primary interest to the designer as this will be the displacement at which the structural response will be maximized. To begin the response spectrum is produced based on the site-specific data input by the user, and the fixed base site specific spectral acceleration is determined. The acceleration will be the same regardless of if the fixed base period, T_{fb} , is assumed as 0.1s or 0.3s, as both values fall within the uniform acceleration segment of the design response spectrum [78]. The iterative calculations to determine D_M and T_M then begin.

Step 1: Initial values of T_M , the period at the maximum displacement, and B_M , the effective damping at the maximum displacement, are assumed as $T_{Mj} = 1.0$ s and $B_{Mj} = 1.0$, where j represents the iteration count.

Step 2: The location-specific spectral accelerations for the base isolated structure, $S_a(T_{Mj})$ is determined using linear interpolation. The upper and lower period bounds, T_{i+1} , and T_i are found that encompass T_{Mj} along with the corresponding values of S_{i+1} and S_i as shown in Figure 5.11.

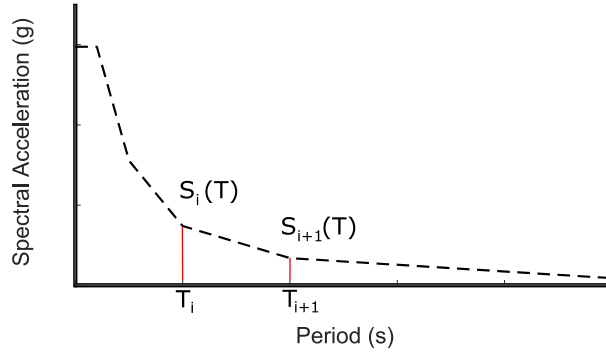


Figure 5.11: Response spectrum interpolation

Step 3: The maximum displacement, D_{Mj} is calculated by:

$$D_{Mj} = \frac{S_a(T_{Mj})gT_M^2}{4\pi^2 B_{Mj}} \quad (5.5)$$

Step 4: The instantaneous isolator stiffness k_{Mj} , and isolator damping, ζ_{Mj} are determined for D_{Mj} using the stiffness and damping regimes of the isolators provided by the designer for isolators with seismic case (case 4) axial loads between W_{max} and W_{min} .

Step 5: The damping coefficient B_{Mj} is determined for $\zeta = \zeta_{Mj}$ using Table 5.2:

Table 5.2 Damping Factor [42]

ζ (%)	B_M
≤ 2	0.8
5	1.0
10	1.2
20	1.5
30	1.7
40	1.9
≥ 50	2.0

Step 6: Using the instantaneous stiffness k_{Mj} determined in step 6 a new T_{Mj+1} is determined using:

$$T_{Mj+1} = 2\pi \sqrt{\frac{W}{k_{Mj}g}} \quad (5.6)$$

Steps 2-6 are repeated and the iteration j increases, such that $j = j + 1$, until the iterative variables converge. The convergence criteria are satisfied when the absolute difference T_{Mj} and T_{Mj+1} is less than 0.001 s.

However, it may be the case that multiple solutions to T_M exist for the range of period around the solved T_M . This is due to the nonlinear characteristics of the isolation system, which can produce multiple possible convergence solutions depending on the initial period assumptions. To ensure that the found solution is unique a factor is applied to the period determined in step 6, and the iterations detailed in steps 1-6 are repeated. This factor is either 1.25 or 0.75 to investigate convergence in the period range around T_M . This ensures that for the displacement range of the isolation system only one solution exists. If the solution is not unique then an error message is displayed. A comparison between the fixed base spectral acceleration and the isolated spectral acceleration is then plotted as shown in Figure 5.12.

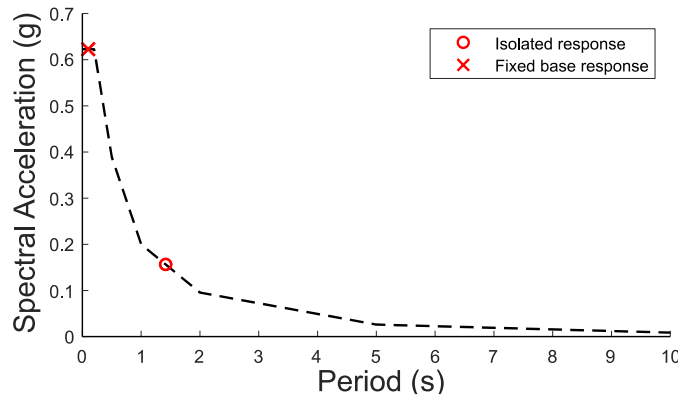


Figure 5.12: Comparison of fixed base and isolated spectral accelerations

After solving the maximum translational displacement, D_M , it is possible to determine the total maximum displacement D_{TM} of each isolator unit. D_M is multiplied by the torsional amplification factors for each isolator producing D_{TM} for each isolator unit.

The program then performs several checks to ensure the results comply with the provisions of both the ASCE and the NBCC. These checks include:

1. Ensuring that the isolated period is at least 3 times the fixed base period
 - $T_M \geq 3 \cdot T_{fb}$
2. Ensuring that the isolated period does not exceed 5s
 - $T_M \leq 5s$
3. Ensuring that the percent damping of the isolation system does not exceed 30%
 - $\zeta_M \leq 30\%$
4. The effective stiffness of the isolation system at D_M is greater than $\frac{1}{3}$ of the effective stiffness at 20% of the maximum displacement
 - $k_M \geq \frac{1}{3}k(0.2D_M)$
5. The lateral displacement across the isolation layer due to wind loads shall be less than 1/500 of the least storey height
 - $D_{wind} < 1/500 \cdot h_{min}$

If the provisions are satisfied the performance of the structure will be acceptable by ASCE and NBCC requirements and further analysis of the response can proceed.

5.3.11 Determine Forces and Response

This program generates the response of the structure and the isolation system. The responses generated include:

- Vertical force distribution
- The displacement of each storey with respect to the foundation
- Interstorey drifts

The vertical force distribution of the fixed base and isolated structures are calculated using the equivalent lateral force procedure from the NBCC such that:

$$F_x = VW_x h_x / \sum_{j=1}^N W_j h_j \quad (5.7)$$

While the isolated vertical force distribution is calculated using equation (4.11) described in section 4.2.4.

$$F_x = C_{vx} V_s \quad (5.8)$$

The cumulative shear force for each storey, V_x , is then determined. A plot of the vertical force distribution is produced, comparing the fixed base and isolated storey forces over the height of the structure as shown in Figure 5.13. The efficiency of the isolation system is determined by comparing the base shear of the isolated and fixed base structures.

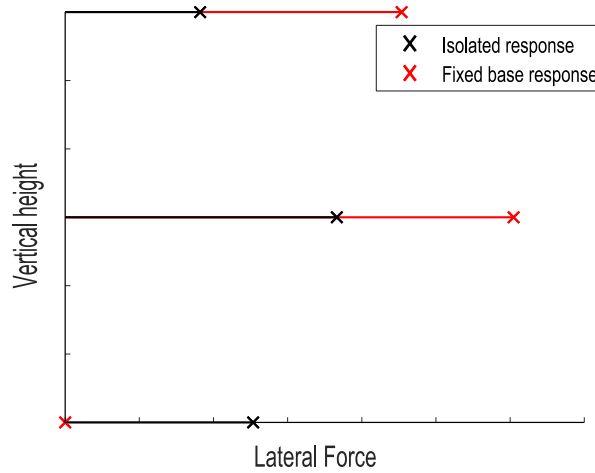


Figure 5.13: Example of a vertical force distribution comparison

The other main response parameters are the displacements of the structure, in particular the displacement of the isolation layer, the interstorey drifts and the floor accelerations. The lateral displacement of each level, d_x , can be determined by solving the stiffness matrix, as shown in equation (5.9). The interstorey drifts are determined for the k^{th} storey using equation (5.10) where d_x and d_{x-1} are the floor displacements above and below storey k . The variable h_k is the height of storey k . The difference between the displacements of the isolated and fixed base structures are then compared by a plot as shown in Figure 5.14.

$$[F] = [K][d] \tag{5.9}$$

$$\Delta_k = \frac{d_x - d_{x-1}}{h_k} \tag{5.10}$$

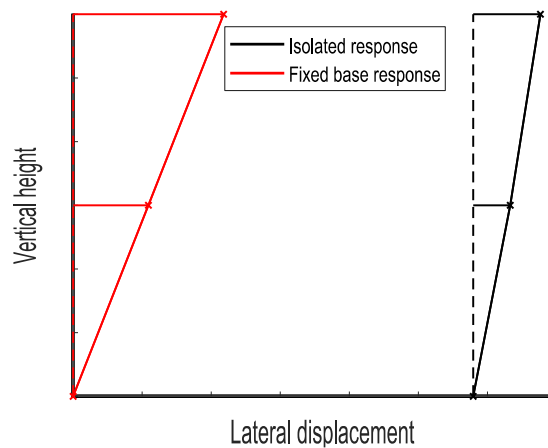


Figure 5.14: Displacement comparison

5.3.12 Analysis Results

The final subprogram within the main program generates the *Analysis_Results* output sheet which contains the following data:

1. A record of each isolator unit, its coordinates, axial load, and maximum displacement
2. The fixed and isolated structural periods
3. The fixed and isolated spectral accelerations
4. A comparison of storey shear between the isolated and fixed base structure
5. A comparison between the interstorey drifts of the isolated and fixed base structures

This data is exported as a spreadsheet to provide the user with an intuitive means of evaluating the results of the seismic analysis. This data is also supported by the figure generated to illustrate the layout of the isolation system, and plots comparing the fixed base and isolated spectral accelerations, the vertical distribution of forces, and the storey displacements. The produced data enables the user to evaluate the efficacy of the isolation system design for the structure. The results generated also form the basis for the design of the isolation system, without requiring the user to perform any specialist engineering design themselves.

CHAPTER 6 ISOLATOR DESIGN

6.1 Introduction

The program methodology described in the previous sections can design and analyze the structure, but this function only reduces the engineering costs. As previously discussed in section 1.2 the other major cost barrier for application of seismic isolation to Part 9 structure is the design and testing cost for the isolator units, which would be mitigated through the development of a catalogue of pretested and certified isolators. While the experimental testing and development of a catalogue of isolators is beyond the scope of this research, it is useful to investigate the feasibility of designing potential isolators specifically tailored for the dynamic and economic realities of Part 9 structures. This section will discuss the design requirements, and proposed criteria for the design of FREIs due to their potentially superior economic characteristics for application in Part 9 structures [52].

6.2 Isolator Stability

The design of FREIs has two main areas of relevance, bearing stability and structural performance. As seismic performance of the superstructure is not directly addressed by the standards for the design of elastomeric bearings, which generally focus on stability and safety, the designer must ensure the characteristics produce a stable bearing regardless of economic performance concerns. To ensure stability of the isolator under the design load-displacement combinations three failure conditions must be investigated and prevented. These failure conditions are buckling, rupture, and rollout. To form a coherent design methodology around these concerns it is important to review the stability requirements in detail, with primary emphasis on those presented in ISO 22762-3 [79] and CSA S6:19 the Canadian Highway Bridge Design Code (CHBDC) [80].

6.2.1 Buckling Stability

As discussed in section 2.2.2 increases in axial load will cause the lateral stiffness of an elastomeric bearing to decrease and, under extreme loading, it may approach zero causing buckling to manifest. Buckling of elastomeric bearings is discussed in ISO 22762-3 [79] and equations (6.1) and (6.2) are provided to determine the critical buckling load under static loading, P_{cr} , and dynamic loading, P_{crD_M} , respectively, as:

$$P_{cr} = \frac{\alpha^3 \pi}{T_r} \frac{\pi}{4} \xi \sqrt{E_b G} \quad (6.1)$$

$$P_{crD_M} \leq P_{cr} \left(1 - \frac{D_M}{a} \right) \quad (6.2)$$

G : Shear modulus
 a : Square bearing side length
 T_r : Total elastomer thickness
 ζ : 1 for circular bearings, or $\frac{2}{\sqrt{3}}$ for rectangular bearings
 E_b : Bending modulus
 D_M : Design maximum lateral displacement

These equations, however, are tailored specifically for SREIs whose reinforcement is rigid in flexure, making them potentially unsuited for the analysis of FREIs. Alternative equations have been derived to investigate the buckling capacity of FREIs by accounting for the fiber reinforcements lack of flexural rigidity [81]. The critical buckling load under static and dynamic loading are thus given by equations (6.3) and (6.4), respectively, as:

$$P_{cr} = \frac{\pi G a^4}{2\sqrt{15} n_e t_r^2} \quad (6.3)$$

$$P_{cr}(D) = P_{cr} \left(1 - \frac{D_M}{a}\right)^3 \quad (6.4)$$

t_r : Elastomeric layer thickness
 n_e : Number of elastomeric layers

These equations allow the designer to investigate the critical buckling capacity of the FREI under static loads at a shear displacement, D_M . However, these equations generally provide very conservative estimates of the critical buckling load under shear displacement due to key simplifying assumptions. For example, a bearing with $G = 0.4$ MPa, shape factor of $S = 11$ and length to height aspect ratio, $R = 2.9$ was found to have a seismic buckling capacity of 12 MPa under $D = 2T$, which is substantially higher than the theoretical capacity of the bearing which is only 2.5MPa [82].

6.2.2 Rollout Stability

Rollout instability is a concern for bearings whose contact surfaces are connected to the surface or foundation through shear connections only, such as shear keys, dowelled connections or simply relying on friction. These connections are unable to resist tension and thus leave the bearing vulnerable to instability at large displacements. Rollout occurs when the overturning moment induced by the lateral seismic force cannot be sufficiently resisted by the axial load applied by the overlying structure. The equilibrium condition can be investigated to determine the maximum allowable shear displacement using:

$$P(a - D_M) = HV \quad (6.5)$$

P : Axial load
 H : Total bearing height
 V : Shear force

Since the shear connections cannot provide a tensile restraint to the shear displacement, displacements past the equilibrium configuration leads to a negative lateral stiffness and thus instability. The factors affecting the rollout of an unbonded elastomeric bearing are shown in Figure 6.1.

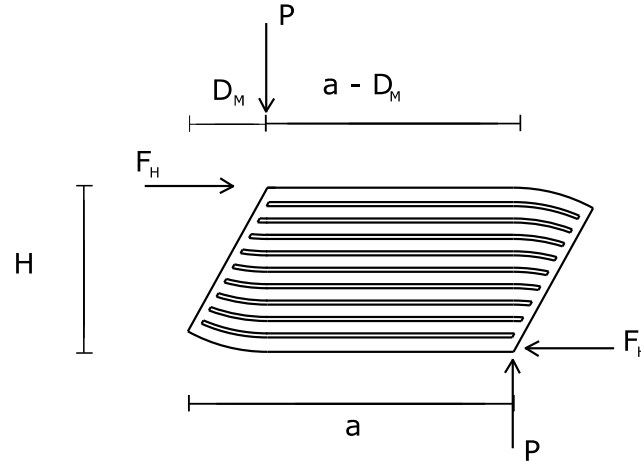


Figure 6.1: Rollout instability

To determine the maximum displacement before rollout occurs a relationship between the applied axial stress and the maximum allowable displacement is produced in equation (6.6) [51]. This relationship is a function of the bearing's geometry, and thus it is not necessary to know the applied shear force to investigate the relationship between axial load and acceptable displacement.

$$D_{max} \leq \frac{a\sigma}{\frac{H}{T_r}G + \sigma} \quad (6.6)$$

Rollout of FREIs can be prevented by ensuring stable rollover occurs. As discussed in section 2.2.2 unbonded FREIs can undergo rollover under large displacements rather than rollout. This is possible for bearings with a length to total height aspect ratio in excess of 2.5, as the larger aspect ratios promote favourable deformation patterns [83].

6.2.3 Rupture Stability Check

Rupture stability is investigated by determining the total internal strain caused by combined shear, and compressive and rotational strains. The allowable internal strain varies between codes and ranges from 5.0 in [84] to 5.5 in [80] and to 7.0 in [85], while ISO limits strain as a function of the type of elastomer [86]. The variability in codes is also present in the equations they present to calculate the strain components. Many of these equations also produce significant errors when compared to the theoretical equations [87]. While simplified equations are desirable to facilitate ease of use the theoretical equations accounting for compressibility of the elastomer and extensibility of the reinforcement are better suited to providing an accurate analysis of the internal strain as well as other relevant physical properties.

The total strain within the bearing, γ , is given by equation (6.7), where γ_d is the shear strain due to shear displacement, γ_c is the shear strain due to compressive strain and γ_r is the shear strain due to rotation. A limit of 5.5 is selected based on the conservative CSA S6 requirements [80]:

$$\gamma = \gamma_d + \gamma_c + \gamma_r \leq 5.5 \quad (6.7)$$

The laterally induced shear strain is given by equation (6.8):

$$\gamma_d = \frac{D_M}{T_r} \quad (6.8)$$

The compressive strain and the compression modulus of rectangular bearings are calculated using equation (6.9) and (6.10) [88]. The variable K_e represents the combined effects of bulk compressibility and extensibility, while λ represents the sensitivity of the pad to compressibility and extensibility where $\lambda = 0$ represents an incompressible elastomer and inextensible reinforcement [87]:

$$\gamma_c = 24S \left(\frac{1+\rho}{\rho} \right) \sum_{n=1,3,5,\dots}^{\infty} \frac{1}{\zeta_{cn} n \pi} \tanh(\zeta_{cn}) \sin\left(\frac{n\pi}{2}\right) \frac{\sigma}{E_c} \quad (6.9)$$

$$E_c = 8\lambda^2 K_e \frac{(1+\rho)^2}{\rho^2} \sum_{n=1,3,5,\dots}^{\infty} \frac{1}{\zeta_{cn}^2 n^2 \pi^2} \left(1 - \frac{\tanh(\zeta_{cn})}{\zeta_{cn}} \right) \quad (6.10)$$

$$\frac{1}{K_e} = \frac{1}{K} + e \frac{t_r}{E_f t_f} \quad \zeta_{cn} = \lambda^2 \frac{(1+\rho)^2}{\rho^2} + \frac{n^2 \pi^2}{4\rho^2} \quad \lambda = cGS^2 \left(\frac{1}{K_e} \right) \quad (6.11 \text{ a b c})$$

K : Bulk modulus of the elastomer

E_f : Effective elastic modulus of reinforcement

ρ : Bearing plan area aspect ratio (equal to 1 for square bearings)

t_f : Thickness of a reinforcement layer

S : Shape factor

σ : Compressive axial stress

c and e : geometry and load dependent coefficients; $c = 12$, $e = 2$ for rectangular bearings

The rotational strain of a rectangular bearing is given by equation (6.12) [89], where θ is the design rotation of a single elastomeric layer:

$$\gamma_r = 12S^2 \frac{(\rho+1)^2}{\rho^2} \sum_{n=1}^{\infty} \frac{1}{\zeta_{rn}^2} \left(1 - \frac{1}{\cosh(\zeta_{rn})} \right) \theta \quad (6.12)$$

$$\zeta_{cn} = \lambda^2 \frac{(1+\rho)^2}{\rho^2} + \frac{n^2 \pi^2}{\rho^2} \quad (6.13)$$

6.3 Testing Requirements

While the equations presented in section 6.2 provide the designer with a method of estimating the stability of the bearing under various loading conditions, testing is still required to ensure the compressive and shear performance matches the theoretical properties. While codes vary on the exact nature and requirements of tests the main properties of interest remain the same. These properties are:

- Compressive properties
- The compressive properties dependence on compressive load and shear displacement
- Shear properties
- The shear properties dependence on compressive load and shear displacement
- Shear displacement capacity

The purpose of testing is fundamentally to provide the designer with a detailed understanding of the properties and performance of the elastomeric bearing that are relevant to seismic isolation. This section will discuss the relevant testing requirements and the data produced by the various tests to provide a detailed view of the properties and loading conditions that must be considered by the designer.

6.3.1 Compressive Properties

ISO 22762-3 Cl. 6.5.2 [79] and ISO 22762-1 Cl. 6.2.1.5.2 [90] provides the designer with the compressive properties of the isolator under the design compressive stress, σ_0 . The test is carried out by applying the design stress, σ_0 , and then subjecting the bearing to 3 cycles of loading with amplitude $\sigma_0 \pm 30\%$ and measuring the vertical deformation of the bearing. After the 3rd cycle the vertical stiffness, k_v , is determined using equation (6.14). For the test results to be accepted the vertical stiffness must be within $\pm 30\%$ of the design value.

$$k_v = \frac{P_2 - P_1}{Y_2 - Y_1} \quad (6.14)$$

$$P_1 = (\sigma_0 - 0.3 \sigma_0)A$$

$$P_2 = (\sigma_0 + 0.3 \sigma_0)A$$

A: Contact surface area

Y_1 : Vertical deformation due to P_1

Y_2 : Vertical deformation due to P_2

6.3.2 Compressive Property Dependence

After the compressive properties have been investigated under the design loading it is important to investigate how the compressive stiffness will vary when subjected to a combined compressive and shear displacement loading. To determine the dependence of k_v on the compressive load, and on the shear displacement two tests are conducted.

The first test investigates the dependence of k_v on the shear displacement of the bearing. This test is identical to the compressive property test described in 6.3.1, however, the test is conducted at a constant shear displacement. The shear displacements to be investigated are given in Table 6.1, where γ_0 is the design shear strain. The vertical stiffness is otherwise determined by the same methods as in section 6.3.1.

Table 6.1: Compressive strain dependence test strains

Shear strain %	0	$0.5\gamma_0$	$1.0\gamma_0$	$1.5\gamma_0$
----------------	---	---------------	---------------	---------------

The second test investigates the dependence of k_v on the applied compressive force and shear displacement. This is done by repeating the test described in section 6.3.1 but with modified loading and shear displacement conditions. The modified loading conditions are presented in Table 6.2. The bearing is additionally subjected to a shear displacement $\gamma = \gamma_0$. The vertical stiffness is otherwise determined by the same methods as in section 6.3.1.

Table 6.2: Compressive stress dependence test stresses

Compressive stress	$\sigma_0 \pm 0.3 \sigma_0$	$\sigma_0 \pm 0.7 \sigma_0$	$\sigma_0 \pm 1.0 \sigma_0$
--------------------	-----------------------------	-----------------------------	-----------------------------

The results from the dependency tests allows the designer to predict the compressive performance of the bearing under conditions that differ from the design seismic loading conditions of $\sigma = \sigma_0$, and $\gamma = \gamma_0$. This is important when the loading conditions of individual isolators within a structure differ from the average conditions significantly. While variable vertical deformation is undesirable, substantial changes to vertical stiffness may have significant implications when investigating the buckling and rupture capacity of the bearing.

6.3.3 Shear Properties

The purpose of the shear property tests as outlined in ISO 22762-3 6.5.3 [79] is to provide the designer with the shear and damping properties of the isolator under the design compressive stress, σ_0 , and at the design shear strain γ_0 . The test is carried out by applying the design stress, σ_0 , and then subjecting the bearing to 3 cycles of shear loading at an amplitude of γ_0 at a period of oscillation equal to the design isolation period. The force displacement hysteresis loop is recorded for each cycle and the effective shear stiffness, k_H , and the equivalent viscous damping ratio, ζ , are determined using the data from the 3rd cycle using equations (6.15) and (6.16) respectively.

$$k_H = \frac{Q_1 - Q_2}{X_1 - X_2} \tag{6.15}$$

$$\zeta = \frac{2(\Delta W)}{\pi k_H (X_1 - X_1)^2} \quad (6.16)$$

Q_1 : Maximum shear force

Q_2 : Minimum shear force

$X_1 = \gamma_0 \cdot T_r$

$X_2 = -\gamma_0 \cdot T_r$

ΔW : Area enclosed by the hysteresis loop

6.3.4 Shear Displacement Capacity

It is expected that the general performance of isolators within an isolation system will conform roughly to $\gamma = \gamma_0$ and $\sigma = \sigma_0$. However, it is important to investigate the ultimate capacity of the bearing to provide the designer with the maximum allowable combined shear and axial loading a bearing can withstand. This ensures that the loading conditions are below the ultimate limits and will not result in stability concerns or failures. The limits of stable performance can be estimated by the equations presented in section 6.2, however, testing is required to ensure that stability is verified.

To evaluate the stability of the bearing the maximum shear capacity, γ_{max} , is established under the maximum load σ_{max} , and, when rollout is a concern, σ_{min} as well. The bearing is loaded with either σ_{max} or σ_{min} and a unidirectional shear deformation is applied at a constant rate until buckling, rupture or rollout occurs, or the test is stopped once the design maximum displacement is reached. If no failure occurs then the maximum displacement reached is designated as γ_{max} , provided that the force-displacement curve has been increasing monotonically.

To provide a relationship between the compressive load and the maximum shear displacement testing can be performed to develop an ultimate property diagram (UPD). This is achieved by applying various stress levels and subjecting the bearing to static monotonic shear loading until stability failure occurs. The stress levels are given in Table 6.3. The results are then used to provide designers with a method of estimating the ultimate capacity of the bearing under variable load conditions such that $\gamma \neq \gamma_{max}$ and $\sigma \neq \sigma_{max,min}$.

Table 6.3: UPD compressive stress loads

Compressive stress	0.5 σ_0	1.0 σ_0	1.5 σ_0	2.5 σ_0
--------------------	----------------	----------------	----------------	----------------

6.3.5 Shear Property Dependence

The variation of shear properties with the axial load conditions has significant implications for Part 9 structures and the development of the isolator catalogue. Variability of properties within the structure can cause additional torsional effects to manifest, however, assuming the average loading conforms roughly to the design conditions of $\gamma = \gamma_0$ and $\sigma = \sigma_0$ the overall structural response should conform generally to the expected design response.

Since custom designs of isolators for each structure are undesirable due to economic concerns it is important to be able to predict how a structure whose average load conditions do not

match the design loading conditions of the isolator will perform. Tests are conducted investigating the dependence of shear and damping properties on shear strain and compressive stress. This investigation allows for the suitability of the bearing to be assessed for a range of structures.

The shear dependency test repeats the experiment described in section 6.3.3 for a range of shear strains to investigate the change of k_H and ζ with respect to the design shear properties. The shear properties are determined between $0.5 \gamma_0$ and γ_{max} at intervals of $0.5\gamma_0$, where the interval between γ_{max} and the preceding test strain is at least $0.5 \gamma_0$. Additionally, it is recommended that the designer investigate $\gamma = 0.1 \gamma_0$ or $0.2 \gamma_0$ to provide a more accurate understanding of the shear properties at small displacements, which is important for accurately investigating the wind induced displacement and required restoring force discussed in section 3.1.3. The compression dependency test repeats the test described in section 6.3.3 for a range of compressive stresses to investigate the change of k_H and ζ with respect to the design shear properties. The test compressive stresses are $\sigma = 0.5 \sigma_0, 1.0 \sigma_0, 1.5 \sigma_0$ and $2.0 \sigma_0$.

The class of the isolator, as defined by ISO 22762-2 [86], is determined by the allowable tolerance of shear properties. S-A allows an individual and global variability of $\pm 15\%$ and 10% respectively, while S-B allows an individual and global variability of $\pm 15\%$ and 25% . Individual variability refers to the properties of each bearing in the system, while global variability refers to the average properties. Individual properties are important when torsion or unequal axial loading may cause significant differences in shear and compressive loading. Deviation of shear properties beyond these limits is prohibited to ensure that the overall system performance will be relatively homogenous regardless of the loading of individual bearings. In Part 9 structures analyzed by the program method, class S-A isolators are preferable as the response of individual bearings will be more homogeneous and ensure that the approximated response does not deviate substantially from the dynamic reality.

6.4 Design Considerations for Part 9 Structures

The fundamental stability considerations and the relevant properties discussed in sections 6.2 and 6.3 are universal to FREI's regardless of the structure augmented with seismic isolation. However, the design of a catalogue of FREIs for Part 9 structures necessitates a design that considers the economic and structural realities of augmenting a Part 9 structure with seismic isolation. This section will discuss several areas of consideration important for the design of isolators for Part 9 structures.

6.4.1 Isolator Shape

The program method described in Chapter 5 approximates the torsional response by assuming the lateral stiffness of the bearings will be homogenous. Additionally employing bearings whose lateral stiffness properties are identical along both primary axes such as square or circular bearings prevents the designer from needing to further detail the isolation system layout by specifying the orientation of individual bearings. Square bearings may have additional potential, as they can be cut from the same large pad, which, while similarly possible for circular bearings, would produce substantially less material waste and may therefore be more economically efficient

to produce in larger quantities. Circular bearings however, have the added benefit of requiring no orientation during construction unlike square bearings which should be oriented to align with the primary structural plan axes. Additionally, it is required that the bearings length to height aspect ratio exceeds 2.5 to prevent the rollout failure condition from manifesting at large displacements as discussed in section 6.2.2.

6.4.2 Superstructure Performance and Shear Displacement

The design of the bearing must be able to provide a sufficient level of protection to the superstructure when applied in the design isolation system. If the isolated period is sufficiently elongated the various response parameters linked to damage (i.e., interstorey drift and floor accelerations), will be suppressed to below the values at which damage is expected to manifest as discussed in section 1.1.4. Elongation of the fundamental period is achieved by ensuring that the collective lateral stiffness of the isolators that compose the isolation layer will be low enough to produce $T \geq T_{min}$, where T_{min} is the isolated period where interstorey drift and floor accelerations are below the damage thresholds of 0.1% and 0.25g, respectively [23, 26].

While $T \geq T_{min}$ is a desirable level of performance to achieve it is undesirable to produce a fundamental period significantly longer than T_{min} . The undesirability of longer periods is due to the increase in the design displacement of the isolation system which can lead to increased costs as the designer must accommodate for larger base displacements [46]. Costs that will increase with displacement include the required size of footings below the isolators, the size of the moat and or the required clearance around the isolation system, and the flexibility of utilities connections. It is thus desirable to control the displacements while preventing damage. Isolated periods shorter than but close to T_{min} may still reduce damage to superficial levels. Thus, it is not always necessary to always ensure $T > T_{min}$ if the expected damage is only superficial and this is deemed acceptable by the designer.

6.4.3 Applicability of Designs

The purpose of the isolator catalogue is to reduce testing and fabrication costs by introducing an element of universality into the design of the bearings. While designing a bearing suitable for all Part 9 structures is unrealistic there are characteristics that make structures more suited to the same bearing design. The period T_{min} is a key parameter when evaluating if a bearing can provide complete seismic protection. If T_{min} of two structures is not close the deviant structures other characteristics such as total weight, W , or number of isolators, n , would need to differ in such a way that the isolator can achieve sufficient performance. By review of the ASCE and NBCC simplified equations discussed in section 5.3.11 the structural characteristics that most strongly predicts T_{min} is the number of storeys and the vertical mass distribution, which play a significant role in determining how the seismic base forces are distributed throughout the structure. The peak interstorey drifts of Part 9 structures with a fixed base period assumed between 0.1 - 0.3 s are mostly independent of the total W , as proportional changes in W throughout the structure will result in proportional increases in both k_k and m_k so that d_x calculated by equation (5.9) remains unchanged. This however, assumes that the fixed base period of the structure remains between 0.1 - 0.3s, which

may not be the case for massive yet relatively slender structures. Additionally, changes in local storey mass that are not reflected proportionally in the other storeys will also lead to alterations in the force distribution, and thus T_{min} .

While T_{min} is theoretically independent of W , the isolated response is not. From equation (4.3) structures with similar $\frac{W}{n}$ ratios subjected to comparable local seismic conditions will achieve a similar period elongation if both structures utilized identical isolators. Under similar conditions the isolated period determined by the methods discussed in sections 4.2 and 5.3 will converge to a similar solution. However, if the $\frac{W}{n}$ ratio or the local seismic conditions deviate significantly between structures using the same isolators the response may converge to different solutions. This can be tolerated so long as the isolation period remains sufficiently elongated and base lateral displacements are not significantly increased. Larger deviations that negatively affect performance would indicate that the isolator is not suitable for the structure. The $\frac{W}{n}$ ratio thus constitutes an important parameter for evaluating if two structures with similar T_{min} requirements can achieve the same isolated period using the same bearing design. Therefore if two structures have similar $\frac{W}{n}$ ratios and have similar design period lengths, then they can likely utilize the same, or similar bearings.

CHAPTER 7 CASE STUDIES

7.1 Program Methodology Validation

To validate the program methodology two base isolated residential structures are simulated and the number and properties of elastomeric bearings required to provide seismic protection for each structure are proposed. The isolated structures are modelled and subjected to time history analysis with west coast ground motions using OpenSees [91]. The theoretical fixed base and base isolated responses are compared to the time history analysis responses. The site conditions and loading are selected to be representative of Vancouver, BC.

7.2 Model Structures

Two structural designs are analyzed to verify the efficacy of the program's analysis for structures typical of British Columbia. Design 1 considers a two storey rectangular structure with a plan area of 255m². Design 1 conforms to contemporary design practices in BC, where single family homes typically have a plan area of 250m² and generally have two storeys [92]. Design 2 considers a single storey rectangular structure with a plan area of 124m² which was chosen to represent the average existing single-family home in BC, which typically have an average plan area around 133m² [93]. Both structures have storey heights of 3m. The floor plans of designs 1 and 2 are shown in Figure 7.1 and Figure 7.2, respectively. A breakdown of the geometric inputs of each design is presented in Table 7.1.

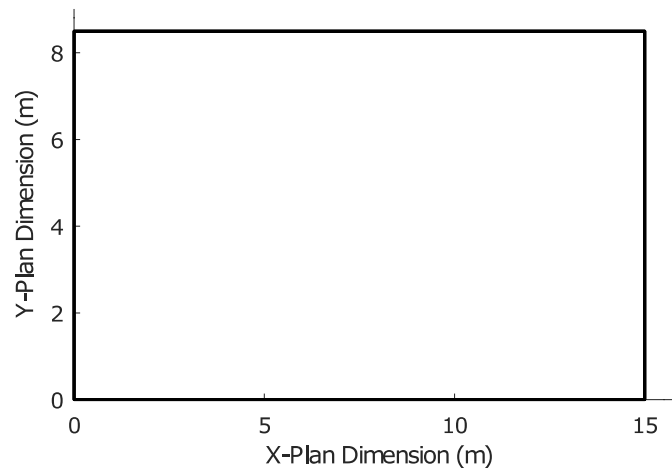


Figure 7.1: Design 1 Ground floor plan and 2nd storey plan

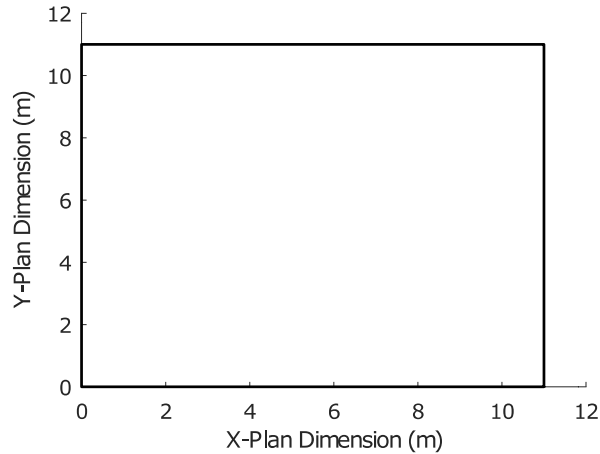


Figure 7.2 Design 2 ground floor plan

Table 7.1: Geometric data

Design	Storey	X1 (m)	X2 (m)	Y1 (m)	Y2 (m)
1	1	15	0	8.5	0
	2	15	0	8.5	0
2	1	11	0	11	0

The dead, snow and live loads applied to the structural areas are given in tables Table 7.2, Table 7.3 and Table 7.4 respectively. All three designs are assumed to be of normal construction for the purposes of determining dead loads in concurrence with the methods described in section 5.3.5. These loads are used to evaluate the structures gravity load and the axial loads of isolators for NBCC load cases 1-4, and the dynamic mass distribution of the structure is determined using load case 4. The two storey OpenSees model was modelled with two different stiffness profiles. Design 1a was modelled with shear proportional stiffness, as assumed by the program method, while design 1b was modelled with a uniform stiffness distribution. This is done to investigate if the assumptions made by the program have a significant impact on response estimation, and to check if the assumption of shear proportional stiffness is conservative. Each design has a fixed base period of 0.3s, the high end of realistic fixed base periods for residential structures [34]. This is due to longer fixed base periods producing a less uniform, and more linear response distribution of the isolated superstructure which leads to response concentrations at the top of the superstructure, in addition to the substantially larger storey displacements and interstorey drifts [70]. The mass distribution of design 1 and 2 is in Table 7.5. The stiffness distribution approximated by the program is determined according to section 5.3.7, and is presented in Table 7.6 while the uniform stiffness distribution of the model is presented in Table 7.7.

Table 7.2: CWC weight class distributed dead loads

Structural Component	Dead Load
Floor	0.5 kPa
Roof	0.5 kPa
Exterior Wall	0.32 kPa
Partition Wall	0.5 kPa

Table 7.3: Snow load values Vancouver

Variable	Value
C_b	0.55
S_r	1.8 kPa
S_s	0.2 kPa
S (snow load)	1.2 kPa

Table 7.4: Distributed live loads

Structural Component	Live Load
Floor	1.9 kPa
Roof	1.0 kPa

Table 7.5: Mass and weight distribution

Level	Design 1		Design 2	
	Mass (kg)	Weight (kN)	Mass (kg)	Weight (kN)
1 (Ground)	15,297	150.1	14,487	142.1
2	17,596	172.6	11,712	114.9
3 (Roof)	12,372	121.4		
Total	45,265	444.1	26,199	257.0

Table 7.6: Program stiffness distribution

Storey	Design 1		Design 2	
	Stiffness (kN/mm)		Stiffness (kN/mm)	
1	18.5		5.1	
2	10.9			

Table 7.7: Model stiffness distribution

Storey	Design 1a		Design 1b		Design 2	
	Stiffness (kN/mm)		Stiffness (kN/mm)		Stiffness (kN/mm)	
1	18.5		16.0		5.1	
2	10.9		16.0			

The structural floor beams of design 1 trace the ground floor perimeter and divide the internal area laterally into three 5.0 m spans, and longitudinally into two 4.25m spans as shown in Figure 7.3 a). The floor beams of design 2 similarly trace the structural perimeter while dividing the internal area via two 5.5m lateral spans and two 5.5m longitudinal spans as shown in Figure 7.3 b). These designs conform to the joist span length limits of the NBCC [6], which limit the maximum allowable unsupported span length. The program designs the isolation system layout by placing isolators at the beam intersection nodes as shown in Figure 7.4 a) and b) for designs 1 and 2 respectively.

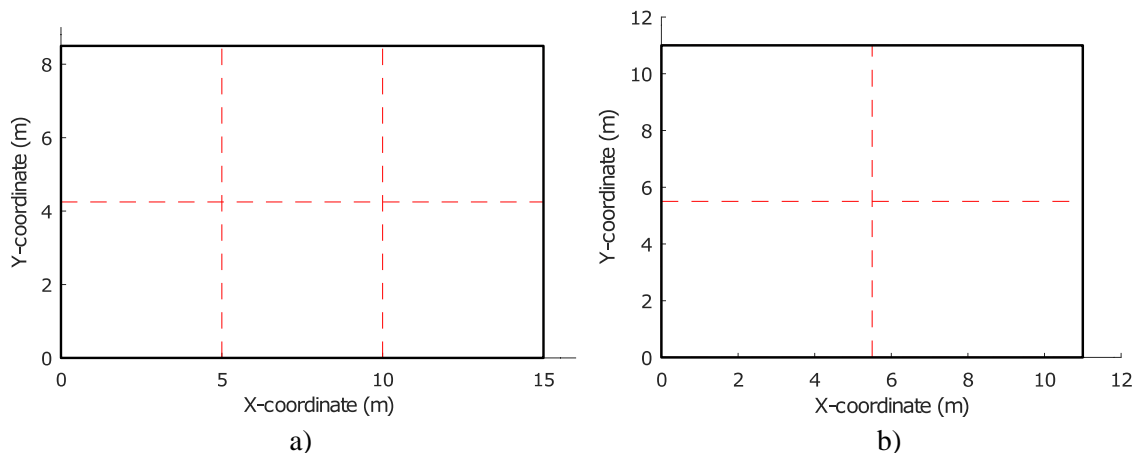


Figure 7.3: a) Design 1 floor beam layout and b) design 2 floor beam layout

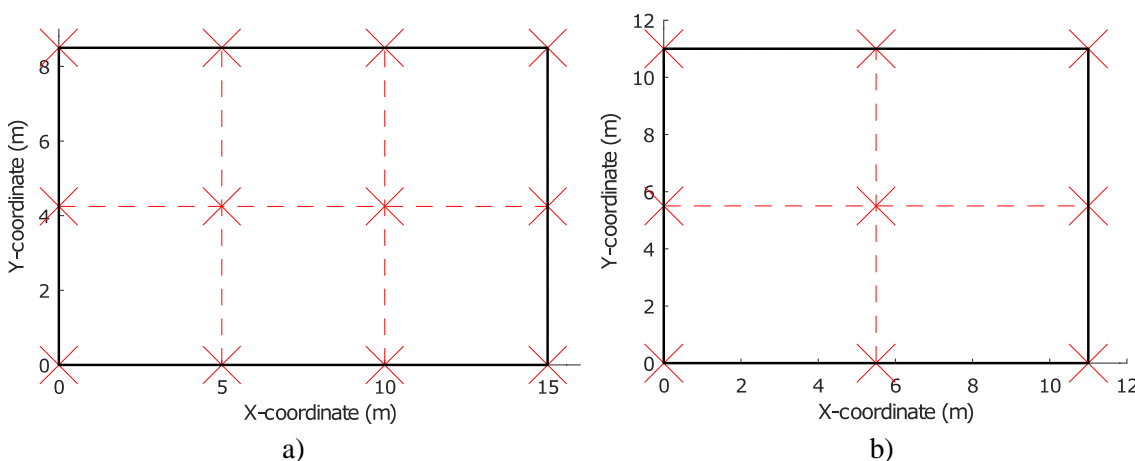


Figure 7.4: a) Design 1 isolator layout and b) design 2 isolator layout

The vertical load on each bearing is determined for each load case using the methods described in sections 5.3.3 - 5.3.5. The approximate axial loads for load cases 1:4 on each isolator of the design 1 and 2 layouts are presented in Table 7.8 and Table 7.9, respectively. The maximum axial load from cases 1-3 is the static axial load and is used to evaluate the rupture and buckling capacity of the bearings under static conditions. The maximum load from case 4 is used to evaluate rupture and buckling under dynamic conditions, and the minimum load of case 4 is used to evaluate rollout instability. The design axial loads for each design are presented in Table 7.10.

Table 7.8: Isolator axial loading of design 1 structure (kN)

Isolator	Load case 1	Load case 2	Load case 3	Load case 4
1	29.9	68.1	60.2	22.9
2	58.7	159.7	141.3	46.4
3	58.7	159.7	141.3	46.4
4	29.9	68.1	60.3	22.9
5	54.1	146.6	128.4	42.4
6	55.1	173.0	144.8	42.8
7	55.1	173.0	144.8	42.8
8	54.1	146.6	128.4	42.4
9	29.9	68.1	60.2	22.9
10	58.7	159.7	141.3	46.4
11	58.7	159.7	141.3	46.4
12	29.9	68.1	60.2	22.9
Average	47.7	129.2	112.7	37.3

Table 7.9: Isolator axial loading of design 2 structure (kN)

Isolator	Load case 1	Load case 2	Load case 3	Load case 4
1	23.3	61.1	56.5	18.9
2	40.0	119.0	110.3	33.5
3	23.3	61.1	56.5	18.9
4	40.0	119.0	110.3	33.5
5	59.9	200.9	180.9	50.3
6	40.0	119.0	110.3	33.5
7	23.3	61.1	56.5	18.9
8	40.0	119.0	110.3	33.5
9	23.3	61.1	56.5	18.9
Average	34.8	102.3	94.3	28.9

Table 7.10: Design axial loads for bearings (kN)

Axial Load Type	Design 1	Design 2
Static Maximum	173.0	200.9
Dynamic Maximum	46.4	50.3
Dynamic Minimum	22.9	18.9

7.3 Isolator Properties

The properties of the bearing used to augment each structure are based on the theoretical dynamic response of the isolated structure, such that the isolated response is kept below theoretical acceleration and drift damage thresholds. This is done by analyzing the theoretical response of the isolated structure for various isolated periods and determining the shortest period capable of providing a design that limits damage to superficial levels, or eliminates it entirely as outlined in section 6.4.2. The number of isolators is determined in accordance with the stability principles

discussed in section 5.3.2, from which the individual maximum stiffness of isolators at the design displacement may be found using equation (7.1). The minimum required isolation period for designs 1 and 2 are 1.35s and 1.0s. The maximum allowable shear stiffness at the design displacement for the designs 1 and 2 are 82.3 kN/m and 74.4 kN/m, respectively:

$$k_{H\ max} = \frac{W}{ng} \left(\frac{2\pi}{T_{min}} \right)^2 \quad (7.1)$$

Using the design axial loads shown in Table 7.10 and the required stiffnesses the design of the bearing can be completed and the physical characteristics selected. The isolator's physical characteristics and performance properties are shown in Table 7.11 and Table 7.12 for both design 1 and 2. The theoretical performance characteristics shown in Table 7.12 and the nonlinear shear properties should be verified via testing and the design be completed using the test data. The theoretic performance would normally serve as a starting point for design and testing, however, due to the scope of the research conducted, performance is approximated using the theoretical design data in lieu of experimental testing.

Table 7.11: Isolator characteristics

Characteristic	Design 1	Design 2
G (shear modulus) (MPa)	0.3	0.3
K (bulk modulus) (MPa)	2000	2000
ζ (damping) (%)	10	10
a (side length) (mm)	251	232
t_r (layer thickness) (mm)	11	10.3
n (number of layers)	9	9
T_r (total thickness) (mm)	99	92.7
R (length to height aspect ratio)	2.54	2.50
S (shape factor)	5.70	5.63

Table 7.12: Isolator properties

Property	Design 1	Design 2
k_{Hi} (initial stiffness) (kN/m)	190.9	174.2
k_V (vertical stiffness) (kN/m)	9873.0	8208.0
D_{max} (Maximum allowable displacement) (mm)	300.0	200.0
P_{min} (design minimum seismic axial load) (kN)	N/A	N/A
$P_{cr}(D)$ (design maximum seismic axial load) (kN)	60.0	47.0
P_{cr} (design maximum static axial load) (kN)	440.0	369.0

Design 1 has a static axial load of 173.0 kN and a dynamic maximum axial load of 46.4 kN, while the design static, and design dynamic axial capacities are 440.0 kN and 60.0 kN respectively. The seismic and static axial loads are substantially less than the isolator's design static and seismic axial loads. The possibility of rollout is suppressed by ensuring a length to total height ratio of 2.5. Thus, rollout does not govern the maximum allowable displacement. Additionally, no minimum

load limit is assigned to these theoretical design bearings as they would be governed by friction, a quality not investigated in this study. The theoretical dynamic buckling capacity is also discounted when establishing D_{max} due to the overly conservative estimation of the equations presented in section 6.2.1. The program assumes the damping of the bearing is constant at 10% while the nonlinear lateral stiffness is approximated as a function of displacement using equation (7.2).

$$k_H = \begin{cases} \frac{Ga(a-d)}{T_r} & d \leq \frac{a}{2} \\ \frac{F_{max}}{d} & d > \frac{a}{2} \end{cases} \quad (7.2)$$

$$F_{max} = \frac{Ga^3}{4T_r} \quad (7.3)$$

A piecewise function is used to provide an approximation of the nonlinear stiffness of the bearing while ensuring the theoretical tangential stiffness remains positive at larger displacements. This is important as equation (7.2) is used to fit a theoretical Bouc-Wen hysteresis profile for the bearings used in the OpenSees models [94]. The design displacements do not exceed $\frac{a}{2}$ and thus the $d > \frac{a}{2}$ approximations are limited to aiding the fit of the hysteresis models, and are not directly used to evaluate the response. The force-displacement Bouc-Wen equation is defined as:

$$F_H = q_d \dot{z} + \alpha_1 k_1 u + \alpha_1 k_1 sgn(u) |u|^\mu \quad (7.4)$$

$$\dot{z} = \frac{\dot{u}}{u_y} \{1 - |z|^\eta (\gamma + \beta sgn(z\dot{u}))\} \quad (7.5)$$

$$u_y = \frac{q_d}{(1 - \alpha_1) k_1} \quad (7.6)$$

F_H : Lateral force

u : Lateral displacement

q_d : Characteristic strength,

k_1 : Initial elastic stiffness,

α_1 : Post-yield stiffness ratio of the linear hardening component,

α_2 : Post-yield stiffness ratio of the non-linear hardening component,

μ : exponent of the non-linear hardening component,

η , β , and γ : hysteretic shape parameters,

u_y : yield displacement

The variables used in the Bouc-Wen equations for the bearings proposed for design 1 and 2 are shown in Table 7.13 and the hysteretic profile of the Bouc-Wen isolators for design 1 and 2 are illustrated in Figure 7.5.

Table 7.13: Model Bouc-Wen Variables

Variable	Design 1	Design 2
k_I (N/m)	$401 \cdot 10^3$	$392 \cdot 10^3$
q_d (N)	752	737
α_1	0.295	0.285
α_2	-0.525	-0.526
μ	1.74	1.71
η	0.120	0.122
β	0.438	0.450
γ	0.431	0.435

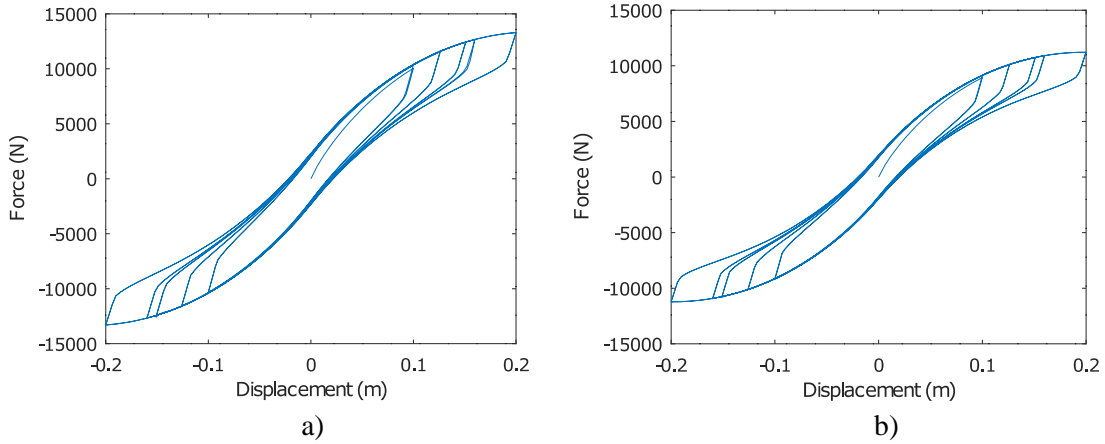


Figure 7.5: a) Force displacement hysteresis of design 1 and b) design 2

7.4 Time History Analysis

The modelled structures are subjected to west coast ground motion records in accordance with the selection and scaling requirements of the NBCC Commentary Appendix J Method A [95]. A minimum of 11 records are required by Method A, with 7 records required per ground motion hazard contribution mechanism (scenario). A total of 21 ground motion records were selected to represent the various hazard source mechanism contributions. The various source mechanisms for Vancouver are a M 6.5 crustal, M 7.5 sub-crustal, and M 9.0 subduction events. Using hazard de-aggregation these scenarios contribute to period domains of 0 - 0.5 s, 0.5 - 2.0 s and 1.0 - 5.0s respectively [96]. The target spectrum domain is selected using equations (7.7) and (7.8) where T_1 is the fundamental period of the structure and $T_{90\%}$ is the lowest period that captures 90% of the mass participation. For the records selected the value of T_1 was chosen as 0.3s and a range of 0 - 1.5s was chosen for the design. For the isolated structures a value of $T_1 = 1.1$ or 1.2 s should have been chosen (with different required period ranges) as this would be the fundamental period for the isolated structures. This was deemed unnecessary as the required period range and subsequent fit did not change significantly. Using the same records also simplifies the comparison between the fixed and base isolated structures.

$$T_{min} = \min[0.2T_1, T_{90\%}] \quad (7.7)$$

$$T_{max} = \max[2.0T_1, 1.5 \text{ s}] \quad (7.8)$$

The ground motion records were obtained from the Engineering Seismology Toolbox online resource [96] which provides crustal, sub-crustal and subduction earthquake records representative of west coast ground motions. These records are synthetically produced; however, their characteristics are tailored to represent realistic west coast records. The selected ground motion records and scale factors are shown in Table 7.14.

Table 7.14: Ground motion records

Magnitude	Record	Distance (km)	Scale factor	Global Scale factor
6.5	1	8.8	0.757	1.03
	2	10.8	0.904	
	3	8.4	0.772	
	4	8.4	0.830	
	5	9.5	1.111	
	6	8.6	0.932	
	7	11.2	1.147	
7.5	8	18.1	0.902	1.03
	9	10.2	0.629	
	10	17.8	1.374	
	11	18.1	1.095	
	12	15.2	0.738	
	13	15.2	0.667	
	14	30.2	1.3705	
9.0	15	112.4	1.6562	1.0
	16	112.4	1.6696	
	17	112.4	1.5022	
	18	156.7	1.8740	
	19	112.4	1.9520	
	20	112.4	1.6607	
	21	112.4	1.6227	

The models developed in OpenSees to validate the program methodology was a dynamically equivalent wireframe model with concentrated mass at nodes, which for the ground level align with the X , Y coordinates of the isolators, and align with the 4 corners of the structure for upper levels of the design structures. The mass of each node is determined based on the supported tributary area, such that the vertical mass distribution and the isolator axial loads between the model and program are identical. Additionally, an eccentricity of 10% of the perpendicular plan direction to loading was applied by biasing the mass towards the negative x -direction to investigate torsional sensitivity. The storey nodes are constrained to act as a rigid diaphragm in alignment with the assumed rigid elastic performance of the floor system. The lateral storey stiffness of the design 1a and design 2 models was assigned as shear proportional, while design 1b was assigned a uniform stiffness distribution. All designs have equal stiffness in both X and Y directions. Lateral stiffness is developed by four massless elastic beam columns located at the corners of each storey. The model structures achieved a period of 0.3s by assigning the design masses to the structure and assigning column stiffnesses that produced a fixed base period of the desired length. The superstructure damping is assumed at 2% for the isolated structure and 5% for the fixed base structure as it is expected that the isolated structure will remain undamaged while the fixed structure will experience

damage [97]. The damping matrix of the fixed and isolated superstructures are approximated using Rayleigh damping. The damping matrix, $[C]$, is constructed using:

$$[C] = a_0[m] + a_1[k] \quad (7.9)$$

$$a_0 = \zeta \frac{2\omega_i\omega_j}{\omega_i + \omega_j} \quad (7.10)$$

$$a_1 = \zeta \frac{2}{\omega_i + \omega_j} \quad (7.11)$$

Equation (7.9) relates the approximated damping matrix to the stiffness and mass matrices of the structure. The variables ω_i and ω_j represent the lower and upper bound angular natural frequency of the modes of the structure, usually selected as the 1st mode and a higher mode. This allows the damping to be approximated for a structure when the primarily contributing modes of vibration fall within the ω_i to ω_j mode bounds. Only the stiffness proportional damping for the base isolated OpenSees models is considered, as the mass proportional damping of isolated structures tends to overestimate the damping and produce consistently lower estimates of the 1st mode's response [97]. For the isolated model $\omega_j = \frac{2\pi}{T_{fb}}$, where $T_{fb} = 0.3$ s, to ensure that the structural modes are included in the damping response. The damping of the isolators is dependant upon the hysteretic characteristics discussed in 7.3.

7.5 Results

The designs are analyzed first as fixed base and then as isolated structures. The selected key performance indicators are the base shear, base displacement, interstorey drift ratios (IDRs) and floor accelerations. The design seismic demand from the time history analysis is determined according to the NBCC Commentary Appendix J [95]. Although 21 records were used for the time history analysis the response is taken as the mean of the 7 highest values of the response parameter. All time history analysis (THA) models were excited in the y -direction due to the torsional response being greatest in this direction. Additionally records 8-21 (see Table 7.14) were not used to evaluate the response of the fixed base structure, as the source mechanism that produced those records does not significantly contribute to the hazard at period ranges shorter than 0.5 s making it inappropriate to include them. The results of the fixed base design's analysis are presented first to act as a benchmark for performance. The results of the isolated structures are then presented and the change in performance is discussed. Lastly the program and time history analysis responses are compared to validate the program method.

7.5.1 Fixed Base Responses

To establish a baseline comparison between the isolated and fixed base structures the base shear determined by the program and by THA are presented in Table 7.15. The base shear response determined by the program is substantially less than the response determined by the THA, however, the program's response is based on capacity-based design which assumes inelastic action and energy dissipation as discussed in section 3.1.2. This method, while able to reduce the global forces experienced by the structure, causes large plastic deformations which result in economic losses. Therefore, it is not reasonable to directly compare the global responses of the program's capacity-based design response and the model's elastic response. If the model structures were designed to perform inelastically the force responses would decrease by a factor of $R_d R_o$ which is taken as $(2.0)(1.7) = 3.4$. This inelastic response is substantially lower and is in line with the expected response. However, the $R_d R_o$ reduction factor is not applied to the other THA recorded responses such as storey displacements as capacity-based design assumes inelastic and elastic displacements are equivalent.

Table 7.15: Fixed base structure base shear

Design	Program	THA	THA/ $R_d R_o$
	V_b (kN)		
1a	71.3	203	59.7
1b		215	63.2
2	28.3	92.7	27.3

The superstructure displacement and acceleration responses of the model are displayed in Table 7.16. The displacements of the structure increase with height which shows that the assumption of first mode dominance is correct. To evaluate the assumption of storey stiffness being proportional to the shear force, the 2 storey model, design 1, was modelled with both shear proportional storey stiffness, design 1a, and uniform storey stiffness, design 1b. For the program response the ratio between the local 2nd level displacement and local 3rd level (i.e., roof) displacement is 1.04. For the shear proportional stiffness model, the ratio is 0.98, while the model with uniform stiffness has a ratio of 1.94.

This indicates that for structures with shear proportional stiffness the level displacements will be relatively uniform while for structures with uniform stiffness the interstorey drifts will be largest at the 1st storey. Additionally, the program's predicted displacement response matched closely with the response of the model when the model was constructed with shear proportional stiffness. Reviewing the interstorey drifts presented in Table 7.17, the interstorey drifts predicted by the program and the shear proportional stiffness model are relatively uniform, whereas the drifts of the uniform stiffness structure are concentrated at the 1st storey. The uniform stiffness model leads to a larger absolute interstorey drift at the 1st storey and proportionally lower drifts at the upper storeys. The floor accelerations (determined based on the elastic response) generally follow a trend of increasing with height with the peak floor accelerations of design 1 occurring when the stiffness was shear proportional rather than uniform. This is expected as the relatively lower stiffness at the top of the structure concentrates the dynamic response at this location. If the true stiffness distribution of the structure is unknown it may be conservative to assume a uniform distribution when evaluating drifts, and a shear proportional stiffness when evaluating peak accelerations

Table 7.16: Fixed base lateral storey displacement and floor accelerations

Design	Program			THA					
	Displacement			Displacement			Floor acceleration		
	1st	2nd	3rd	1st	2nd	3rd	1st	2nd	3rd
	(mm)	(mm)	(mm)	(mm)	(mm)	(mm)	(g)	(g)	(g)
1a	0	13.3	26.1	0	10.4	21.0	0.44	0.60	1.03
1b ¹				0	13.0	19.7	0.44	0.66	0.82
2	0	18.7		0	18.0		0.44	0.86	

¹No program analysis was conducted for a uniform stiffness assumption (design 1b).

Table 7.17: Fixed base interstorey drifts

Design	Program		THA	
	IDR (%)		IDR (%)	
	1st	2nd	1st	2nd
1a	0.44	0.43	0.35	0.35
1b			0.43	0.22
2	0.62		0.60	

The ratio between the program and THA response (THA/Program) are illustrated in Table 7.18. The base shear responses predicted by the program are generally conservative. The drifts predicted by the program were conservatively overestimated to a similar proportion as the base shears suggesting that the assumed correlation between V_b and superstructure response is valid. Additionally, the drifts of design 1b were not underestimated. However, if the program were modified to assume a uniform stiffness profile the overestimation would likely approach a similar degree of conservatism. Overall, the program was able to predict the magnitude and profile of the response closely to the reality especially when accounting for variability in ground motion as well as the inclusion of torsion.

Table 7.18: Difference factor between the program and THA (THA/program)

Design	V_b	Peak IDR
1a	0.84	0.80
1b	0.89	1.0
2	0.96	0.97

7.5.2 Base Isolated Responses

A comparison between the total base displacement, lateral base displacement and base shear of the program and THA responses are shown in Table 7.19. The isolated base shear values of design 1 are roughly 10% lower in the model than those determined by the program, which is a similar trend for the fixed base structure. The program lateral base displacement, D_M , of design 1 is 7% higher than the THA D_M while the program V_b of design 1 is 10% higher. It is expected that as D_M decreases V_b decreases at a slower rate due to the stiffening of the bearing, and so a minimum of a 3% discrepancy in expected base shear is present. This 3% discrepancy in the data is accounted for by the fact that the fitted stiffness of the bearing used for the model is about 10% softer than the

theoretical bearing used by the program, so even at equal displacements V_b will be proportionally less for the model due to the reduced stiffness. A similar issue appears in design 2, however, the fit for that bearing was within a 5% difference, and the discrepancy is also proportionally less. This resulted in the THA displacements of design 2 exceeding the values determined by the program. The torsional response of design 1 and 2 were 5% and 1%, respectively, which are both substantially less than the 15% minimum required by the ASCE standards. The low torsional response of design 2 is due to the square plan area producing a more torsional resistant design. This is due to the proportionally shorter eccentricity length as both eccentricities are based on $0.1D_p$, where D_p is the plan length perpendicular to the direction of loading.

Table 7.19: Base isolated displacement and base shear

Design	Program				THA			
	D_M	D_{TM}	V_b	T_M	D_M	D_{TM}	V_b	T_M
	(mm)	(mm)	(kN)	(s)	(mm)	(mm)	(kN)	(s)
1a	122	140	144	1.23	113	119	130	1.17
1b					113	119	130	1.17
2	99.4	114	89.1	1.08	106	106	82.9	1.12

The superstructure displacement and acceleration responses of the model are displayed in Table 7.20. The displacements of the structure are concentrated overwhelmingly at the base and then increase slowly with height, confirming that the assumption of first mode dominance is correct. For design 1 the ratio between the roof and 2nd level displacement determined by the program is 1.2, while design 1a and design 1b models both have ratios of 1.5. Interestingly, the ratio of 2nd level to roof displacement is identical between design 1a and design 1b implying that the relative force distribution profile within the superstructure was not significantly affected by storey stiffness assumptions. Both models exhibit a more uniform force distribution which is expected for isolated structures. Floor accelerations generally increase with height, with little notable difference between the shear proportional and uniform stiffness models. The interstorey drifts shown in Table 7.21 indicate that the program was able to accurately predict the peak drifts, however, the program did overestimate the 2nd storey drift suggesting that the program overestimated the linearity of the force response.

Table 7.20: Base isolated lateral storey displacement and floor accelerations

Design	Program						THA		
	Displacement			Displacement			Floor acceleration		
	1st	2nd	3rd	1st	2nd	3rd	1st	2nd	3rd
	(mm)	(mm)	(mm)	(mm)	(mm)	(mm)	(g)	(g)	(g)
1a	122	128	133	113	119	123	0.39	0.34	0.41
1b				113	119	123	0.39	0.34	0.40
2	99.4	109		106	113		0.36	0.37	

Table 7.21: Base isolated interstorey drifts

Design	Program		THA	
	IDR (%)		IDR (%)	
	1st	2nd	1st	2nd
1a	0.20	0.17	0.20	0.13
1b			0.20	0.13
2	0.32		0.24	

The ratio between the program and THA responses are illustrated in Table 7.22. The program responses were moderately conservative with the predictions of base shear and lateral displacement being within 10% of the THA responses. The mandated 15% minimum torsional amplification proved to be very conservative compared to the THA results as design 1 exhibited a maximum of 5% amplification while design 2 exhibited only 1% amplification. The peak interstorey drifts were closely estimated by the program, with the 1 storey (design 2) structure being conservatively overestimated.

Table 7.22: Difference factor between program and THA (THA/program)

Design	T_M	D_M	D_{TM}	V_b	Peak IDR
1a	0.95	0.930	0.849	0.903	1.0
1b	0.95	0.930	0.849	0.903	1.0
2	1.04	1.07	0.930	0.930	0.75

7.5.3 Evaluation of Isolated Performance

A comparison between the fixed base and isolated spectral accelerations determined by the program are shown in Figure 7.6 for designs 1 and 2. For both designs the period is extended to a length in excess of 1s and the spectral acceleration is reduced to approximately half of their fixed base values. The responses of the fixed and isolated structures determined by the program and from the THA are shown in Table 7.23 and Table 7.24.

Generally, the isolated base shears are 2-3 times greater than the inelastic fixed base responses. However, the base shear of the isolated response includes the excitation of the foundation masses which contributes to the base shear but does not contribute to the superstructure response. A more useful comparison is to compare the ground level shears of fixed and isolated structures by comparing V_b of the fixed structures to V_s of the isolated structures, as these parameters represents the peak shear within the fixed and isolated superstructures respectively. The increase in the peak superstructure shear is still 1.49-1.74 times greater within the isolated structures, however this is substantially less than the increase in base shear. While the shear forces may have increased the elastic performance of the isolated structures is still significantly superior to the fixed structures. This is illustrated by the reduction of peak THA drifts by 50% in line with the reduction of the spectral acceleration. In addition, the peak elastic floor accelerations were reduced by 50 - 60% from the elastic fixed base response. The increase in storey shears is somewhat counter intuitive as generally forces correlate directly with response. However, due to the nature of capacity-based design lower forces are achieved which preserve life safety but at the cost of inflicting significant damage upon the structure. Therefor even though the isolated structure

experiences greater forces the economic performance is substantially greater. The isolated responses did, in some cases, not reduce the drift to below the 0.1% and 0.25g thresholds where no damage is expected. However, it did succeed in limiting drifts to levels where the interstorey drift causes only superficial and easily repairable damage, whereas before drifts were approaching the range consistent with moderate levels of damage. Additionally, the peak floor accelerations (PFAs) were also kept within the superficial damage range with the internal floor accelerations kept at levels below the peak acceleration. In contrast the fixed based structure elastic floor accelerations reached levels where extensive damage is expected, leading to significant property damage to the household's contents. This is due to the relatively short isolation periods which were significantly shorter than in other existing designs. This suggests that superior levels of performance could be achieved by employing softer bearings than those employed in this testing regime.

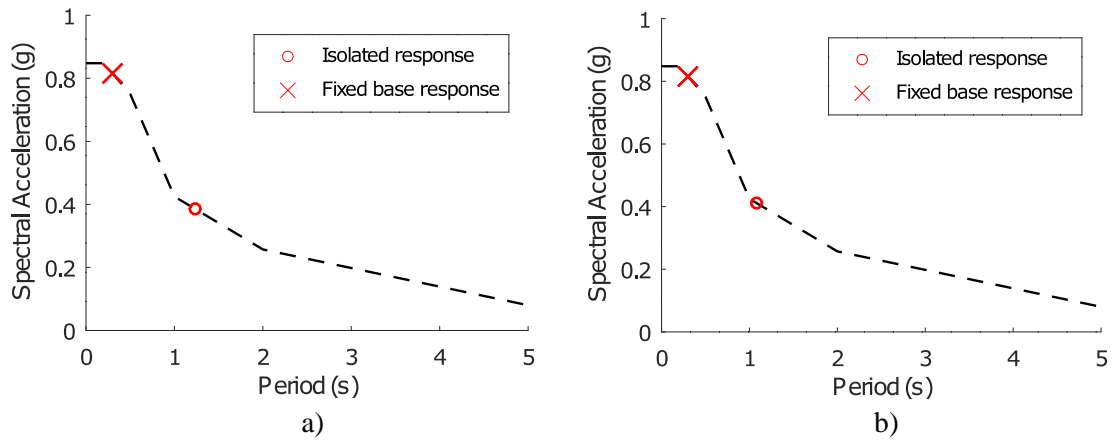


Figure 7.6: a) Design 1 response spectrum comparison and b) design 2 response spectrum comparison

Table 7.23: Program responses

Design	V_b	V_b	V_s	Peak drift	Peak drift
	Fixed ($R_d R_o$)	Isolated	Isolated	Fixed	Isolated
1a	71.3	144	106	0.44	0.19
1b				0.44	0.19
2	28.3	89.1	49.2	0.62	0.32

Table 7.24: THA responses

Design	V_b	V_b	V_s	Peak drift	Peak drift	PFA	PFA
	Fixed	Isolated	Isolated	Fixed	Isolated	Fixed	Isolated
1a	59.7	130	111	0.35	0.18	1.03	0.41
1b	63.2	130	111	0.43	0.21	0.82	0.40
2	27.3	82.9	43.3	0.60	0.24	0.86	0.37

CHAPTER 8 CONCLUSIONS AND RECOMMENDATIONS

8.1 Introduction

To address economic barriers to the adoption of seismic isolation for Part 9 structures a program methodology has been developed to design the isolation system of a Part 9 structure and analyze its performance. To validate the program, numerical analysis of two numerical models were conducted in OpenSees and subjected to time history analysis under west coast ground motions. This chapter provides a summary of the conclusions of each chapter and provides recommendations for future improvements and study.

8.2 Conclusions

Despite recent advances in life safety design single family Part 9 structures continue to remain vulnerable to large economic losses from moderate to large seismic events. Seismic isolation is an anti-seismic design method that has proven to be effective at reducing or eliminating damage to the superstructure and its contents. However, due to the high cost of testing and specialist design this technique is generally rarely applied, often only to higher importance structures. To address the seismic risk and enable adoption of seismic isolation for Part 9 structures methods to eliminate cost barriers are required.

The economic vulnerability of Part 9 structures is discussed extensively in Chapter 1, while Chapter 2 provides a comprehensive review of the seismic protection capabilities of seismic isolation in addition to discussing the economic viability of seismically isolated Part 9 structures. By reviewing existing research on low-cost seismic isolation, it is shown that substantial work has gone into developing economically viable bearings for use in Part 9 structures. Due to economic considerations FREIs are suggested as a preferable design bearing. However, substantial cost barriers remain, especially regarding testing and engineering design costs which have yet to be fully addressed. Therefore further research on removing these cost barriers was required to further improve economic viability.

Chapters 3 and 4 review the existing ASCE and NBCC requirements of seismic isolation and the adaption of the ASCE simplified methods to be in compliance with NBCC requirements for analyzing Part 9 structures. Chapter 5 discusses the proposed program methodology, its assumptions, and its limitations. The program determines the dynamic response of the isolated structure using the ELF procedure. The design of the isolation system, structural characteristics, and bearing characteristics are required designer inputs. To simplify the number and detail of the required inputs to quantities known by a Part 9 designer. The location and number of isolator bearings, the axial load on the bearings, and storey stiffnesses are approximated. Bearing placement and numbers are determined based on the existing Part 9 floor support system requirements. These simplifications allow the isolation system to be designed in compliance with existing gravity Part 9 load path requirements. The storey stiffnesses are represented as proportional to the fixed base shear force at each storey allowing the storey stiffnesses to be solved from the structure's characteristic equation and an assumed first mode period. Some assumptions are also required to enable ease of design and compliance with requirements. For example, the connection between the

isolation layer and isolation system is a rigid diaphragm. The elastomeric bearings, regardless of axial loading or displacement differences within the isolation system are assumed to possess the same shear properties. This significantly simplifies the analysis by assuming a uniform response based on average load conditions.

Chapter 6 discusses the design of elastomeric bearings and the associated standards and requirements. The three main stability characteristics are the buckling, rupture and rollout of the bearings, however, different standards present variable criteria and requirements complicating design. It was concluded that square bearings would be the preferred shape due to the symmetry of properties in both X and Y directions as well as the ease of mass fabrication. It was also concluded that T_{min} , the isolated period at which damage is prevented, is a preferable target when designing Part 9 bearings. Additionally, it was found that T_{min} of a structure is directly related to the structure's geometry and local seismic hazard and that if two structures had a similar T_{min} and $\frac{W}{n}$ ratio then they could achieve similar levels of performance with the same bearing design.

Chapter 7 presented the validation of the program by comparing the responses determined by the program to the THA responses. Two structures were considered. The first was analyzed with shear proportional and uniform stiffness to investigate the assumption of shear proportional stiffness. The shear proportional model's response profile matched closely with the program's analysis response. However, it was noted that the interstorey drifts were largest when a uniform stiffness model was used while floor accelerations were largest when the stiffness was shear proportional. The program conservatively estimated the structures responses for both fixed and isolated scenarios and generated response profiles like the response of the models. Isolation was able to successfully reduce the damage states from potential serious levels of economic loss to superficial levels, suggesting that the designed theoretical bearings proved suitable for the considered structures. The levels of torsional excitation of the models were substantially less than the 15% minimum required by ASCE.

8.3 Recommendations for Future Research

While the program methodology showed promise in the program's capacity for predicting the response of isolated structures, significant research is still required to further develop the program methodology of analyzing isolated Part 9 structures. Areas of future research include:

8.3.1 Rigid Floor Diaphragm

The interface between the isolation system is assumed to behave as a rigid diaphragm. However, it is possible that the wooden floor systems common in Part 9 structures may be sufficiently flexible to invalidate this assumption. Isolation systems that are relatively lightly loaded uniformly, or do not have significant torsional excitation may behave as a rigid diaphragm. The assumption of rigidity should be investigated for common wood diaphragms systems to confirm the validity and extent of differential displacements between isolators.

8.3.2 Isolation Layer Design and Axial Loading

The program currently designs the isolation system layout based on the user's input of the location of lateral and longitudinal floor beams and places the bearings at the intersection of these members. An investigation of real Part 9 structure floor beam systems should be undertaken to validate the efficacy of this approach in locating isolators at load bearing points. Additionally, the axial loads on the bearings are approximated via finite element methods and do not account for the occurrence of overturning moments that will alter the axial loads. An investigation of the true loading distribution within real Part 9 structures should be undertaken to assess the efficacy of the program's approximate method, and the effects of overturning accounted for in the program methodology.

8.3.3 Structural Geometry Considerations

Currently the program methodology is limited to rectangular and L-shaped structures. While these plan types compose most Part 9 structures built, other structural variations such as garages and basements are not currently accounted for. Additionally, while it is assumed that the internal load paths are too complicated to include in the program method this has not been fully investigated. Further developments should be made to account for the unique geometry and loading of garages, and the feasibility of analyzing Part 9 structures with basements should be assessed.

8.3.4 Storey Stiffnesses

The program currently assumes that the structure's storey stiffnesses are proportional to the storey shears. The program was able to determine storey displacements close to the shear proportional model, however, it should be verified that storey stiffnesses of Part 9 structures do indeed conform to the shear proportional assumption. If it is an unknown quantity, it may be necessary to assume either shear proportional stiffness or uniform stiffness and determine the response based on which scenario produces more conservative estimates. This, however, would lead to potentially excessively conservative results. Alternatively, due to the apparent similarity of performance between the shear proportional and uniform stiffness models it may be that the true stiffness distribution is not relevant to the performance of the isolated structure. Thus, further research is required to investigate the storey stiffness distributions.

8.3.5 Superstructure Performance

Currently it is assumed that the superstructure design of the Part 9 isolated structure will not differ significantly from the fixed base structure. As seen in Chapter 7 the isolated superstructure may have larger forces than the inelastic fixed base structure. However, damage is expected to be less due to the structure remaining elastic. This may not be the case if the superstructure is still designed within the framework of capacity-based design as plastic hinges may still form due to the relatively higher forces experienced by the isolated structure. To ensure this does not occur the

isolation system should be designed such that the isolated structure's forces are below the fixed base forces. In addition, it is also recommended that T_{min} be set as a preferable target to ensure that damage is prevented. It may not be feasible to achieve this level of performance with a system composing purely elastomeric bearings and research should be conducted on creating systems capable of achieving the desired levels of performance.

REFERENCES

- [1] BBC News, "History of Deadly Earthquakes," 2018. [Online]. Available: <https://www.bbc.com>.
- [2] Earthquakes Canada, "Earthquake Search," 2019. [Online]. Available: www.nrcan.gc.ca.
- [3] Insurance Bureau of Canada, "Study of Impact and the Insurance and Economic Cost of a Major Earthquake in British Columbia and Ontario/Quebec," AIR Worldwide, Boston, 2013.
- [4] M. Lamontagne and F. Brian, "Perception of earthquake hazard and risk in the province of Quebec and the need to raise earthquake awareness in this intraplate region.," *Seismological Research Letters*, vol. 87, no. 6, pp. 1426-1432, 2016.
- [5] British Columbia, "Population Estimates - Province of British Columbia," 2021. [Online]. Available: www.gov.bc.ca.
- [6] National Research Council of Canada, National Building Code of Canada 2015, Ottawa: Canada, 2015.
- [7] National Resources Canada, "Simplified Seismic Hazard Map for Canada, the provinces and territories," [Online]. Available: <http://www.seismescanada.nrcan.gc.ca>.
- [8] N. J. Balfour, J. F. Cassidy, S. E. Dosso and S. Mazzotti, "Mapping crustal stress and strain in southwest British Columbia," *Journal of Geophysical Research*, vol. 116, 2011.
- [9] Columbia, "Subduction zones and earthquakes," 2011. [Online]. Available: www.ldeo.columbia.edu/.
- [10] J. Cassidy, G. Rogers, S. Lamontagne and J. Adams, "Canada's Earthquakes: The Good, the Bad, and the Ugly," *Geoscience Canada*, vol. 37, no. 1, 2010.
- [11] M. Lamontagne, S. Halchuk, J. F. Cassidy and G. C. Rogers, "Significant Canadian Earthquakes of the Period 1600–2006," *Seismological Research Letters*, vol. 79, no. 2, pp. 211-223, 2008.
- [12] Natural Resources Canada, "The M9 Cascadia Megathrust Earthquake of January 26, 1700," 2018. [Online]. Available: <https://www.earthquakescanada.nrcan.gc.ca/historic-historique/events/17000126-en.php>.
- [13] W. DuPont and I. Noy., "What Happened to Kobe? A Reassessment of the Impact of the 1995 Earthquake in Japan.," *Economic Development and Cultural Change*, vol. 63, no. 4, pp. 777-812, 2015.
- [14] J. Adams and P. Basham, "The seismicity and seismotectonics of Canada east of the Cordillera," *Geoscience Canada*, vol. 16, no. 1, 1989.

- [15] M. Lamontagne, "Earthquakes in Eastern Canada: A Threat that can be Mitigated," Natural Resources Canada, Ottawa, 2008.
- [16] Swiss Re, "Earthquake risk in eastern Canada: mind the shakes," Swiss Re, Zurich, 2017.
- [17] Natural Resources Canada, "The Charlevoix earthquake of 1663," 2021. [Online]. Available: <https://www.earthquakescanada.nrcan.gc.ca/historic-historique/events/16630205-en.php>.
- [18] A. M. Tarabia and R. Y. Itani, "Seismic Response of Light-Frame Wood Buildings," *Journal of Structural Engineering*, vol. 123, no. 11, pp. 1470-1477, 1998.
- [19] M. C. Comerio, "Housing Issues After Disasters," *Journal of Contingencies and Crisis Management*, vol. 5, no. 3, 1997.
- [20] CUREE, "Woodframe Project Case Studies," CUREE, Richmond, 2001.
- [21] K. J. Tierney, "Business Impacts of the Northridge Earthquake," *Journal of Contingencies and Crisis Management*, vol. 5, no. 2, 1997.
- [22] Canadianvisa, "Median Household Income," 2021. [Online]. Available: <https://canadianvisa.org/life-in-canada/facts/household-income>.
- [23] I. P. Christovasilis and A. Filiatrault, "Seismic Testing of a Full-Scale Two-Storey Light-Frame Wood Building: NEESWOOD Benchmark Test," MCEER, Buffalo, 2009.
- [24] A. Pomonis, E. So and J. Cousins, "Assessment of facilities from the Christchurch New Zealand Earthquakes February 22nd 2011," Seismological Society of America Annual Meeting, Memphis, 2011.
- [25] K. M. McMullin and D. Merrick, "Seismic Performance of Gypsum," CUREE, Richmond, 2002.
- [26] H. Aslani and E. Miranda, "Probabilistic Earthquake Loss Estimation and Loss Disaggregation in Buildings," John A. Blume Earthquake Engineering Center, Stanford, 2005.
- [27] S. Taghavi and E. Miranda, "Response Assessment of Nonstructural Building Elements," PEER, Berkeley, 2003.
- [28] A. Martelli, M. Forni and P. Clemente, "Recent Worldwide Application of Seismic Isolation and Energy Dissipation and Conditions for Their Correct Use," in *World Conference of Earthquake Engineering*, Lisbon, 2012.
- [29] J. Kelly, "Aseismic base isolation: review and bibliography," *Soil Dynamics and Earthquake Engineering*, vol. 5, no. 4, pp. 202-216, 1986.
- [30] F. Naeim and J. Kelly, *Design of Seismically Isolated Structures: from Theory to Practice*, John Wiley & Sons, 1999.

- [31] S. Nagarajaiah and S. Xiaohong, "Response of Base-Isolated USC Hospital Building in Northridge Earthquake," *Journal of Structural Engineering*, vol. 126, no. 10, 2000.
- [32] K. Kasai, A. Mita and H. Kitamura, "Performance of Seismic Protection Technologies during the 2011 Tohoku-Oki Earthquake," *Earthquake Spectra*, vol. 29, no. 1, 2013.
- [33] H. Aslani and E. Miranda, "Optimization of Response Simulation for Loss Estimation Using PEER's Methodology," in *World Conference on Earthquake Engineering*, Vancouver, 2004.
- [34] M. J. Tait, R. G. Drysdale, H. Toopchi-Nezhad, B. Foster and M. G. P. Raaf, "Seismic Isolation of Residential Wood Frame and Low-Rise Masonry Buildings," McMaster University, Hamilton, 2011.
- [35] P. Clemente and G. Buffarini, "Base isolation: design and optimization criteria. Seismic isolation and protection systems," *The Journal of the Anti-Seismic Systems International Society*, vol. 1, no. 1, pp. 17-40, 2010.
- [36] C. J. Derham, J. M. Kelly and A. G. Thomas, "Nonlinear natural rubber bearings for seismic isolation," *Nuclear Engineering and Design*, vol. 84, no. 3, p. 417–428, 1985.
- [37] H. B. Seed, C. Ugas and J. Lysme, "Site-Dependant Spectra For Earthquake-Resistant Design," *Bulletin of the Seismological Society of America*, vol. 66, no. 1, pp. 221-243, 1976.
- [38] A. Chopra, *Dynamics of Structures Theory and Application to Earthquake Engineering*, Upper Saddle River: Pearson Prentice Hall, 2007.
- [39] J. M. Kelly, "The Role of Damping in Seismic Isolation," *National Information Service for Earthquake Engineering*, vol. 28, no. 3, 1999.
- [40] P. Buffarini and C. a. G., "Optimization criteria in design of seismic isolated building," in *American Insitute of Physics*, Melville, New York, 2008.
- [41] N. Mostaghel and J. Tanbakuchi, "Response of Sliding Structures to Earthquake Support Motion," *Earthquake Engineering and Structural Dynamics*, vol. 11, pp. 729-748, 1983.
- [42] ASCE, *Minimum Design Loads and Associated Criteria for Buildings and Other*, Reston: Published by American Society of Civil Engineers, 2017.
- [43] N. Fallah and G. Zamiri, "Multi-objective optimal design of sliding base isolation using genetic algorithm," *Scientia Iranica*, vol. 20, no. 1, 2013.
- [44] Y.-P. Wang, L.-L. Chung and W.-H. Liao, "Seismic Response Analysis of Bridges Isolated with Friction Pendulum Bearings," *Earthquake Engineering and Structural Dynamics*, vol. 27, p. 1069—1093, 1998.
- [45] M. Pranesh and R. Sinha, "VFPI: an isolation device for aseismic design," *Earthquake Engineering and Structural Dynamics*, vol. 29, 2000.

- [46] E. Jampole, *High-friction sliding seismic isolation for enhanced performance of light frame structures during earthquakes*, Ann Arbor: ProQuest LLC, 2016.
- [47] C. Tsai, P.-C. Lu, W.-S. Chen, T.-C. Chiang, C.-T. Yang and Y.-C. Lin, "Finite element formulation and shaking table tests of direction-optimized-friction-pendulum system," *Engineering Structures*, vol. 30, no. 9, 2008.
- [48] T. A. Morgan and S. A. Mahin, "Achieving reliable seismic performance enhancement using multi-stage friction pendulum isolators," *Earthquake Engineering and Structural Dynamics*, vol. 39, 2010.
- [49] N. C. Van Engelen, "Fiber-reinforced elastomeric isolators: A review," *Soil Dynamics and Earthquake Engineering*, vol. 125, 2019.
- [50] H. Toopchi-Nezhad, M. Tait and R. Drysdale, "Influence of thickness of individual elastomer layers (first shape factor) on the response of unbonded fiber-reinforced elastomeric bearings.," *Journal of Composite Materials*, vol. 47, pp. 3433 - 3450., 2013.
- [51] J. M. Kelly, *Earthquake-Resistant Design with Rubber*, New York, NY.: Springer-Verlag, 1997.
- [52] J. Kelly, "Analysis of fiber-reinforced elastomeric isolators," *Journal of Seismology and Earthquake Engineering*, vol. 2, no. 1, 1999.
- [53] J. Kelly, "Seismic Isolation Systems for Developing Countries," *Earthquake Spectra*, vol. 18, no. 3, p. 385–406, 2002.
- [54] G. Russo and M. Pauletta, "Sliding instability of fiber-reinforced elastomeric isolators in unbonded applications," *Engineering Structures*, vol. 48, pp. 70-80, 2013.
- [55] H. Toopchi-Nezhad, M. Ghotb, Y. Al-Anany and M. Tait, "Partially bonded fiber reinforced elastomeric bearings: Feasibility, effectiveness, aging effects, and low temperature response," *Engineering Structures*, vol. 179, pp. 120-128, 2019.
- [56] I. G. Buckle and R. L. Mayes, "Seismic Isolation: History, Application, and Performance - A World View," *Earthquake Spectra*, vol. 6, no. 2, 1990.
- [57] S. Chimamphant and K. Kasai, "Comparative response and performance of base-isolated and fixed-base structures," *Earthquake Engineering and Structural Dynamics*, vol. 45, no. 5, 2015.
- [58] S. Nagarajaiah and S. Xiaohong, "Response of Base-Isolated USC Hospital Building in Northridge Earthquake," *Journal of Structural Engineering*, vol. 126, no. 10, 2000.
- [59] M. CELEBI, "Successful Performance of a Base-Isolated Hospital Building During the 17 January 1994 Northridge Earthquake," *The Structural Design of Tall Buildings*, vol. 5, pp. 95-109, 1996.

- [60] J. Asher, S. Hoskere, R. Ewing, R. Mayes, M. Button and D. Van Volkinburg, "Performance of seismically isolated structures in the 1994 Northridge and 1995 Kobe earthquakes," in *Structures Congress*, New York, 1997.
- [61] R. L. Mayes, "Using Seismic Isolation and Energy Dissipation to," in *New Zealand Society for Earthquake Engineering*, Christchurch, 2012.
- [62] M. N. Fardis, "Capacity design: early history," *Earthquake Engineering & Structural Dynamics*, vol. 47, no. 14, pp. 2887-2896, 2018.
- [63] M. Melkumyan, "Savings in Consumption of Concrete and Steel and in the Related Cost of Various Reinforced Concrete Frame Buildings with Shear Walls Due to Implementation of Base Isolation Strategy," *Scientific Review*, vol. 4, no. 8, 2018.
- [64] J. M. Kelly and D. Konstantinidis, "Low-Cost Seismic Isolators for Housing in Highly-Seismic Developing Countries," in *Conference on Seismic Isolation, Energy Dissipation and Active Vibrations Control of Structures*, Istanbul, 2007.
- [65] W. Taniwangsa, P. W. Clark and J. M. Kelly, "Natural Rubber Isolation Systems for Earthquake Protection of Low-Cost Buildings," Earthquake Engineering Research Center, Berkeley, 1996.
- [66] UC San Diego , "Seismically Isolated Unibody Residential Buildings for Enhanced Life-Cycle Performance (2014)," 2014. [Online]. Available: <http://nees.ucsd.edu/projects/2014-seismically-isolated-unibody/>.
- [67] M. Walters, "Seismic Isolation – The Gold Standard of Seismic Protection," *Structure Magazine* , pp. 11-14, July 2015.
- [68] Habitat Insurance Agencies Ltd, "Available In BC: Earthquake Deductible Buyback Insurance," Habitat Insurance Agencies Ltd, July 2017. [Online]. Available: <https://www.habitatinsurance.com/blog/now-available-in-bc-earthquake-deductible-buyback-insurance/>.
- [69] R. H. DeVall, "Background information for some of the proposed earthquake design provisions for the 2005 edition of the National Building Code of Canada," *Canadian Journal of Civil Engineerin*, vol. 30, no. 2, pp. 279-286, 2003.
- [70] K. York and K. Ryan, "Distribution of Lateral Forces in BaseIsolated Buildings Considering Isolation System Nonlinearity," *Journal of Earthquake Engineering*, vol. 12, no. 7, pp. 1185-1204, 2008.
- [71] B. D, M. C. Constantinou and W. A. S, "An equivalent accidental eccentricity to account for the effects of torsional ground motion on structures.," *Engineering Structures*, no. 69, pp. 1-11, 2014.
- [72] E. Wolff, C. Ipek, M. Constantinou and L. Morillas, "Torsional response of seismically isolated structures revisited," *Engineering Structure*, vol. 59, 2014.

- [73] C. W. a. C. M. C. Winters, "Evaluation of Static and Response Spectrum Analysis Procedures of SEAOC/UBC for Seismic Isolated Structures," National Center for Earthquake Engineering Research, New York, 1993.
- [74] M. K. Bednarek, *Seismic Base Isolation for Residential Structures in Canada*, University of Windsor, 2020.
- [75] Natural Resources Canada, "National Building Code of Canada seismic hazard values," 2018. [Online]. Available: <https://earthquakescanada.nrcan.gc.ca/hazard-alea/interpolat/calc-en.php>.
- [76] MathWorks Inc, *MATLab*, Natick, Massachusetts: MathWorks Inc, 2018.
- [77] The Canadian Wood Council, *Engineering Guide for Wood Frame Construction*, Ottawa: The Canadian Wood Council, 2014.
- [78] Cadbull, "cadbull.com," Cadbull, 2019. [Online]. Available: <https://cadbull.com>. [Accessed 27 10 2021].
- [79] ISO, "Elastomeric Seismic-Protection Isolators-Part 3: Applications for Buildings," ISO, Geneva, 2018.
- [80] Canadian Standards Association (CSA), *Canadian Highway Bridge Design Code*, Mississauga: Canada: CSA, 2019.
- [81] J. M. Kelly and M. R. Marsico, "Stability and Post-buckling Behavior in Nonbolted Elastomeric Isolators," *The Journal of the Anti-Seismic Systems International Society*, vol. 1, no. 1, pp. 41-54, 2010.
- [82] M. de Raaf, M. Tait and H. Toopchi-Nezhad, "Stability of fiber-reinforced elastomeric bearings in an unbonded application," *Journal of Composite Materials*, vol. 45, no. 18, p. 1873–1884, 2011.
- [83] N. C. Van Engelen, M. J. Tait and D. Konstantinidis, "Model of the Shear Behavior of Unbonded Fiber-Reinforced Elastomeric Isolators," *Journal of Structural Engineering*, 2014.
- [84] AASHTO, *AASHTO LRFD bridge design specifications*, Washington, DC: AASHTO, 2017.
- [85] BSI (British Standards Insitute), *Anti-seismic Devices*, London: BSI, 2018.
- [86] ISO, *Elastomeric seismic-protection isolators - Part 2: Applications for bridges - Specifications*, Geneva: ISO, 2018.
- [87] N. C. Van Engelen, "Evaluation of Design Equations for Critical Properties of Reinforced Elastomeric Bearings and Recommended Revisions," *Journal of Structural Engineering*, vol. 147, no. 9, 2021.

- [88] J. M. Kelly and N. C. Van Engelen, "Single series solution for the rectangular fiber-reinforced elastomeric isolator compression modulus," Pacific Earthquake Engineering Research Center, Univ. of California, Berkeley, CA, 2015.
- [89] N. C. Van Engelen, "Rotation in rectangular and circular reinforced elastomeric bearings resulting in lift-off," *International Journal of Solids and Structures*, vol. 168, pp. 172-182, 2019.
- [90] ISO, *Elastomeric seismic-protection isolators - Part 1: Test Methods*, Geneva: ISO, 2017.
- [91] OpenSees, *OpenSees*, Berkeley, 2021.
- [92] Canada Mortgage and Housing Corporation, "Overview of Residential Property Living Areas in British Columbia, Nova Scotia and Ontario," *Housing Market Insight*, May 2019.
- [93] Statistics Canada, "Canadian Housing Statistics Program," 03 05 2019 . [Online]. Available: <https://www150.statcan.gc.ca/n1/daily-quotidien/190503/dq190503b-eng.htm>. [Accessed 28 06 2022].
- [94] OpenSees, "Elastomeric Bearing (Bouc-Wen) Element," 19 October 2016. [Online]. Available: [https://opensees.berkeley.edu/wiki/index.php/Elastomeric_Bearing_\(Bouc-Wen\)_Element](https://opensees.berkeley.edu/wiki/index.php/Elastomeric_Bearing_(Bouc-Wen)_Element). [Accessed 10 September 2022].
- [95] National Research Council of Canada, *Structural Commentaries (User's Guide – NBC 2015: Part 4 of Division B)*, Ottawa: Canada, 2017.
- [96] G. M. Atkinson, "Earthquake time histories compatible with the 2005 National building code of Canada uniform hazard spectrum," *Canadian Journal of Civil Engineering*, vol. 36, no. 6, pp. 991-1000, 2009.
- [97] K. Ryan and J. Polanco, "Problems with Rayleigh Damping in Base-Isolated Buildings," *Journal of Structural Engineering*, vol. 134, no. 11, pp. 1780-1784, 2008.

APPENDIX A BASELINE PROGRAM PROCESS

For ease of explanation the existing design methodology can be separated into 14 steps which across 2 main phases. The 1st phase consists of steps 1-9 and calculates of initial variables and performs the iterations required to determine the properties of the system at its maximum expected displacement. The second phase consists of steps 10-14 and investigates if the system is code compliant and determines the remaining response parameters based on the properties determined in steps 1-9.

Step 1: Step 1 is where the known input parameters are added into the analysis. The inputs can be grouped into several different subtypes such as structural inputs, location inputs and isolator inputs. The structural inputs include:

- x : the structural width;
- y : the structural length;
- z_i : the uniform height of the storeys;
- N : the number of storeys;
- ST : the weight class of the structure;
- T_b : The fixed base period of the structure.

The structural inputs describe the fundamental dimensions of the structure which can be used to determine the structural mass distribution. These inputs are restricted to simple rectangular structure with uniform floor plans and masses and storey stiffnesses. The weight class of a structure can either be normal or heavy as classified by the Canadian Wood Council (CWC) [77]. The classification of structures as either normal or heavy weight was intended to augment Part 9 of the NBCC by providing a designer with the expected dead loads associated with different construction methods. Each classification has a prescribed range of distributed dead loads for the floors, exterior walls, the roof, and partitions as shown in Table 5.1.

While the heavy weight construction loads have a range of values the program currently selects the upper bound to remain conservative by default. It should also be noted that while the total floor, roof and partition wall loads are based on the plan area of the structure the exterior wall loads are based on the total surface area of the exterior walls. The estimates of structural weight provided by the CWC classification are used to determine the total dead loads of each storey. The fixed base period of the structure is also included to enable the program to generate a profile of the isolated force distribution in later steps and to provide the user with a comparison between the isolated and fixed base performance of the structure. The value of T_f , is assumed based on the typical period range of 0.1-0.3 s for low rise wood frame, and masonry structures [34]. It is possible for the user to determine and input the fixed base period of the structure, but if no value is inputted 0.3 s is selected as the fixed base period. This is considered as the worst-case scenario because the force at the top level is larger, leading to a generally less desirable response.

The location inputs consist of factors that affect the loading of the structure due to the site-specific hazard. Ideally the site location would be what was inputted into the code, however, since it is currently unfeasible to incorporate an accurate catalogue of local hazards for each site location parameters are inputted directly. The location inputs include:

S_s : The 1-in-50 year ground snow load;
 S_r : The 1-in-50 year associated rain load;
 C_b : The basic roof snow load factor;
 $S_a(T)$: The design response spectrum data.

The snow and rain hazard data are used to determine the roof snow loads, 25% of which is then added to the total structural load. The design response spectrum values for various periods is also required by to calculate the instantaneous design spectral acceleration can be determined, $S_a(T_i)$ for each iteration.

The isolator inputs are the properties of the isolator being considered. Currently the properties of 5 different isolators are incorporated into the program directly. The inputs related to each isolator are:

$k(D_i)$: The isolator stiffness as a function of displacement;
 $\zeta(D_i)$: The isolator damping as a function of displacement;
 L_{min} , L_{max} : The range of vertical pressure that an individual isolator can carry without changing the isolator properties;
 b_i d_i : The plan dimensions of the rectangular isolator unit;
 d_{max} : The maximum displacement isolators can undergo.

The isolator properties given in the inputs allow the instantaneous response of the structure to be determined during each iteration. The range of compressive pressure that can be applied to the isolators, and the maximum allowable displacement of isolators are required to ensure that the stresses and strains applied to the isolator will not substantially alter its performance or cause damage. It should be noted that only the case 4 load case provided by the NBCC is considered. This means that the maximum load on the isolators, and the potential for buckling is currently ignored.

Step 2: Initial Variables are calculated such as:

W : the effective seismic weight of the structure above the isolation interface

W_{min} , W_{max} : The minimum and maximum weight that an individual isolator can carry without changing the isolator properties

N_{min} , N_{max} : The range of the number of isolators

The ranges of weight per isolator and number of isolators are given by:

$$W_{min} = \frac{L_{min}}{x_i y_i} \quad W_{max} = \frac{L_{max}}{x_i y_i}$$

$$N_{min} = \frac{W}{W_{max}} \quad N_{max} = \frac{W}{W_{min}}$$

The maximum load limit per isolator is used to determine the minimum number of isolators required, while the minimum vertical load required constrains the maximum number of isolators that can be used. The upper and lower limits provide the program with upper and lower bounds of analysis to consider, which result in two design scenarios to be generated during the design of the system. Initially the program selects N_{min} for initial analysis while later steps will select N_{max} and the two boundary designs may be compared. This approach assumes that the load will be evenly distributed between all isolator units, and no attention is given by the program to the design of the isolator layout itself.

Step 3: Initial guesses of the design period T_M and the design damping coefficient B_M are assumed such that $T_{Mj} = 1.0$ s and $B_{Mj} = 1.0$, where j represents the iteration count.

Step 4: The location-specific spectral accelerations for the base isolated structure, $S_a(T_{Mj})$ is determined using linear interpolation.

Step 5: The maximum displacement, D_{Mj} is calculated by:

$$D_{Mj} = \frac{S_a(T_{Mj})gT_M^2}{4\pi^2 B_{Mj}}$$

Step 6: The instantaneous isolator stiffness k_{Mj} , and isolator damping, ζ_{Mj} are determined for D_{Mj} using the stiffness and damping regimes of the isolators.

Step 7: The damping coefficient B_{Mj} is determined for $\zeta = \zeta_{Mj}$ using Table 5.2.

Step 8: Using the instantaneous stiffness k_{Mj} determined in step 6 a new T_{Mj} is determined using:

$$T_{Mj} = 2 \sqrt{\frac{W}{k_{Mj}g}}$$

Step 9: Steps 4-8 are repeated and the iteration j increases such that $j = j + 1$, until the iterative variables converge. The convergence criteria is satisfied when the absolute difference T_{Mj} and $T_{M(j+1)}$ is less than 0.001 s. It should be noted that using T_M as the convergence metric did not result in substantial errors or convergence issues for the other iterative parameters.

Step 10: Since the stiffness and damping regime functions of the isolators are nonlinear it is possible for multiple solutions to exist, and there exists the possibility that the solution converged to in step 9 is not unique. To ensure the solution found is unique a factor of 1.25 and 0.75 are applied to T_M and the program performs the iterations of steps 4-8 again. If the new solution found from the offset starting conditions is the same as that found in part 9 the solution is unique. If the solutions do not converge the nonlinearity of the isolators makes simplified analysis impossible and either a new isolator should be selected or an expert consulted.

Step 11: The program evaluates the key parameters for compliance with the code requirements. The period is checked against the fixed base period to ensure $T_M \geq 3T_{fb}$ and the maximum design displacement D_M is checked to ensure it does not exceed the maximum allowable isolator displacement such that $D_M \leq d_{max}$.

Step 12: The foundation base shear, superstructure base shear above the isolation interface, and the force distribution are calculated using equations (4.7), (4.8) and (4.11) respectively. The force distribution is not strictly necessary for the design of an isolated structure whose superstructure is built according to Part 9 of the NBCC. However, the force distribution is a useful metric to compare the performance of the fixed base and isolated structures and to evaluate if the response is reasonable.

Step 13: Steps 3-12 are repeated using the maximum number of isolators.

Step 14: The results of the analysis are summarized as 2 graphs. The first graph displays the efficiency of the system

APPENDIX B BEAM LAYOUT

The Isolator layout program places isolators at the corners of the exterior walls as a default. Additional isolators required to carry gravity loads are placed at the intersections between floor beams. The longitudinal and lateral floor beams are defined by a X and Y coordinate respectively. From this data the intersections of the lateral and longitudinal floor beams are used to determine the coordinates of isolator units. The program constrains the number of lateral and longitudinal floor beams to 4 in each direction for a rectangular structure and 1 in each direction for areas A, B and C for L-shaped structures as illustrated in Figure B.1 a) and b) respectively.

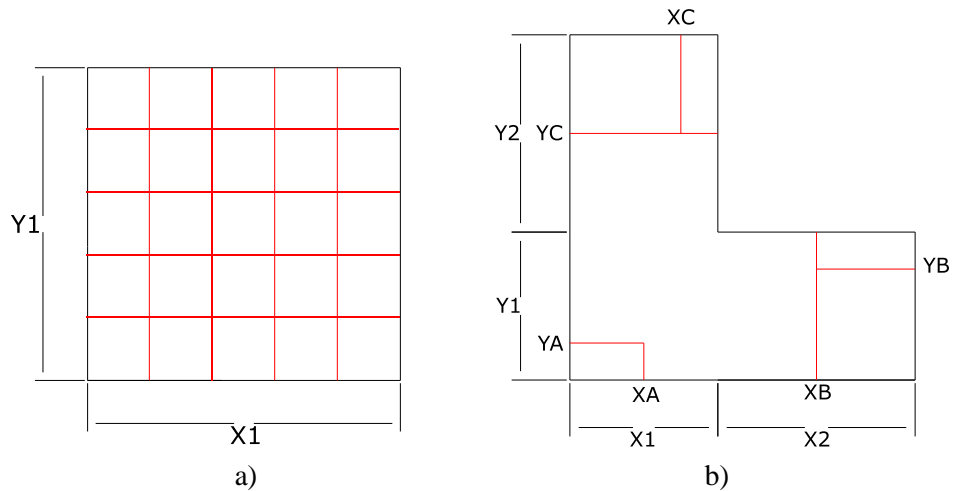


Figure B.1 Floor beams for a) Rectangular and b) L-shaped structures

This constraint is due to the realistic expected size of structures. The NBCC allows traditional joist lengths of up to 5.6m, but a more common span length is roughly 3-4 m based on common practices. With those average span lengths, it is unreasonable to expect a structure that's maximum plan area is limited to 600m² between all storeys, and usually generally conforming to much less, to have substantially more internal spans. Larger structures that would be exempt from this assumption would not be applicable to Part 9 and would require custom detailing outside the scope of this project.

The ground floor plan type is identified as rectangular or L-shaped. Depending on the plan type the program will interpret the inputs to determine the positions of isolator units. For structures with rectangular ground floor plans the user can enter the X coordinates of the longitudinal floor beams by selecting values for $X_{bearing1}$ up to $X_{bearing4}$, while the Y coordinates are entered by selecting values for $Y_{bearing1}$ up to $Y_{bearing4}$. For structures with less lateral or longitudinal floor beams than 4, the user should leave the inputs on the input sheet blank. From these inputs the intersection of the lateral and longitudinal floor beams is used to determine the coordinates of isolator units. Figure B.2 illustrates the layout of foundation floor beams of an arbitrary rectangular structure in red dotted lines.

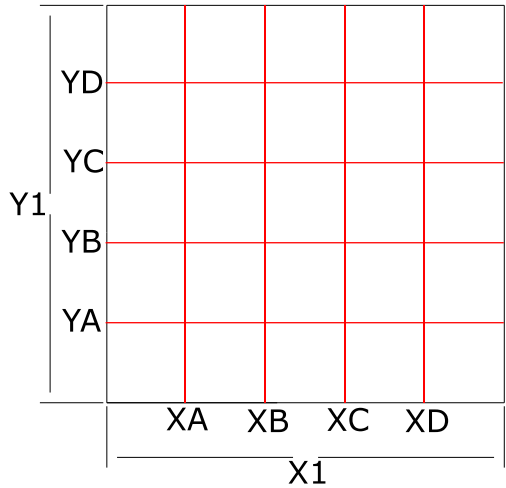


Figure B.2 Floor beams and isolator layout of example structure

For L-shaped structures the method of selecting floor beams is more constricted. An L-shaped structure is divided into 3 primary areas: A, B and C, which correspond to the areas as shown in Figure B.3.

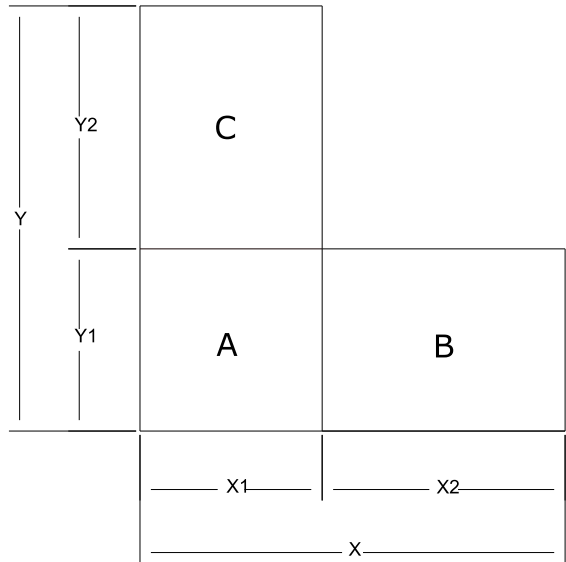


Figure B.3 Division of a L-shaped structure

As previously mentioned, floor beams for this type of structure are limited to one longitudinal and one lateral beam per primary area. Such that the user may input X_A , X_B , X_C and Y_A , Y_B , Y_C for the longitudinal and lateral beams respectively, as illustrated in Figure B.4.

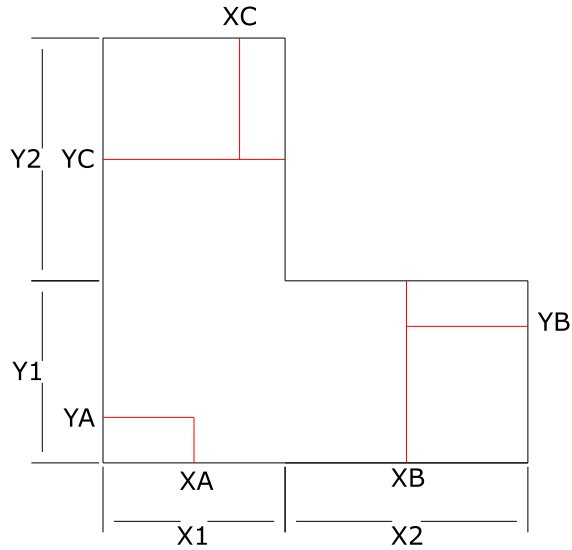


Figure B.4 L-shaped structure floor beam layout

In addition to these floor beams the user may also opt to include beams along the borders between AB and AC to produce a layout as shown in Figure B.5.

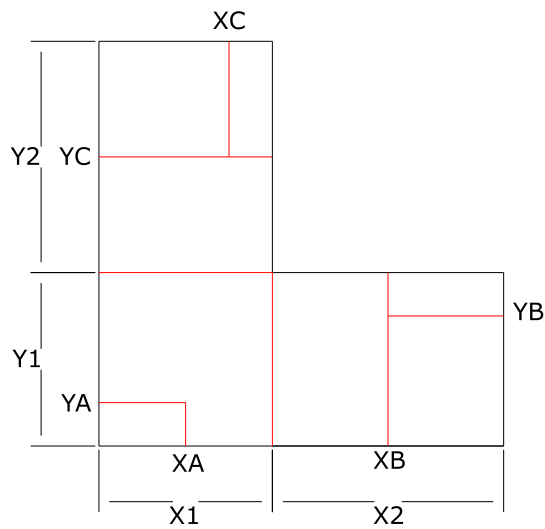


Figure B.5 L-shaped structure floor beam layout with AB and AC borders

The user may also wish to further expand the floor beams by extending XA YA and XB and YC such that they intersect with the bordering floor beams between AB and AC to produce a layout as shown in B.6.

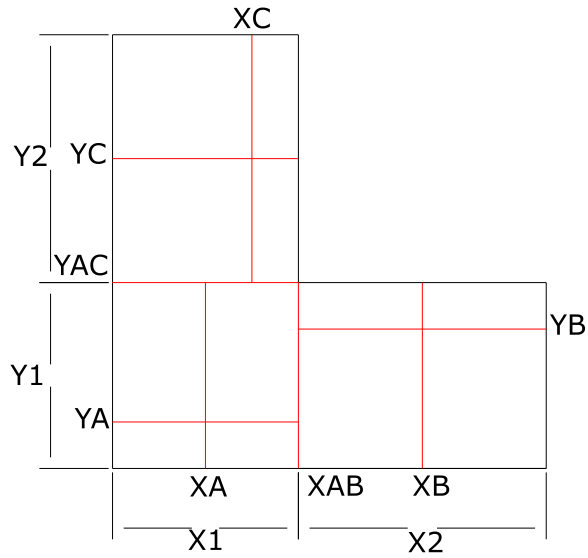


Figure B.6 L-shaped structure with AB and AC borders connected

In the 3 cases presented the user may select their preferred layout by inputting variables *ClearAB* *ClearAC* as 2, 1 and 0 for the cases shown in figures Figure B.4, Figure B.5, and B.6 respectively. The program then generates a record of the number of isolators required, and their individual coordinates for further use in later subprograms.

VITA AUCTORIS

NAME: Nolan Stratton
PLACE OF BIRTH: Toronto, ON

YEAR OF BIRTH: 1998

EDUCATION: Bishop Allen Academy, Toronto, ON, 2016
University of Windsor, B.A.Sc., Windsor, ON, 2020
University of Windsor, M.A.Sc., Windsor, ON, 2022